Study and modelling of the prefractionation and distillation of work-arising-gases-derived synthetic crude oil

Master's Thesis

Dimitrios Dimitriadis

TUDelft

TATA STEEL

Study and modelling of the prefractionation and distillation of work-arising-gases-derived synthetic crude oil

Master's thesis

by

Dimitrios Dimitriadis

to obtain the degree of Master of Science

in Sustainable Energy Technology

at the Delft University of Technology

Student Number:	4749812	
Project Duration:	August 8th, 2019 – March 24th, 2020	
Thesis Supervisors:	Prof. dr. ir. Wiebren de Jong	TU Delft
	PDEng. Frank Sauerhöfer Rodrigo	Tata Steel
	Dr. Stanley Santos	Tata Steel
Thesis Committee:	Prof. Dr. ir. Wiebren de Jong	TU Delft
	Asst. prof. Dr. R. Delfos	TU Delft
	Asst. Prof. Dr. H. B. Eral	TU Delft

Abstract

The steel-making industry has a large carbon footprint, mostly due to the use of coke and coal to reduce the iron oxides from iron ore into carbon rich iron, which is then used to produce low-carbon steel. The reduction reaction happens in the blast furnace, which releases CO and CO_2 to the atmosphere. In the interest of reducing the carbon footprint of the steel-making process, the captured blast furnace gases can be used in methanol or liquid hydrocarbons production, by using the GTL process. Blast furnace and basic oxygen furnace off-gases can be converted to syngas with the addition of hydrogen or via the water-gas shift reaction with the addition of steam. The syngas can be converted into synthetic crude oil (syncrude) with the use of the Fischer-Tropsch technology. Syncrude can then be fractionated and upgraded or refined into final products, such as motor gasoline, jet fuel and diesel fuel.

The purpose of this study was to create a theoretical model for the distillation of synthetic crude oil (syncrude) into straight-run naphtha, kerosene and gas oil fractions, at a scale of 235 kt_{feed}/year. To that end, a process model was created that receives the output of a Co-LTFT process as raw feed. The raw feed was prefractionated to remove the majority of the unreacted syngas, inert gases, light hydrocarbons (C_1-C_4) and water. The remaining stream was syncrude, primarily composed of alkanes and 1-alkenes in the C_{5-50} range.

A Base Case was designed in ASPEN plus, with a distillation unit with two steam strippers and three pumparounds. The goal was to receive the syncrude and separate naphtha, kerosene and gas oil cuts, with least 90% purity and recovery of the components. The Fenske-Underwood-Gilliland method was used to estimate the number of stages and reflux ratio of the column, and the Kirkbride method was used to find an initial estimate for the feed stage. The TBP curves of the cuts were compared with similar cuts from literature and found to be similar.

The Base Case underwent a sensitivity analysis in order to ascertain the effect of different design and process parameters on the separation quality and utility consumption. The parameters that were tested are cold condensate temperature, feed stage, condenser duty, feed temperature and stripping steam flow rate to the ADU. According to the sensitivity analysis results, for optimal separation between the syncrude and the other gases in the raw feed, the gases must be purged at a temperature of -70°C. Furthermore, the optimal configuration for the distillation of the given syncrude into naphtha, kerosene and gas oil fractions with at least 90% purity and recovery is as follows: The ADU has 40 equilibrium stages and a condenser duty of approximately -5.7 MW. The feed must be heated to 310°C and enter the column at stage 37. The stripping steam flow rate must be around 1.3 kg/s.

Five alternative processes were modelled as well, with similar inputs to the column model, and the results of the distillate separation quality and utility consumption were documented as well. The alterations of the alternative cases include replacing the stripping steam with a reboiler in one of the strippers, adding a stripper from where an additional product was drawn, concentrating the pumparound duty on the condenser, using a vacuum distillation unit to fractionate the residue of the atmospheric distillation unit, and employing a heat integration network.

The most important conclusions are listed. Firstly, the side strippers must use low pressure stripping steam instead of reboilers. Next, the minimum number of products must be drawn off in order to minimize utility consumption at a given separation quality. Furthermore, heat integration can save up to 50% in total utility consumption (heat and cooling water). It is recommended that further research, including a cost estimation, is conducted on refineries that produce on-specification final products.

Preface

Dear reader,

This project report is the distilled product of 8 challenging months of work in the R&D dept. of Tata Steel Nederland Technology B.V., in collaboration with the Process and Energy dept. of TU Delft. It also is my Thesis for the title of Master of Science in Sustainable Energy Technology at TU Delft, which marks the end of my journey as a student and the start of my professional career. During those 8 months, I learned a lot of new things; both from an academic standpoint and from a professional standpoint. I hope that this is reflected in this project report.

Tata Steel Europe is the second largest producer of steel in Europe, with the branch in IJmuiden producing over 7 million tonnes of high quality steel annually. The learning experience from working in such a challenging and competitive work environment has been invaluable. As such, I believe it is my duty to show my gratitude by acknowledging the people who played an important role in successfully carrying out this project.

First and foremost, my thanks go to mr. Jan van der Stel, Manager of the Blast Furnace Development & Alternative Ironmaking group, for providing me with the opportunity to carry out this Thesis project in Tata Steel.

Second, I would like to thank dr. Frank Sauerhöfer Rodrigo, dr. Stanley Santos, and Prof. dr. ir. Wiebren de Jong, for being my supervisors and mentors during those 8 months. Their guidance, insight and sharing of their knowledge were catalysts in carrying out the project.

I would like to extend my thanks to the other employees of Tata Steel R&D, my fellow interns, and my friends from TU Delft, for making those 8 months memorable, for their support, and for providing their insight.

Last but not least, my heartfelt gratitude goes to my family, for providing me with the necessary support to pursue my dream to become an engineer, as well as for their words of encouragement and understanding during my studies.

Dimitrios Dimitriadis

IJmuiden, March 2020

List of Figures

x

List of Tables

List of abbreviations

ADU	Atmospheric Distillation Unit
AGO	Atmospheric Gas Oil
AHSS	Advanced High Strength Steel(s)
AR	Atmospheric Residue
ASF	Anderson-Schultz-Flory
ASTM	American Society for Testing and Materials
BoD	Basis of Design
EoS	Equation(s) of State
FT	Fischer-Tropsch
FTR	Fischer-Tropsch Reactor
FTS	Fischer-Tropsch Synthesis
FUG	Fenske-Underwood-Gilliland
GO	Gas Oil
GTL	Gas-to-Liquids
HC	Hydrocarbon(s)
HEN	Heat Exchanger Network
HGO	Heavy Gas Oil
HK	Heavy Key
HPS	High Pressure Steam
HTFT	High-Temperature Fischer-Tropsch
HVGO	Heavy Vacuum Gas Oil
LK	Light Key
LPG	Liquefied Petroleum Gas
LPS	Low Pressure Steam
LTFT	Low-Temperature Fischer-Tropsch
LVGO	Light Vacuum Gas Oil
PFD	Process Flow Diagram
PR	Peng-Robinson
TBP	True Boiling Point
VD	Vacuum Diesel
VDU	Vacuum Distillation Unit
VGO	Vacuum Gas Oil
VLE	Vapor-Liquid Equilibrium
VR	Vacuum Residue
WAGs	Work's Arising Gases
WGS	Water Gas Shift

List of symbols

Latin

a	Relative volatility
B	Bottom product (of ADU) molar flow rate
c_p	Specific heat
C_p	Heat capacity flowrate
D	Distillate product (of ADU) molar flow rate
F	Feed (of ADU) molar flow rate
H	Enthalpy
i	Subscript indicating component i
K	Volatility
L	Reflux (of ADU) molar flow rate
m	Mass
m	Number of stages above feed stage
n	Number of carbon atoms
N	Total number of stages in column
n	Moles
p	Pressure
p	Number of stages above feed stage
q	Vapor fraction of feed
Q	Heat
R	Reflux ratio (of ADU)
R	Ideal gas constant
S	Entropy
T	Temperature
U	Internal energy
V_m	Molar volume
V	Volume
x_i	VLE concentration of component i in liquid phase
x_n	Molar fraction of compounds with carbon number n
y_i	VLE concentration of component i in vapor phase
Z_{Fi}	Molar fraction of component i in the feed

Greek

α	α-value, catalyst and temperature dependent value in ASF distribution
Δ	Prefix indicating difference between two values
θ	Root of second Underwood equation

Table of Contents

1. Introduction

1.1.   Problem background

Demand for steel globally is forecasted to increase by 30% until 2050 [1]. The current amount of CO_2 emitted by the iron and steel industry is 2.8 Gt/year, and it is forecasted to increase to 3.1 Gt/year by 2040. This will account for 8% of global CO_2-equivalent emissions and about 34% of global industry energy production-based emissions.

Iron ore must be processed in order to reduce the iron oxide compounds to elemental iron, as well as to remove impurities. Three methods are used currently for the reduction of iron ore: blast furnace reduction, direct reduction, and electric arc furnace reduction. The three methods will be briefly described in the next paragraphs.

Blast furnaces are large towers wherein iron ore and coke are loaded in alternating layers from the top, while hot air (in the order of 1000°C), possibly enriched with oxygen, is loaded from pipes (tuyeres) at the bottom [2]. Oxygen reacts with coke, producing carbon monoxide, and the carbon monoxide reacts with the iron oxides in a series of reactions that eventually produce elemental iron. The temperature in the interior of the furnace is in the order of 2200°C. The products of the blast furnace are: from the bottom, a molten iron phase with few impurities, called pig iron, and a liquid slag phase, which contains most of the impurities; from the top, the blast furnace gases (rich in CO and CO_2). A schematic of the interior of a blast furnace is shown in Figure 1.1.
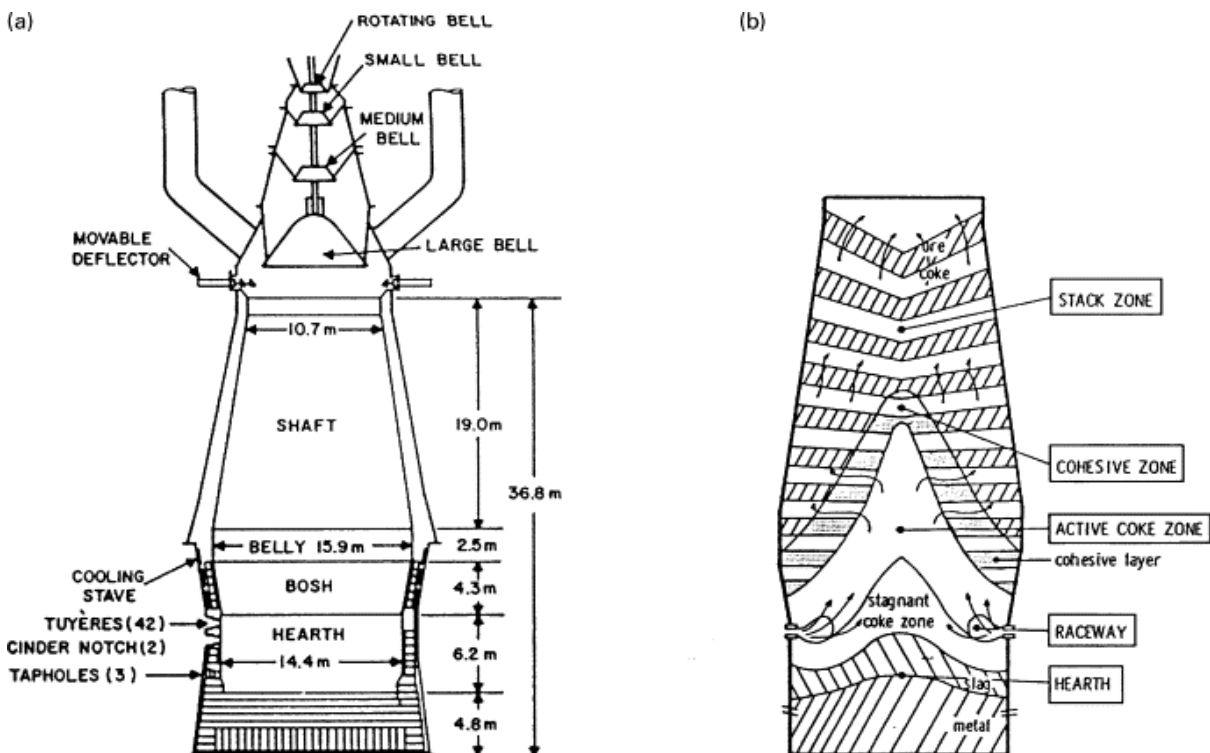
Figure 1.1: Schematic of the interior of a blast furnace. Left side (a) shows a cross-section of the empty blast furnace; right side (b) shows a cross-section of the coke and ore layers. Reprinted from [3].

In direct reduction processes, the aim is to reduce the iron oxides from the ore at a temperature below the melting point of iron, usually below 1200°C [4,5]. Solid iron oxide pellets, mostly from scrap metal, are added at the top of the direct reduction reactor. There, they are heated

and brought into contact with the reducing gas. The reducing gas is syngas, with >95% concentration of CO and H_2. Then, the reduced iron, also named "sponge iron" in the case of direct reduction, is cooled and exits from the bottom of the reactor, where it is cleaned from impurities (such as silicon gangue) [6]. The syngas is recovered and reformed to increase the concentration of CO and H_2. The sponge iron may then be used for steel production. The direct reduction process is more energy efficient than the BF process, due to the low reaction temperature [7]. The concentration of iron in the product of both blast furnaces and direct reduction reactors, around 95%. However, direct reduced iron is more susceptible to oxidisation and must quickly be processed to steel. Figure 1.2 depicts the schematic of a typical direct reduction process.
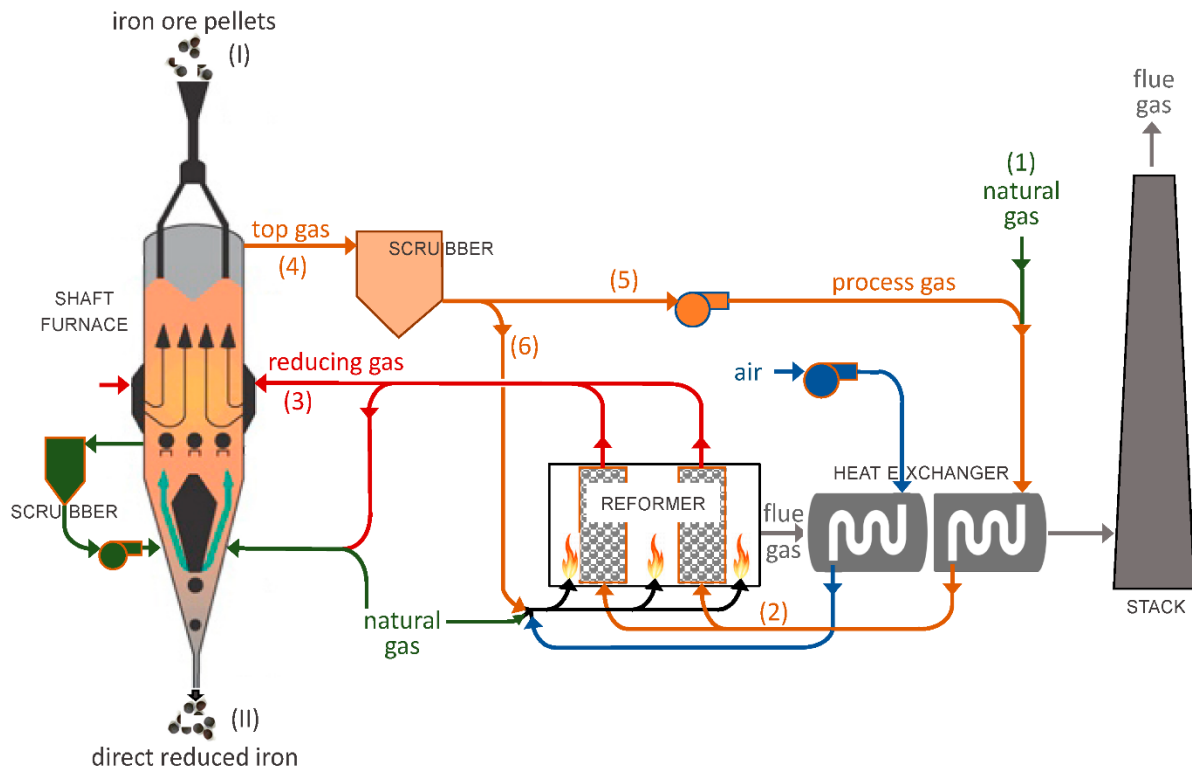
Figure 1.2: Schematic of a typical direct reduction process. Reprinted from [8].

Electric arc furnaces operate by heating and melting scrap iron in a furnace with electrodes that produce an electric arc [9]. The furnace is loaded with shreds and slabs of scrap metal, and possibly some pig iron or sponge iron. The top of the furnace has electrodes connected to a DC power source, while the bottom of the furnace is electrically connected to the neutral. The electrodes come into contact with the top layer of the scrap, and the voltage applied gradually increases. Oxygen is blown into the furnace to accelerate scrap melting. The temperature at the inside of the furnace reaches around 2000°C, and locally (at the electrode point of contact) up to 3000°C. to Eventually, the scrap melts, forming a layer of slag (containing the impurities) on the top of the molten iron bath. Electric arc furnaces offer lower energy requirements compared to blast furnaces, since the feedstock is not ore. Furthermore, they can start and stop easily. A schematic of an electric arc furnace is shown in Figure 1.3.
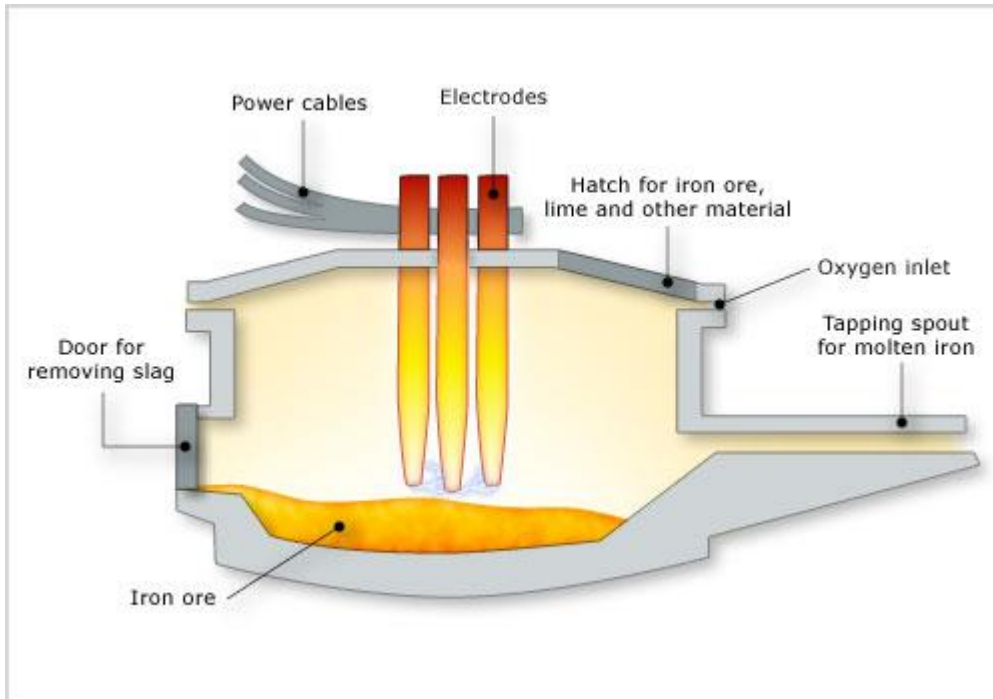
Figure 1.3: Schematic of an electric arc furnace. Reprinted from [10].

Currently, approximately 95% of primary steel (steel produced directly from iron ore) is produced in blast furnaces, which have an average of 2.3 tonnes CO_2 emitted per tonne steel produced. The rest of the primary steel is produced with the direct reduction method (DRI) in combination with electric arc furnaces (EAFs). EAFs process the majority of secondary (recycled) steel as well. The emissions from DRI with gas as the input are about 1.1 tonne CO_2 per tonne steel produced, while EAFs produce 0.4 tonnes CO_2 per tonne steel produced, which can decrease even more if the electricity source is zero-carbon. The average CO_2 emissions per tonne of steel (including recycled steel) are about 1.85 tonnes per tonne steel produced [1,11–13].
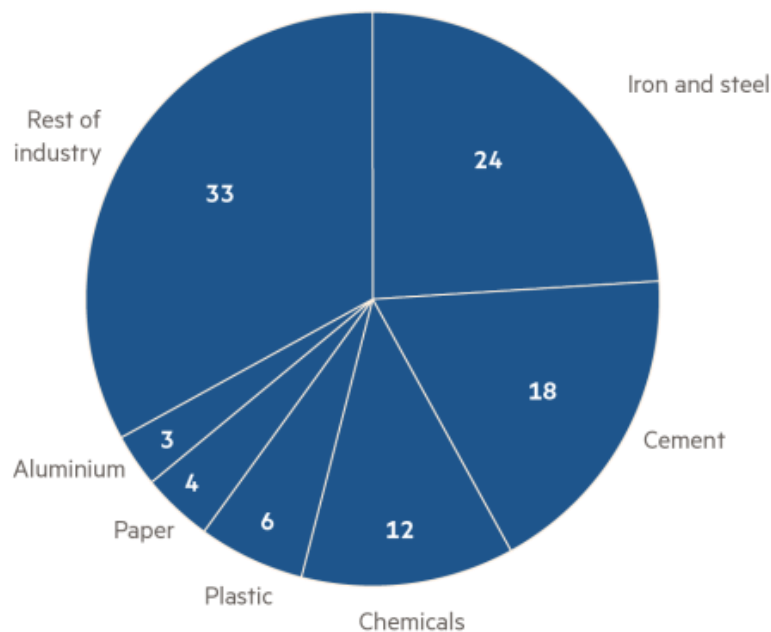
Figure 1.4: Total industry CO_2 emissions by subsectors (%). Source: Financial Times ©. Reprinted from [14].

1. Introduction

As shown in Figure 1.4, the iron and steel industry is responsible for 24% of all industry CO_2 emissions. Overall, it is responsible for 7-9% of all CO_2 emissions [13,14].

According to the World Steel Association, the steel industry has reduced CO_2 emissions per tonne by 60% since 1960 [13]. The trendline of energy used per tonne of steel produced, which was in steady decrease over the past few decades, is plateauing. As of the last few years, the energy demand to produce 1 tonne of crude steel is 20 GJ, and there is a 15-20% potential for further decrease. Energy purchases amount to 20-40% of the final product cost, meaning that there is a strong fiscal, in addition to the environmental, incentive to reduce direct energy use [11–13].

Some methods that are already being used to preserve raw materials and decrease direct energy use are [15]:

- Recycling of scrap steel either after consumer use, or even before consumer use (for example, manufacturing defects). Steel, as a material and by itself, is infinitely recyclable [13]. The amount of end-of-life steel that is being recycled currently is 83%. Reasons that this number is not 100% include high concentration of impurities such as copper, existence of steel in inaccessible constructions (such as underground ones), and corrosion. Furthermore, impurities accumulate during recycling, which necessitates downcycling. Downcycling is the use of recycled steel in applications with more lax specifications for the finished product (such as construction steel). Using scrap steel instead of iron ore that needs reducing can save up to 80% energy per unit mass of final product. However, the current global pool of steel is too small and too young for recycling to have a meaningful impact in CO_2 emissions reduction. This means that efforts that aim to reduce CO_2 emissions in the overall steel making process should aim not only at recycling end-of-life steel products, but reducing emissions in the primary steel production process as well.
- Manufacturing of higher quality, stronger steel, that aims at having a longer life cycle (thus directly preserving raw materials) and requiring less material for the same application. For example, a truck made from stronger steel would weigh less than a conventional one, requiring less emissions of fuel per km travelled. It is estimated that up to 150 Mtonnes of CO_2 equivalent could be saved if the current vehicle body structures used more Advanced High Strength steels instead of the steels being used currently.

Capturing waste gases and removing some of the raw material processing steps can reduce total CO_2 emissions by 80% in Tata Steel [14]. Since there is little potential for a further decrease of CO_2 emissions in the steel making process, while the global steel demand is steadily increasing, the industry is looking at other methods to mitigate the problem of CO_2 emissions in primary steel making. Those are [1,13]:

- Use of H_2 to reduce iron ore, producing H_2O in the process instead of CO_2. Depending on the energy source used to produce the H_2, this will either decentralize CO_2 production, or completely mitigate it if renewable sources are used.
- Use of electrolysis to reduce iron ore. Similarly to the measure mentioned above, depending on the source of electricity, this may lead to a complete elimination of CO_2 emissions during reduction, if renewable energy sources are utilized.
- Use of biomass derived charcoal rather than mined coal in order to reduce iron ore. Biomass is considered low in carbon emissions or carbon-neutral during combustion, since the CO_2 emitted during combustion is CO_2 that has been captured by the

atmosphere. Thus, the only net contribution of biofuel in CO_2 emissions is from non-renewable fuel CO_2 emissions that occur during production and transport.

- Carbon Capture and Storage (CCS). This method aims to produce a highly pure CO_2 stream downstream of the blast furnace, which can be later transported to a suitable storage site instead of being released to the atmosphere.
- Carbon Capture and Utilisation (CCU). Similar to the above method, this method aims to capture the work arising gases (WAGs) of the blast furnace. However, this method uses them as feedstocks for processes that produce fuels or other chemicals instead of storing them.

Large quantities of carbon-free hydrogen or electricity are currently not readily available, and it is not possible to use these methods with the already existing infrastructure of the steel manufacturing industry. However, the latter three methods have the following advantages: they can be used in tandem, and it is not necessary to build new blast furnaces in order to successfully implement them. Instead, the coal may be partially substituted with charcoal depending on availability, and steel plants can be retrofitted with carbon capturing equipment from which the WAGs will be captured on site and transported to facilities that can upgrade them to hydrocarbon based fuel or other chemicals [12].

The general process by which gaseous hydrocarbons are converted to liquid hydrocarbons is called Gas-to-Liquids (GTL). The umbrella term that encompasses all feedstock-to-liquids (XTL) processes is *indirect liquefaction*. The GTL process that is relevant to the scope of this project will be explored briefly in chapter 2.2.

The WAGs can be captured with the use of CCS technology. Captured WAGs can be used for the production of syngas ($CO+H_2$). Using the Fischer-Tropsch technology, which has been well established as a method to convert syngas to liquid fuel in the last century, syngas can be converted into synthetic crude oil (syncrude). The Fischer-Tropsch method is used, instead of other methods for utilisation of WAGs (such as methanol production), in order to Synthetic fuel production leads to:

- Lower direct CO and CO_2 emissions [16].
- Valorisation of the WAGs [17].
- Sulphur-lean, carbon-neutral liquid hydrocarbon production.

Tata Steel operates blast furnaces in order to melt and reduce iron ore. Blast furnace operation causes CO and CO_2 emissions (WAGs), which are harmful to the environment. Fuel produced by capturing CO and CO_2 is considered to be low in carbon emissions, since combustion of such fuel is not a net contributor of CO and CO_2 in the atmosphere, excluding fuel used during production of the fuel itself [18,19]. If renewable sources or energy are used during fuel production, processing and transportation, the fuel produced with CCU is considered carbon neutral. Sulphur-lean feedstock, such as the WAGs of Tata Steel, can be used to produce sulphur-lean liquid fuel [16,20,21]. The demand for carbon neutral and sulphur-lean liquid fuel, as well as the price thereof, is expected to increase by 2050 [22].

Tata Steel is conducting research on the use of the Fischer-Tropsch method, as well other methods of indirect liquefaction, for the production of liquid fuel from WAGs. In order to assess the feasibility of the Fischer-Tropsch indirect liquefaction process, it is necessary to have a preliminary model which is able to simulate the fractionation and refining process of syncrude. The present work is part of this study that Tata Steel is conducting.

The formation of syncrude from syngas has been modelled in a previous study done by Kumar in 2019 [17]. In that study, a kinetic model of a multi-tubular fixed bed Fischer-Tropsch reactor

with a recycle loop was created. The modelling of the process took place in ASPEN Plus. The reactor kinetics developed by Todic et al. [23] were used to model the FTS product distribution. The products had an 86.6% C_{5+} hydrocarbon selectivity and a C_{5+} hydrocarbon production of 235 kton/year.

1.2. Project objective

The present study is a continuation of the study done by Kumar [17]. The objective of this project is to model a syncrude separation/refining process in ASPEN Plus for the assessment of the feasibility of straight-run fuel production from WAGs derived syncrude, at a scale of 235 kton/year of syncrude. The feed to the process is a Co-LTFT syncrude product with water, inert gases and unreacted syngas. The process should be designed to separate the water, the unreacted syngas and the hydrocarbon stream, which will be fractionated into different end-products. A sensitivity analysis of some design parameters of the Base Case will be carried out in order to ascertain their effect on the separation quality of the streams. Alternative process configurations will be modelled as well in order to assess the separation quality and the utilities consumption compared to the Base Case. The distillation of the atmospheric residue under vacuum will also be modelled in one of the cases.

1.3. Thesis structure

Chapter 2 contains the relevant theoretical background for the GTL process, the atmospheric and vacuum distillation processes, and the typical oil fraction names and specifications. Chapter 3 reviews state of the art literature with respect to modelling of the distillation process. Chapter 4 contains the basis of design for the project. Chapter 5 contains the results and the discussion thereof for the Base Case process and the alternative processes. Chapter 7 contains a sensitivity analysis on the Base Case. Chapter 8 contains the conclusions from the findings of the project. Chapter 9 contains recommendations for future research. The Appendix contains information on the selection of the suitable property method package, volatilities of the raw feed components, details on the mass balance of the column and tables with the stream properties.

2. Theoretical background

2.1. Introduction

Creating liquid fuel from blast furnace gases shares a lot of similarities with the gas-to-liquid process, which is well documented in the literature.

Syncrude, also known as synthetic crude oil, is the product of the Fischer-Tropsch synthesis. Its composition depends on various factors, such as: FTS process feed composition (H_2/CO ratio), temperature (categorized as high when it is around 270°C, and low when it is around 220°C), and type of catalyst used (cobalt or iron). The FTS upstream of the battery limits of this project uses a cobalt catalyst low temperature FTS process (Co-LTFT) to produce syncrude, so only the Co-LTFT Fischer-Tropsch synthesis will be described in this chapter. Features of syncrude produced by these means typically are [16]:

- Low branching, which means low concentration of branched isomers of any specific carbon number alkane compared to the total amount of the same alkane.
- Relatively longer carbon chains on average in the product, which implies more heavy oils and waxes and less volatile or gaseous compounds.
- Relatively low amount of unsaturated hydrocarbons.

Thus, Co-LTFT derived syncrude is mostly made up of linear alkanes and 1-alkenes, and about half of its mass is made up of waxes [16,21].

2.2. Gas-to-liquids conversion

The process of indirect liquefaction, also referred to as XTL (feed-to-liquids), is the process by which an organic feed (e.g., natural gas, biomass, etc.) is converted to liquid fuels through a series of processes. An overview of the indirect liquefaction process is shown in Figure 2.1.

Feed	Feed-to-syngas	Syngas-to-syncrude	Syncrude-to-product	Products
Coal	Gasification	Fischer-Tropsch	Refinery processes	Fuels
Natural gas	Reforming	Syngas-to-methanol		Chemicals
Biomass	Partial oxidation	Kölbel Engelhardt		
Waste		Syngas-to-oxygenates		
Oil shale				
Oil sands				
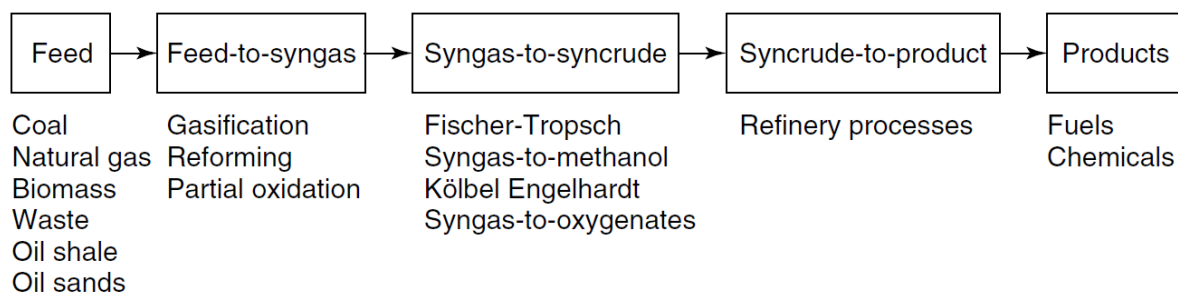
Figure 2.1: Indirect liquefaction overview. Reprinted from [16].

In the context of this project, the GTL (gas-to-liquids) process is shown as three separate processes:

- Feed-to-syngas: formation of syngas (synthesis gas), CO and H_2, from the feedstock type.
- Syngas-to-syncrude: Fischer-Tropsch synthesis (FTS) for the catalytic conversion of syngas to syncrude (synthetic crude oil).
- Syncrude-to-product: Separation and upgrading or refining of syncrude to final products.

The gasification process may differ depending on the feedstock type. Furthermore, there are other methods of conversion of syngas to liquid, such as methanol production. In the scope of this project, only the Fischer-Tropsch synthesis method will be explored.

An example overview of a GTL process with an FTS reactor and gas loop is shown in Figure 2.2.
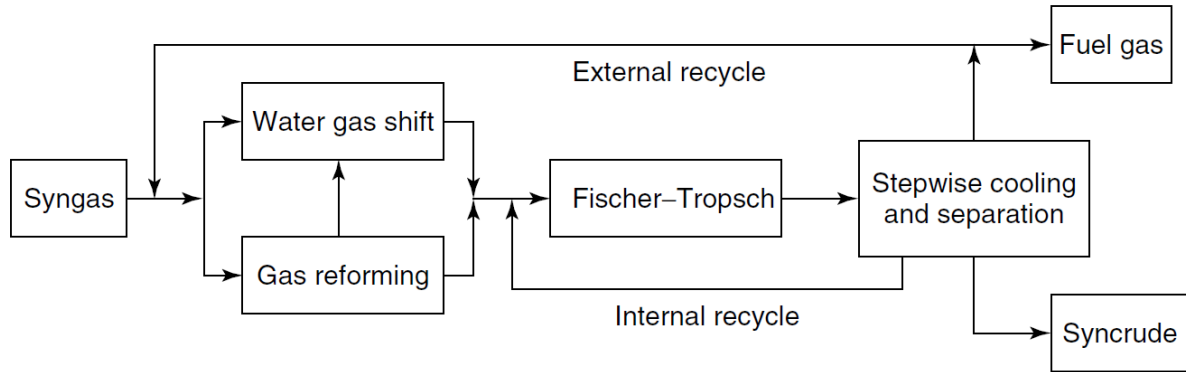
Figure 2.2: GTL process with syngas conditioning and FTS gas loop. Reprinted from [16].

The overall energy efficiency of GTL is usually around 30% (LHV basis) [16], so it should be reserved for instances where the feedstock is not useable, and conversion to liquid fuel is mandatory.

The following subsections will give a brief introduction into the overall GTL method using the FTS process, with larger emphasis in the types of process that relate to the type of syncrude used in this project.

2.2.1. Syngas production

Syngas can be produced by many different methods: partial oxidation from carbon sources such as methane, steam reforming of methane, autothermal reforming, etc. In the case of this project, there is CO, CO_2 and H_2O produced as work arising gases which are used as feedstock for syngas production. An external source of H_2 can be provided to produce more CO by means of the water gas shift reaction (WGS):

$$CO(g) + H_2O(g) \rightleftharpoons CO_2(g) + H_2(g) \qquad -40.6 \, kJ/mol \qquad (2.1)$$
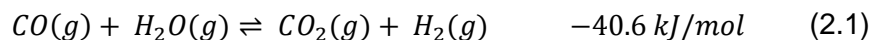
H_2 may need to be added to adjust the H_2/CO ratio in the syngas. H_2/CO is an important parameter that affects product selectivity in the FTS reaction. The process of manipulating the H_2/CO ratio is called conditioning.

Other parameters that affect syncrude composition but are unrelated to syngas production, such as FTS reactor temperature and catalyst choice, are detailed in the following subchapter.

2.2.2. FTS

The Fischer-Tropsch process was discovered by Franz Fischer and Hans Tropsch in Germany in 1925 [16,21]. It consists of a series of reactions by which syngas is converted to liquid hydrocarbons. The product of the FTS is called syncrude. Syncrude composition depends primarily on the temperature and the type of the catalyst used in the reactor. Other parameters that affect the reaction products are reaction temperature, H_2/CO ratio and type of reactor. The process is called low temperature Fischer-Tropsch (LTFT) if the reactor temperature is

between 200-240°C, whereas in high temperature Fischer-Tropsch (HTFT) processes, the reactor temperature is in the 330-350°C range. The catalyst type is usually iron-based in the HTFT process (Fe-HTFT), and it can be either iron- or cobalt-based in the LTFT processes (Fe-LTFT or Co-LTFT, respectively).

An overview of the effect of these parameters on syncrude composition is shown in Table 2.1.

Table 2.1: Influence of FTS operating parameters on product selectivity. Reprinted from [16].

Selectivity parameter	Operating parameter being increased			
	Temperature	Pressure	Space velocity	H_2:CO ratio
Carbon number distribution	Lower α-value	Higher α-value	No change[a]	Lower α-value
Methane selectivity	Increases	Decreases	Decreases	Increases
Alkene selectivity	$-$[b]	$-$[b]	Increases	Decreases
Oxygenate selectivity	$-$[b]	Increases	Increases	Decreases
Aromatic selectivity	Increases	$-$[b]	Decreases	Decreases
Syngas conversion	Increases	Increases	Decreases	$-$[b]

[a]Some change is possible if secondary reactions like re-incorporation, hydrogenation, or cracking are significant.
[b]The direction of change depends on a more complex relationship.

In all cases, syncrude composition generally follows the Anderson-Schultz-Flory (ASF) carbon number distribution, or an approximation of it [16]. The ASF model uses the following equation:

$$x_n = (1 - \alpha) \cdot \alpha^{n-1} \tag{2.2}$$

where:

n is the number of carbon atoms,

x_n is the molar fraction of a carbon chain C_n with n carbon atoms,

α is a constant that depends on the catalyst type and temperature of the FTS. In the following paragraphs, it is referred to as α-value.

The prediction of carbon chain length distribution is accurate for most of the hydrocarbons. The largest discrepancies are in the C_1-C_2 range, primarily due to the high selectivity of the FTS for methane, as well as due to the ethene to methane reaction. Furthermore, there are some secondary reactions taking place in the n<12 carbon number range in LTFT reactors, affecting selectivity in a way that is not adequately predicted by having a single α-value for all values of n. Product distribution is more accurately described by a relatively lower α-value (larger x_n) for n≤8, and a higher α-value for n≥12, with a crossover region for 8<n<12 [16]. An example of an ASF distribution of LTFT-derived syncrude is shown in Figure 2.3.
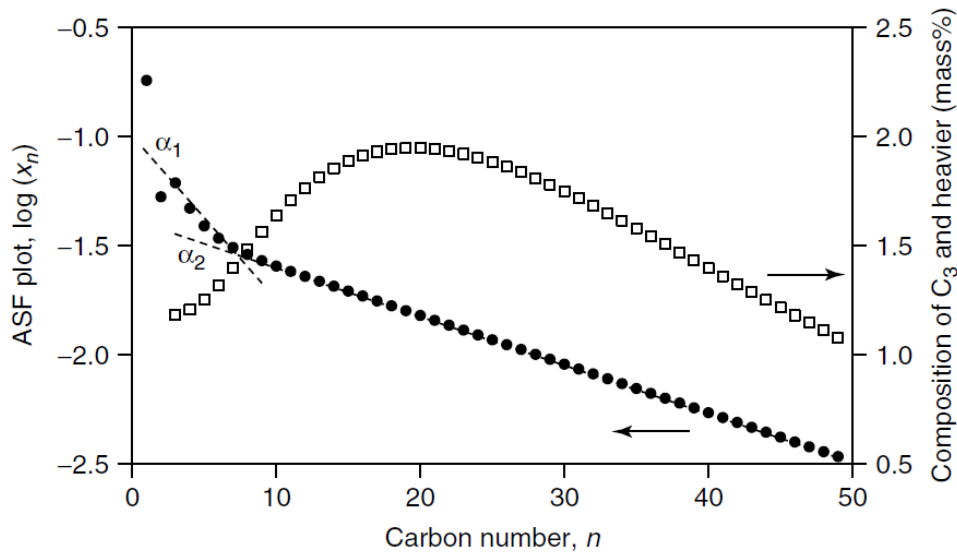
Figure 2.3: ASF semilogarithmic plot of the molar fraction (x_n, left axis, black) of all the components with total carbon number n and the corresponding mass fraction (right axis, white) versus carbon number (n) of an LTFT-derived syncrude. Reprinted from [16].

The syncrude that is used as raw feed in the process modelled in this project is created via a Co-LTFT process. The Co-LTFT-derived syncrude composition approximately follows an ASF distribution with an α-value of around 0.85 to 0.95. More specifically, the expected syncrude composition is:

- Mostly linear alkanes, some alkenes (mostly linear 1-alkenes) in the smaller C_n range.
- About 50% of the total mass is at the C_{23+} range (waxes), almost exclusively linear alkanes.
- Very small amounts of aromatics and oxygenates.
- Almost no nitrogen- or sulphur-containing compounds.

More details on the typical Co-LTFT syncrude composition is shown in Table 2.2 and Table A.1 of the Appendix.

Table 2.2: Typical syncrude compositions of syncrude derived from different FTS types. Reprinted from [16].

Product fraction	Carbon range	Compound class	Syncrude composition[a] (mass%)		
			Fe-HTFT	Fe-LTFT	Co-LTFT
Tail gas	C_1	Alkane	12.7	4.3	5.6
	C_2	Alkene	5.6	1.0	0.1
		Alkane	4.5	1.0	1.0
LPG	C_3-C_4	Alkene	21.2	6.0	3.4
		Alkane	3.0	1.8	1.8
Naphtha	C_5-C_{10}	Alkene	25.8	7.7	7.8
		Alkane	4.3	3.3	12.0
		Aromatic	1.7	0	0
		Oxygenate	1.6	1.3	0.2
Distillate	$C_{11}-C_{22}$	Alkene	4.8	5.7	1.1
		Alkane	0.9	13.5	20.8
		Aromatic	0.8	0	0
		Oxygenate	0.5	0.3	0
Residue/wax	$C_{22}+$	Alkene	1.6	0.7	0
		Alkane	0.4	49.2	44.6
		Aromatic	0.7	0	0
		Oxygenate	0.2	0	0
Aqueous product	C_1-C_5	Alcohol	4.5	3.9	1.4
		Carbonyl	3.9	0	0
		Carboxylic acid	1.3	0.3	0.2

[a]The syncrude composition is expressed as the total mass of product from Fischer−Tropsch synthesis, excluding inert gases (N_2 and Ar) and water gas shift products (H_2O, CO, CO_2, and H_2). Zero indicates low concentration and not necessarily a total absence of such compounds.

2.2.3. Prefractionation

The output of the FTS reactor, in addition to syncrude, contains unconverted syngas, CO_2, H_2O and inert gases. At the temperature and pressure conditions of the reaction, the product has a vapor and a liquid phase, with the latter being composed mostly of waxes. The FTR output is cooled down to ambient temperature, in order to condense the heavier volatiles of the syncrude and the water that are present in the gas phase. The cooled stream enters a 3-phase separator, where a gas phase and two liquid phases, an organic phase and an aqueous phase, are separated. The liquid stream containing the organic phase is called the hot condensate, since it condenses at a higher temperature. The hot condensate contains most of the syncrude. The aqueous phase is called reaction water. It is mostly made up of water, potentially with some dissolved light alcohols, carboxylic acids and other oxygenates (collectively <2% on a mass basis [16]), and it is processed in a water treatment facility before being discarded. The gas phase is subcooled to temperatures below 0°C, so that the rest of the hydrocarbons condense. The cooled stream then enters a flash drum to separate the liquid from the gas phase. The liquid stream containing the rest of the syncrude is called cold condensate and is fed into the downstream processing units. The remaining gas stream is called tail gas and contains the inert gases, unreacted syngas, and may contain C_1-C_2 hydrocarbons if the subcooling temperature was above -100°C. The cold and hot condensate

streams are then processed in the downstream units [16,21,24,25]. An overview of the prefractionation of LTFT syncrude is shown in Figure 2.4.
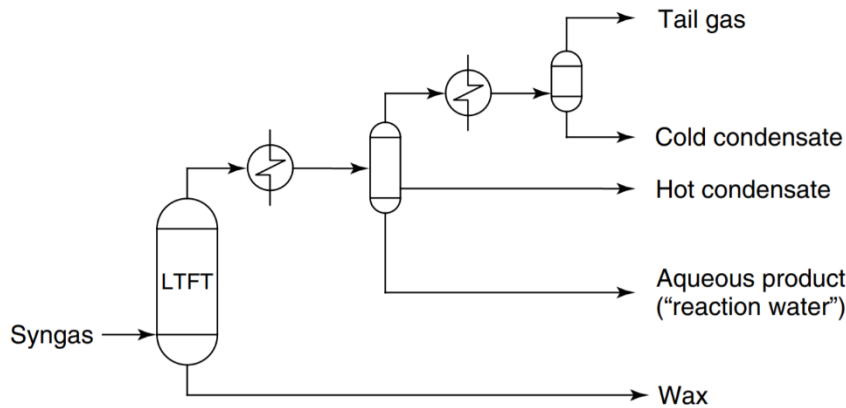
Figure 2.4: Overview of LTFT syncrude prefractionation. Adapted from [16].

2.3. Atmospheric distillation

Distillation is a separation operation used in many industrial processes, including the refining/upgrading part of the oil industry. The goal of the distillation process is to separate the different components of the feed mixture into products depending on the relative volatilities of the components. In the case of syncrude, there are usually certain recovery and composition or purity constraints for the components in each product. Products of petroleum distillation are called cuts [1].

2.3.1. Operating principles

Distillation commonly takes place after removal of the unwanted gases (e.g., N_2, CO, CO_2) and water from the FTR output, leaving only the hydrocarbons as feed to the column. The main products of the (synthetic) crude distillation process, also referred to as "cuts" in industrial practice, are naphtha, kerosene, atmospheric gas oil, vacuum gas oil and residue. Distillation products that have not undergone any upgrading or refining process are also referred to as "straight-run products", e.g., "straight-run kerosene" [21,24–26].

The process of separating the more volatile components of the distillation column feed from the less volatile works by creating a temperature gradient along the height of the distillation column. The temperature gradient along the column height creates a different vapor-liquid phase equilibria (VLE) on each stage, with higher heavy components concentration in the lower stages and higher light components concentration in the higher stages. This works because the temperature gradient causes each stage of the column to have a different vapor-liquid equilibrium, with heavier compounds to be present in the liquid phase and lighter compounds to be present in the vapor phase of each stage.

Liquid flows down to the higher temperature stages, where the equilibrium shifts, making the liquid phase have higher concentration of heavier components by vaporizing some lighter components. The opposite happens with the vapor: it flows up to the stage above where the temperature is lower, condensing some of the heavier elements and leaving lighter elements in the vapor phase. Eventually, this will increase the presence of the lightest components in the liquid phase of the lowest temperature stages, and the heaviest components in the highest temperature stages. Liquid is then drawn off, and the distillate (top) and residue (bottom) streams have different composition according to the design specifications.

The temperature gradient is maintained by a condenser at the top of the column, while heat is provided at the bottom by preheating the feed and either a kettle reboiler, or injection of high-pressure stripping steam. Steam can be used in the main column and the strippers to reduce the partial pressure of the hydrocarbons, making them vaporize at lower temperatures. The feed is initially heated in heat exchangers that draw heat from the pumparounds or the hot streams that exit either of the distillation units. Typically, it is heated up to 200-250°C. The feed then enters the fired heater and is heated up to 330-370°C [16,21,24,25,27].

The feed enters the column partially vaporized. The feed stage is also called the flash zone sometimes when it refers to the section of the column at which the feed vaporizes. The part of the column below the flash zone is called the stripping section, while the one above the flash zone is called the rectifying section. The heavier components in the feed tend to stay in the liquid phase, which flows downwards, and the lighter components tend to vaporize and flow upwards. The distillation column contains internals that facilitate contact and mass transfer between the liquid and vapor phases. Those internals may be trays, structured packing or random packing.

Trays work by allowing vapor to bubble through the liquid that is retained by a weir (dam) on the side of the tray. Trays are the most common type of internals in atmospheric distillation units of crude oil [24,25].

Packing works by providing a 3D lattice network which increases surface area for mass exchange between the liquid and vapor phases. Compared to trays, they offer a lower pressure drop, approximately one fourth the pressure drop per stage. For this reason, they are most commonly used in vacuum distillation units [24,25].

In crude oil distillation, there is no reboiler for the main column. Heat is provided in the column by the feed preheating furnace and the stripping steam. Typical stripping steam conditions are provided in Chapter 3. The reason is that in order to provide adequate separation of the gas oil fraction from the atmospheric residue, the necessary temperature at the reboiler stage is in the order of 450°C. At that temperature, the syncrude is at risk of thermal cracking or coke deposits.

Thermal cracking is undesirable for multiple reasons [16,20,21]:

- It is a carbon rejection process. This means that the overall amount of fuel that can be produced given a certain amount of feed decreases.
- There is no cracking selectivity, which means that there will be a substantial amount of C_4 and lighter compounds produced, the production of which happens at the expense of naphtha, kerosene or gas oil.

Coking is also undesirable, as it lowers the plate efficiency and increases maintenance cost and downtime.

Therefore, the temperature is limited at 400°C or lower in the entire column [16,21]. In order to achieve that, heat is provided in the column by stripping steam and the feed. Stripping steam achieves the same separation quality as a reboiler at a lower temperature. Steam decreases the partial pressure of the components, making them vaporize in order to reach the equilibrium partial pressure. This causes higher vaporisation rates at the same temperature.

2.3.2. Troubleshooting

Under normal operating conditions, the vapor and liquid phase exchange mass and energy while flowing in countercurrent mode. This operating mode can be adequately represented by

the double film theory. According to that theory, the liquid and vapor phases are both continuous, and separated by an interface. Boundary layers are formed for both phases at the interface, where heat and mass transfer take place (by conduction and diffusion, respectively). The values of the heat and mass transfer coefficients depend on the properties of the phases and the hydrodynamic conditions (which affect boundary layer thickness). As long as the two phases are in thermodynamic equilibrium (there is no heat or mass accumulation or consumption, the operation is steady state), then the transfer flows must be equal. At those conditions, which span over a large operating domain, the diffusion coefficients and the boundary layer thickness at the vapor-liquid interface are constant and the column operates at a high efficiency. A large deviation from the operating point where the coefficients are constant causes a lot of problems in the fluid mechanics of the column internals. The main problems that may appear can be summed up in the following categories [28]:

- Dumping: Caused by too low liquid flow rate, causing the column to be filled up with vapor.
- Weeping: Caused by too low vapor flow rate. The effect this has on the distillation process is that liquid "weeps" down from the sieve or bubble caps, with little mass exchange taking place between the two phases, and tray efficiency dropping as a result of that.
- Entrainment: Caused by high vapour flow rate. The effect this has is that liquid is entrained at the form of droplets above its tray. At the extreme case, the liquid on a specific stage may reach the stage above it. Separation quality decreases due to the mixing of the liquids of different stages.
- Flooding: Caused by high liquid flow rate. The effect this has is that the weir floods over and a part of the liquid goes to the lower stage through the downcomer without exchanging mass with the vapour. At the extreme case, the column completely fills up with liquid.

A qualitative chart of the stable operating region and the problematic operating regions is shown in Figure 2.3.
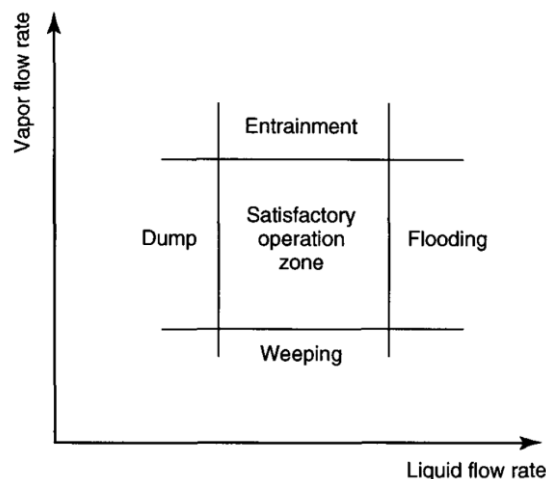

Figure 2.5: Column stable operating domain. Reprinted from [28].

2.3.3. Sizing

Typical atmospheric crude units can be 2 to 14 m in diameter [29]. A unit of about 8 to 9 m in diameter can be expected to have around 50 m height, 40 to 60 bubble cap trays, and an output in the order of 40.000 m^3/day [29]. The numbers vary depending on the volume flow of

the feed, the type of crude and the separation quality requirements. The lighter distillates (naphtha) are drawn at the top, and progressively heavier distillates are drawn at progressively lower stages as side draws. Steam strippers are often used to strip side draws from lighter gases and enhance key component separation. Components of the feed that do not vaporize at the temperature and pressure conditions in the column are drawn as atmospheric residue from the bottom.

Reflux is the downward flow of condensed liquid from the condenser in the column. Fractionation quality improves by increasing the reflux rate. The same effect can be achieved with the pumparounds, but the terms *reflux rate* and *reflux ratio* are reserved for liquid flow due to the condenser. Increasing the reflux rate improves fractionation quality by increasing liquid and vapor residence time, facilitating better mass transfer between phases. The ratio of liquid drawn at the top of the column to liquid returned to the top stage is called reflux ratio and it is one of the most important operating parameters of the column [24,28].

The reflux ratio R is defined as

$$R = \frac{L}{D} \qquad (2.3)$$

where

D is the distillate (top product) flow rate, and

L is the reflux.

Increasing the reflux ratio increases the energy consumption of the column, but also improves the separation quality for a given number of stages. Therefore, increasing reflux ratio with the same separation quality goal decreases the necessary number of stages. Theoretically, the minimum number of stages for a given separation quality goal can be achieved with infinite reflux ratio, which is mathematically described as:

$$\frac{F}{L} = \frac{D}{L} = \frac{B}{L} = 0$$

where

F is the column feed flow rate, and

B is the bottom product flow rate.

Conversely, decreasing R with the same separation quality goal, increases the necessary number of stages. Theoretically, at $R=0$, an infinite number of stages is necessary. A more thorough explanation will be given at subsection 2.3.4.

A pumparound works by drawing liquid from the side of the column and pumping it into a higher stage after cooling it. Stage and duty can be decided by optimisation algorithms, or reference to similar refineries in commercial experience. Usually, the draw-off stage is 1-3 stages below the pumb-back stage, as shown in Chapter 3. Pumparounds increase manufacturing complexity compared to having just a condenser with the collective duty of the pumparounds and condenser of the unit, but the heat drawn from the column can be more readily recovered as it is at a higher temperature than in the condenser. The goal of the pumparound is to increase the reflux rate internally in the column, and a higher reflux increases separation quality. Shifting a fraction of the condenser duty to a specific column section facilitates separation between the components that reside in those equilibrium stages

compared to adding that same duty in the condenser. Pumparounds typically have a flow rate in approximately the same order as the feed flow rate.

2.3.4. Initial estimates

The equations that govern the distillation process have multiple variables and degrees of freedom. Before beginning to use an equation solver or simulation software, the designer must first set the values of the independent variables. For a distillation column with no reboiler, the independent variables are the number of stages, the feed stage, the distillate rate and the reflux ratio. In the case of a partial condenser, either the vapor/liquid distillate ratio, the vapor flow rate, or the distillate flow rate, is also required.

There are multiple methods of finding an initial estimate for the number of stages and feed stage. The most well-known method is the McCabe-Thiele method. It only works for a binary mixture, that is, the feed must contain only two components. The components are labelled with the subscript LK (for light key) and HK (for heavy key), with the light key being the more volatile of the two.

Despite not successfully implementing the McCabe-Thiele method in this project, the basic principles behind it are discussed because they are helpful in illustrating the basic concepts of the distillation process and how changing different parameters affects others.

The McCabe-Thiele method assumes that the mole specific latent heat of the two components are equal. Furthermore, it assumes that relative volatility is constant with temperature. Another assumption that is made is perfect mixing in each stage (uniform concentration of any component and uniform stage temperature) [30]. This means that for every mole of liquid that converts to gas, one mole of gas is converted to liquid [24,28]. The McCabe-Thiele method is applicable even in non-ideal systems, such as azeotropes (e.g. ethanol-water or isopropanol-water distillation) [30].

The first step is to create a 2D graph where the horizontal axis represents the molar fraction of the light key in the liquid phase, while the vertical axis represents the molar fraction of the light key in the vapor phase. The interval of both axes is from 0 to 1. The next step is drawing the vapor-liquid equilibrium (VLE) curve. For a two-component mixture, this can be done by using the formula:

$$y = \frac{ax}{1 + x(a - 1)}$$

in which a is the relative volatility, calculated as:

$$a = \frac{K_{LK}}{K_{HK}}$$

in combination with the expressions for volatility,

$$K_i = \frac{y_i}{x_i}$$

where x_i is the vapor the vapor–liquid equilibrium concentration of component i in the liquid phase and y_i is the vapor the vapor–liquid equilibrium concentration of component i in the vapor phase. The molar balance of a binary mixture is expressed as:

$$y_{HK} + y_{LK} = 1$$

$$x_{HK} + x_{LK} = 1$$

16

The next step is to draw the operating line of the rectifying section and feed line. The rectifying line passes from the point x_D, y_D, with x_D the target molar fraction of the light key in the distillate and $x_D = y_D$, and it has a slope equal to $L/(D+L)$, where L is the reflux molar flow rate and D is the distillate flow rate.

The feed line passes from the point x_F, y_F, with x_F being the molar fraction of the light key in the feed and $x_F = y_F$, and it has a slope of $q/(q-1)$, where q is the liquid fraction of the feed, also known as feed quality. Feed quality is mathematically defined in this subchapter, with equation (2.7). In theory, q may take values below 0, indicating that the feed is superheated vapor, or values above 1, indicating that the feed is subcooled liquid. However, in crude distillation applications, its value is between 0 and 1, typically in the range of 0.4 to 0.6 [28].

The intersection of the feed and rectifying line and the point x_B, y_B, with x_B being the target molar fraction of the light key in the bottom product and $x_B = y_B$, are the two points that create the operating line of the stripping section.

The final step is drawing the theoretical equilibrium stages. The first equilibrium stage is represented by a horizontal line, starting from the (x_D, y_D) point and ending at the intersection with the VLE curve. The next equilibrium stage is found by drawing a horizontal line which starts at the vertical projection of the previous point on the rectifying line and ends at the intersection with the VLE curve.

This process continues until an equilibrium stage passes the intersection of the rectifying and stripping line. From that point on, the process continues as before, with the only difference being that the subsequent equilibrium stages start on the stripping line, instead of the rectifying line. The process ends when an equilibrium stage intersects the VLE curve at a point x_{final} such that $x_{final} \leq x_B$. The total number of stages drawn is the minimum number of stages that would be necessary to achieve the desired separation at the given reflux ratio. The feed stage is the stage that passes over the feed line and rectifying line intersection, starting from the top of the column. An example application of the McCabe-Thiele method for estimating the total number of stages and feed stage is shown in Figure 2.4.
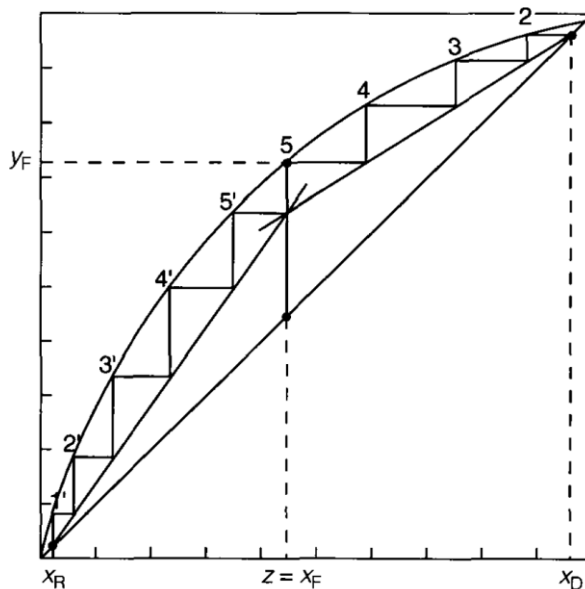

Figure 2.6: Application of the McCabe-Thiele method. Reprinted from [28].

Due to the multicomponent feed, and the oversimplifying assumptions, the McCabe-Thiele method fails to give a feasible solution to the problem posed by this project when modelling

the feed into a binary stream of two pseudocomponents. It is nevertheless a useful qualitative tool for showing how varying the vapor fraction of the feed (parameter q) and the reflux ratio (effectively parameter L, since D is a given and the reflux ratio is defined as L/D) affects the number of stages necessary for a certain separation quality in the column.

The minimum number of stages, N_{min}, can be achieved as the reflux ratio tends to infinity. A very large L/D ratio causes the stripping line to intersect the feed line closer to the x=y line, allowing for longer equilibrium stage lines. This operation mode is called *total reflux.*

If the minimum reflux ratio, R_{min}, is used in a column, it is seen that the intersection of the stripping and rectifying operating lines tends to intersect the VLE curve. This forces progressively smaller and smaller equilibrium stage lines, and the number of theoretical stages required reaches infinity. This operation mode is called *minimum reflux* in literature. Those principles hold true even for multicomponent distillation in complex columns with multiple feeds and multiple side products. Two example applications of the McCabe-Thiele method with minimum and total reflux is shown in Figure 2.6.
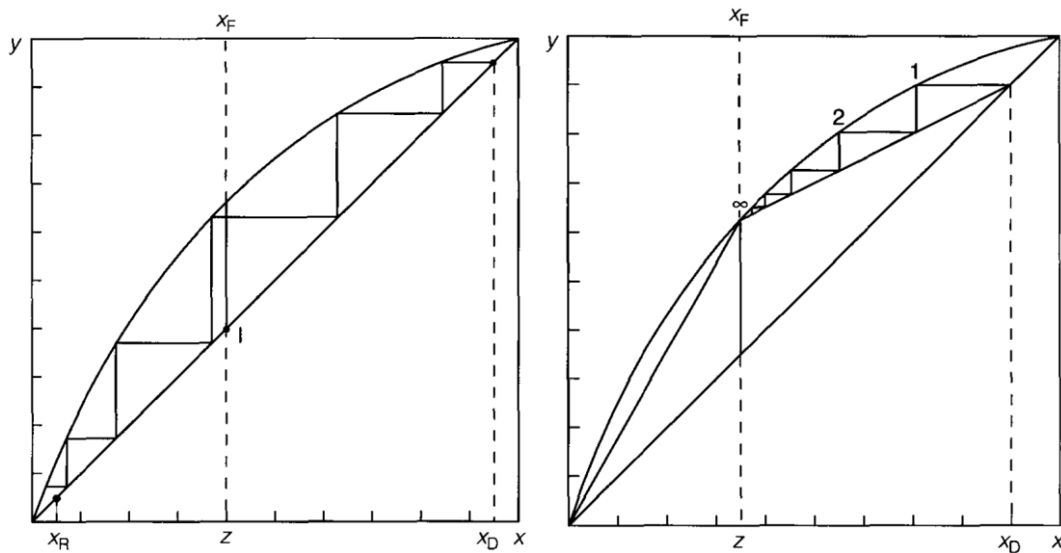
Figure 2.7: Application of the McCabe-Thiele method at total (left) and minimum (right) reflux. Reprinted from [28].

In order to find a more accurate estimate for the number of stages and reflux ratio, the Fenske-Underwood-Gilliland (FUG) method is used. The FUG method is used as follows: The Fenske equation is used to calculate the minimum reflux ratio, then the Underwood equation is used to calculate the minimum number of stages and then the Gilliland correlation is used to estimate the theoretical number of stages [24,25,28,31–34]. The Fenske and Underwood equations, and equations that represent the Gilliland correlation are explained in the following paragraphs.

The Fenske equation entails selecting two components among the feed components to represent the distillate and bottom products, setting separation requirements, and using those to estimate the minimum number of stages necessary. The selected components may be either real components of the feed, usually adjacent in volatility (K-value), although this is not a restriction, or they may be pseudocomponents that are chosen as having K-values representative of the aggregate the composition and volatility of the distillate and bottom products. Those are called the light key and heavy key, the light key being the one with the higher volatility.

The Fenske equation is:

2. Theoretical background

$$N_{min} = \frac{\log\left(\left(\frac{x_{LK}}{x_{HK}}\right)_D \left(\frac{x_{HK}}{x_{LK}}\right)_B\right)}{\log(a_{LK})} \tag{2.4}$$

Where a_{LK} is the relative volatility of the light key with respect to the heavy key,

$$a_{LK} = \frac{K_{LK}}{K_{HK}}$$

and x the molar fraction of the light or heavy key in the distillate or bottom product.

is the relative volatility of the light key component with respect to the heavy key. It is noted that volatilities and thus relative volatilities are functions of temperature; thus, the Fenske equation assumes that relative volatility is constant along the column height. Then, N_{min} is the minimum number of stages, including the condenser and reboiler stages if applicable. In this problem there is no reboiler so only the condenser is included. Another assumption of the Fenske method is that it assumes a large enough number of stages (i.e., infinite), in order to achieve the required separation at minimum reflux.

The Underwood equation is used to determine the minimum required reflux ratio, given the feed conditions and the purity requirements of the distillate. The distillate requirements and feed composition have already been set by the basis of design, so the only remaining independent variable is the feed temperature which is set at a value that is in accordance with data from literature and commercial experience.

The Underwood equation is:

$$\sum_{i=1}^{N_{comp}} \frac{a_i x_{Di}}{a_i - \theta} = R_{min} + 1 \tag{2.5}$$

where:

N_{comp} is the total number of components,

a_i is the relative volatility of component i with respect to the heavy key element that was selected for the Fenske equation:

$$a_i = \frac{K_i}{K_{HK}}$$

x_{Di} is the molar fraction of component i in the liquid phase of the distillate,

R_{min} the minimum reflux ratio,

and θ is the root of the equation:

$$\sum_{i=1}^{N_{comp}} \frac{a_i Z_{Fi}}{a_i - \theta} = 1 - q \tag{2.6}$$

where:

Z_{Fi} is the molar fraction of component i in the feed

q is the feed quality, defined as:

$$q = \frac{H_G - H_F}{H_G - H_L} \tag{2.7}$$

Where H_G, H_F and H_L are the molar enthalpies of the vapor phase of the feed, the sum of the feed, and the liquid phase of the feed, respectively.

The equation used to calculate θ has N_{comp}-1 roots, each of them between two consecutive a_i values. The solution has to be found iteratively by the goal seek method, and θ must be bound by:

$$a_{LK} > \theta > a_{HK}$$

in order for the solution to have meaning. This means that the initial guess for θ, θ_0, must be

$$a_{LK} > \theta_0 > a_{HK}$$

otherwise, the iterative goal seek process of finding the θ value that solves equation (2.6) will converge at a wrong value for R_{min}.

After determining θ, the value of R_{min} can be calculated by using equation (2.5).

The final step in this method is using the Gilliland correlation for determining the actual stage number and reflux ratio. The Gilliland correlation is a curve, based on experimental data, that estimates the actual number of stages N and the actual reflux ratio R based on the minimum reflux ratio R_{min} and the minimum number of stages N_{min}.

The Gilliland correlation curve is seen in Figure 2.8., where:

$$x = \frac{R - R_{min}}{R + 1}$$

and

$$y = \frac{N - N_{min}}{N + 1}$$
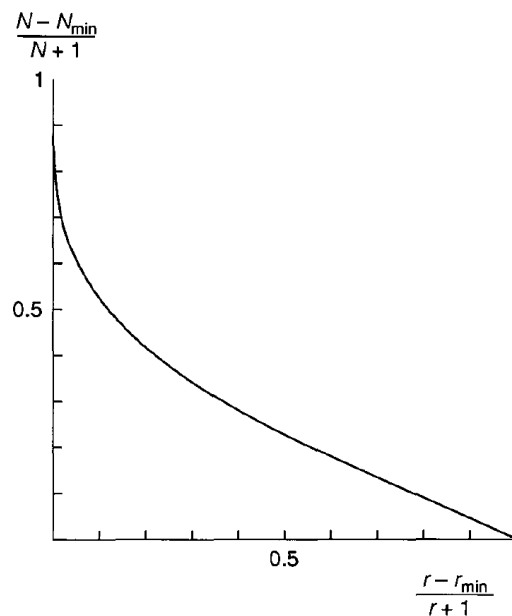
Figure 2.8: The Gilliland correlation. Reprinted from [28].

Two equations that best fit the Gilliland correlation curve are the Molokanov equation and the Edjulee equation [28]. The Molokanov equation, which better fits the Gilliland correlation curve, is given by:

$$y = 1 - \exp\left(\left(\frac{1 - 54.4x}{11 + 117.2x}\right) * \left(\frac{x - 1}{\sqrt{x}}\right)\right)$$

(2.8)

While the simpler Edjulee equation is given by:

$$y = 0.75 * (1 - x^{0.5668})$$

Since in either case there are two unknowns (R and N) and one equation, one of the variables must be fixed. In literature the method most commonly used is fixing R by multiplying R_{min} with a factor between 1.1 and 1.5. A good approximation is to use:

$$R = 1.2R_{min}$$

(2.9)

at which point calculating the number of stages becomes easy by applying the Molokanov equation (2.8) [28].

The feed stage location can be estimated using Kirkbride's equation [35]:

$$\frac{m}{p} = \left(\left(\frac{B}{D}\right)\left(\frac{z_{HK}}{z_{LK}}\right)_F\left(\frac{x_{LK,B}}{x_{HK,D}}\right)^2\right)^{0.206}$$

(2.10)

where m and p are the stages above (and including) and below the feed stage. It therefore holds that:

$$N = m + p$$

which means that an initial estimate for the number of stages between the condenser and the feed stage can be calculated by:

$$m = N\left(\frac{m/p}{m/p + 1}\right)$$

2.3.5. Distillation process configuration

This subchapter contains general design guidelines that can be made about the majority of commercial crude distillation columns. The design of any new column, including for this project, is not bound by these guidelines. However they are good estimations for validation of the initial steps in the design process, as well as for the final results [16,21,24,25,28].

- The overall refinery process starts with a heat exchanger network wherein the hot product streams from the distillation unit are used to preheat the cold feed. The feed is then heated in the fired heater up to a temperature of 330-370°C.
- Upon entering the column, approximately 50-60% of the crude mass should flash (vaporize). This does not necessarily mean that the other 40-50% has to become atmospheric residue, but rather that the mass vapor ratio in the feed has to be approximately 50-60%.
- The number of stages has to be approximately 35-60 in the entire column, with approximately 4-6 stages in the stripping section and approximately 8-11 stages

separating between any two-consecutive draw-off trays. Side strippers can be anywhere between 4 and 10 stages.

- The pressure drop per stage can be expected to be approximately 0.01 atm, and the pressure drop between the flash zone and the overhead condenser usually does not exceed 0.35 atm.
- Typical crudes are distilled into 3 products (naphtha, kerosene, atmospheric gas oil) plus an atmospheric residue product. The residue may be distilled under vacuum in order to produce vacuum diesel, light vacuum gas oil, heavy vacuum gas oil and vacuum residue. In the case of the ADU, the products are drawn off from side strippers.
- Pumparounds are used to ensure adequate liquid flow in all stages and higher reflux, which leads to better separation quality.
- Crude composition may vary during the operation lifetime of a distillation unit, and product specifications may change. Therefore, the design needs to support flexibility of the operating parameters in order to facilitate those potential variations.

2.4. Vacuum distillation

Atmospheric residue is processed in a vacuum distillation unit (VDU). VDUs, being distillation columns, have the same basic operating principles as ADUs. Thus, this section will only focus on the similarities and differences VDUs present when compared to ADUs.

The similarities with atmospheric distillation are [16,21,24,25,28,29]:

- A temperature gradient is applied over the column height in order to achieve a different VLE on each stage, leading to higher heavier components concentration in the lower stages and higher lighter components concentration closer to the top of the column.
- Heat to the feed is provided by the feed preheating furnace, where the outlet temperature is higher than the ADU's furnace, in the order of 400-425°C. The furnace aims at vaporising 40-80% of the feed on a mass basis. The risk of coking is lower in this type of column due to the lower residence times compared to ADUs, so the temperature may be higher.
- Stripping steam is still used to provide additional heat and reduce hydrocarbon partial pressure, facilitating better separation. Reboilers are not used. A condenser as well as pumparounds are still used to generate reflux.
- Side strippers can be used if high purity is required in one of the products, e.g., in the production of lubricants.

The differences with atmospheric distillation are [16,21,24,25,28,29]:

- The main difference is that VDUs operate at a much lower pressure, usually ranging between 0.01-0.05 bara compared to 0.5-2 bar for ADUs.
- The vacuum at the top is maintained with the use of 3-stage steam ejectors.
- The column internal type is packing in this type of unit, since the pressure drop is about 25% that of a corresponding unit with trays. Low pressure drop is necessary to maintain low pressure along the entire height of the VDU.
- The condenser is not necessary if the overhead distillate flow rate is very low compared to the feed rate. In this case, reflux is generated only by the pumparounds, with the topmost pumparound returning liquid to the top stage.
- Side strippers are usually not necessary, since in most cases the light and heavy vacuum gas oils are both used as feedstock in other units downstream, such as fluid

catalytic crackers (FCC) or hydrocrackers, the goal of which is to convert the waxy paraffins in VGOs into lighter components.

Due to the very high flash zone temperature and the high feed vaporisation rate, the components in the wash zone (below the flash zone) are susceptible to coking. In order to prevent drying of the bottom stages, especially in the cases where the vacuum residue flow rate is very low compared to feed rate, there is a stream (overflash) going from directly below the flash zone to the wash zone. The overflash ensures adequate liquid flow in the wash zone.

2.5. Oil fractions

Characterisation of a given crude oil or a cut necessitates the use of an "assay", which in petroleum engineering is a compilation of data about the crude that defines the crude. The most important piece of data, always included in any assay, is a distillation curve. One type of distillation curve is the True Boiling Point (TBP) curve. Cuts from petroleum distillation are typically defined by their ASTM (American Society for Testing and Materials) boiling ranges. Either end of the boiling range is called a cut point. Cut points is the name used to collectively refer to the temperature at which a specific amount of the crude has evaporated and are determined by the true boiling point (TBP) curve of the crude. A TBP curve is a plot of the percentage of the crude (or crude cut) volume that is boiled off at a given temperature. It can be experimentally verified in distillation columns with a very large number of stages and a very large reflux ratio (batch distillation method). The distillate at any given temperature is a plot point, and the temperature increases until the crude is completely boiled off. Recently, more advanced, more accurate and faster methods for drawing TBP curves have been developed, such as mass spectrometry [25].

An example TBP curve where the cut points of naphtha, kerosene, gas oil and residue from the Bintulu plant in Malaysia is shown in Figure 2.7. Another example TBP curve from a typical Middle Eastern crude is shown in Figure 2.8.
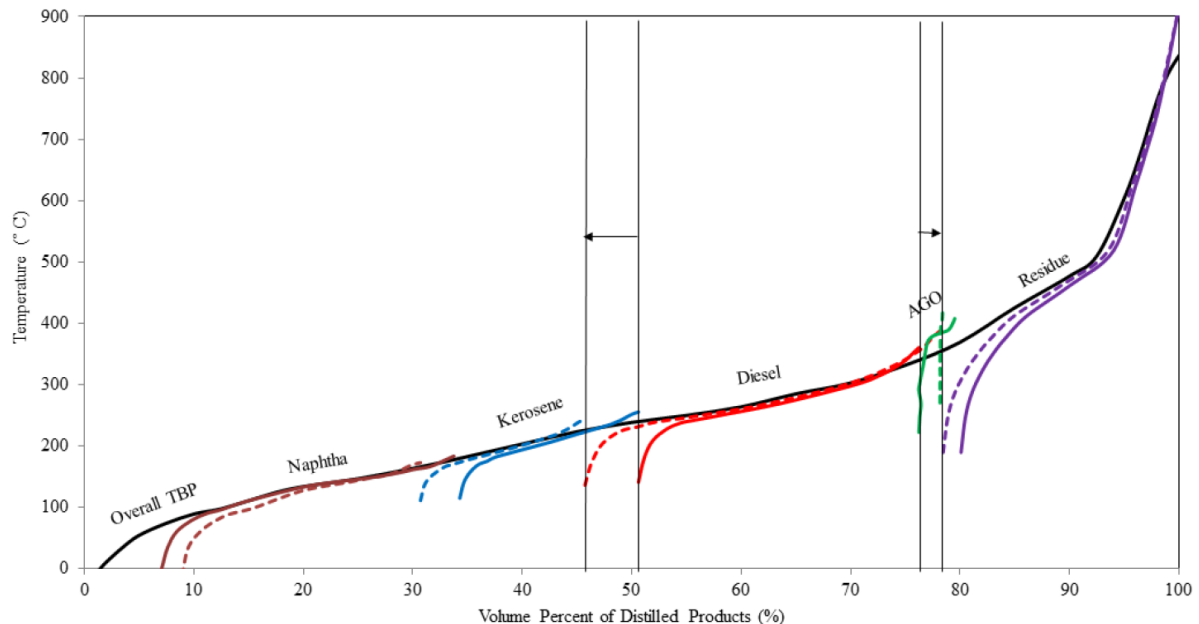
Figure 2.9: TBP curves from the Bintulu syncrude processing plant. Reprinted from [34].
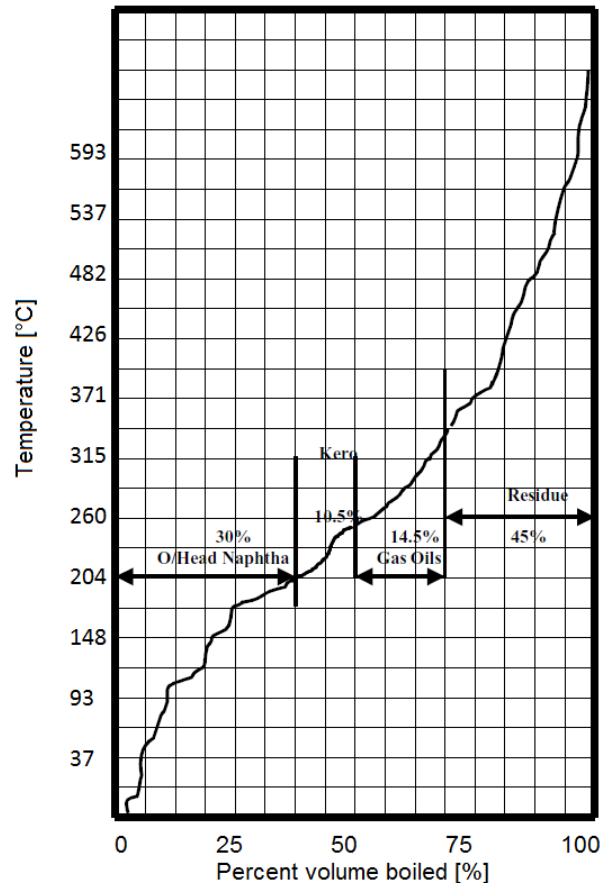
Figure 2.10: TBP curve for a typical Middle Eastern crude and its cuts. Adapted from [25].

The main cuts in atmospheric distillation are naphtha, kerosene and gas oil [15,24]. There are other cuts as well, such as LPG, or the atmospheric residue which can be further distilled under vacuum. A brief description of each cut along with its uses and nomenclature of the most common cut points is provided [15]:

- Fuel gas: C_1-C_2 gases have little economic value and are used as fuel for the refinery operations that require heat in almost all cases.
- LPG: Liquid Petroleum Gas has different specifications depending on country. Generally, it is a mixture of butane (including isobutane) and propane. Proper separation from the lighter gases requires distillation under pressure (higher than atmospheric).
- Naphtha: The term naphtha is used for hydrocarbons that have a cut point between 32 and 193°C. Sometimes light and heavy naphtha (32-88°C and 88-193°C) are drawn separately from the distillation column. In some occasions, all the hydrocarbons below 193°C are drawn as overhead distillate from the column, and further separation into LPG, light naphtha and heavy naphtha takes place in a separate downstream unit. The most common uses of naphtha are:
  - Feed for refinery operations that upgrade naphtha to motor gasoline. A high octane number is required for use of naphtha as fuel, which necessitates further refining to increase the content of branched and cyclic compounds.
  - Feedstock for olefin and aromatic production for the petrochemical industry, by using thermal cracking and catalytic reforming respectively.
- Kerosene: Kerosene is mainly used as aviation fuel after further refining. Therefore, the primary specifications for kerosene are the flash point (the temperature at which

the vapors ignite from an ignition source, i.e., a spark) and the freezing point. The flash and freezing points for jet fuel with lax specifications are +38 and -40°C, respectively. Those constraints limit the cut points to between 193-271°C.

- Gas oil: Gas oil is the precursor of diesel fuel. Gas oil is sometimes referred to in literature as diesel for that reason, but for the scope of this project the term gas oil is reserved for the distillation cut and the term diesel is reserved for the fuel. The cut points of gas oil are 271-425°C. Sometimes it is separated in light and heavy gas oil with cut points at 271-321°C and 321-425°C respectively. Heavier diesel can be used for marine applications, while lighter diesel is preferentially used in colder climates.

- Vacuum gas oil: Atmospheric residue from the bottom of the atmospheric tower can be further distilled into light and heavy vacuum gas oil in a vacuum distillation tower. Their cut points are 425-510°C and 510-564°C, respectively. Vacuum gas oils may be used as lubricants or as feedstock for cracking units that produce lighter hydrocarbons in the gas oil, kerosene and naphtha cut range.

- Vacuum residue: Vacuum residue is not an actual cut with specifications, but rather simply the leftover product from the bottom of the vacuum tower, that is heavy waxes that boil above 565°C. Straight-run vacuum residue is of low value. Also, it creates problems, such as coking on the catalyst of cracking reactors during refining operations, so it usually does not undergo any refining. Instead is used in other applications, e.g., asphalt, or it is blended with gas oils to meet heavy fuel oil specifications.

2. Theoretical background

3. Literature review

The goal of this chapter is to review the state of the art, with regards to modelling of the distillation process, in recent literature.

3.1. Review of theses and journal articles

Chen conducted modelling of a distillation unit with its associated feed preheating train for their PhD thesis in 2008 [31]. The design of the column was carried out using the FUG method. A prefractionation column was used upstream of the ADU in order to recover the crude oil from the raw feed. The main column has 25 stages, three pumparounds, and three strippers which have three stages each. The column with the side strippers is "decomposed" [sic] into four smaller columns representing the original, with each small column having a stripping section (which corresponds to the stripping section of the main ADU or a side stripper in the original) and a rectifying section (which corresponds to the stages of the rectifying section between the side stripper draw-off trays in the original). The stripping steam to feed molar ratio of the main column is approximately 25% and the stripping steam to stripper product molar ratio is approximately 50%. The stripping steam to the main column is high pressure superheated steam at 260°C and 4.5 bar. The feed enters at 370°C and the condenser duty causes a molar reflux ratio of 1.6 in the column. The 5%, 50% and 95% boiling points of the products are used to characterize them. The distillate products of the main column are off gas, naphtha, kerosene, light gas oil and heavy gas oil, with atmospheric residue as the bottom product.

The design of the Heat Exchanger Network (HEN) was carried out by using pinch analysis. The minimum approach temperature was taken to be 10°C. Simplifying assumptions, such as constant heat capacity with respect to temperature, were made.

The work concluded that the FUG method can be used to accurately determine design and process parameters with the use of an iterative method that selects the appropriate key components and characterizes products by the three TBP curves mentioned earlier. Pumparound location and duty are important factors in process optimisation. Pinch analysis is recommended for heat integration. Heat integration is highly important in distillation process design and analysis for saving cost and energy.

Liu conducted an optimisation study of a distillation process and the associated HEN for his Master's thesis in 2012 [27]. The study reports itself to be based on Chen's [31] application of the Fenske method. The model used in this study is more simplified in design and more robust in convergence. The Fenske method is used for the initial column configuration and an iterative "trial and error" method is used in order to meet product specification goals. In this study, the Fenske method considers the complex column with the side strippers as follows: The strippers and top product of the original correspond to the top product of the Fenske method column, and the bottom product of the original corresponds to the bottom product of the Fenske method column. As such, this is a more simplified approach. The results of the Fenske method are then applied in a rigorous process model which gives results for the product composition. The parameters of the Fenske method are adjusted until the rigorous model returns satisfactory results.

The process model is similar to Chen's as well, with the crude being preheated by recovering heat from the distillate products before entering the fired heater and the ADU. The ADU has 27 stages in total. The feed stage is the 22nd, and the feed temperature is 370°C. High pressure

stripping steam is injected at the bottom stage at a steam to feed molar ratio of approximately 7%. The bottom strippers utilize low pressure steam, at a steam to product molar ratio of approximately 15%, while the top stripper uses a reboiler. The top two strippers have 4 stages each, and the bottom stripper has two. The distillate products of the column are off gas, light naphtha, heavy naphtha, light gas oil and heavy gas oil, with atmospheric residue as the bottom product.

According to Liu, rigorous methods are evaluated as more accurate and the shortcut methods as more suitable for optimisation problems due to the ease of convergence and flexibility of input. It is concluded that the Fenske method is adequate at predicting product composition and column configuration, as long as it is coupled with a rigorous method to evaluate the suitability of the light and heavy key selection. Iterative "trial and error" methods are applicable to obtain the optimal design and process parameters of distillation if coupled with shortcut distillation models.

Ochoa-Estopier et al. published a journal article in 2014 reviewing and comparing the suitability of shortcut, rigorous and statistical models for distillation of Venezuela Tia Juana Light crude oil and presented an example of a distillation model developed with the use of artificial neural networks [32]. To that end, an interface between MATLAB and ASPEN HYSYS was created. An iterative process is carried out with the use of a shortcut model that requires certain process parameters as input. Product specifications are compared to the goal product specifications. Sets of process parameters for the next iteration are created in MATLAB by use of a neural network. The neural network aims at matching the product specifications and utility consumption of the ASPEN HYSYS model to the ones set as goals.

The results of the final distillation configuration were reported. The column has three pumparounds and three strippers. The distillate products are light naphtha, heavy naphtha, light gas oil and heavy gas oil. The column has 41 stages, and the three side strippers have 6, 7 and 5 stages from top to bottom. The feed stage is the 35th, and there is high pressure steam injected at the bottom at 260°C and 4.5 bar. The steam to feed molar ratio is approximately 43%, the stripper to bottom product molar ratio of the strippers is 235%, and the reflux ratio is 4.17.

Ochoa-Estopier et al. concluded that rigorous models are the most suitable for distillation process simulation. However, they are not robust to changes in the input parameters, meaning that changes in input parameters may cause the simulation to fail to converge. Furthermore, rigorous models have longer simulation run times compared to shortcut models. Therefore, shortcut models are more appropriate for optimisation problems for both grassroots designs of processes (i.e., from scratch) and retrofit designs of processes (i.e., changes in existing processes) if coupled with an optimisation algorithm. Statistical models are the most robust and easy to converge, but they may suffer in accuracy depending on the data used for the regression. Artificial neural networks can be used in conjunction with the FUG method to automate the process of optimisation and deliver accurate results with robust simulation convergence.

Luo et al. published a journal article in 2014 proposing a systematic optimisation approach of the cost function for a crude oil distillation process [33]. In the article, the distillation process is described as follows: There is a distillation unit with three pumparounds and three steam strippers. The products from the three-phase separator of the condenser are off gas, water and naphtha. The stripper products are, from top to bottom, kerosene, diesel and atmospheric gas oil (AGO). A heat exchanger network recovers heat from the products to heat up the feed. The feed is then heated up to 370°C in the furnace, becoming partially vaporized.

The column has 31 stages, the feed stage is the 29th, and the stripper draw off stages were the 10th, the 13th and the 24th, respectively. The column is operated at a pressure slightly higher than atmospheric, with 1.47 bar at the bottom stage and 1.31 bar at the top.

The atmospheric residue, which contained components with a boiling point above 350°C, was heated at 394°C and fed into the vacuum distillation column. The VDU had 14 stages and operated at a pressure of 0.039 bar at the bottom and 0.027 bar at the top. There are 3 pumparounds and 3 side products, namely Vacuum Diesel (VD), LVGO and HVGO. The naphtha, kerosene, Diesel, AGO and VD products were considered straight-run products, while the LVGO and HVGO were feedstock for downstream units.

Luo et al. modelled their distillation process using the SCFrac model of the ASPEN Plus software (which uses the FUG method as well). The heat integration was conducted by using the pinch analysis tool of ASPEN Plus, with a minimum temperature difference of 15°C.

The optimisation results result in optimal steam flow rates that give a steam to feed molar ratio of approximately 12% for the main column and an average steam to bottom product molar ratio for the strippers of approximately 15%.

The researchers concluded that shortcut models of distillation units are adequate at predicting the composition and boiling points of the distillation products. Furthermore, crude oil and product composition have a major influence on heat recovery.

3.2. Conclusions from the literature review

All distillation unit models reviewed in literature share the following common points [27,31–33]:

- The Fenske-Underwood-Gilliland method is used either for the initial parameter estimation of a model that later is optimised by an iterative process that uses a more rigorous model, or it is used for the entire modelling.
- Experimental data validates the use of the aforementioned methods.
- Distillation columns typically have design parameters in the ranges shown below:
    - Number of stages: between 25 and 45 for ADUs, between 10 and 14 for VDUs, between 2 and 7 for the side strippers.
    - Operating pressure: At or slightly above atmospheric for ADUs, in the order of 30 mbar for VDUs.
    - Pressure drop along the entire unit: in the order of 10-15% for ADUs, and around 25% for VDUs.
    - Number of pumparounds: Typically, three.
    - Number of side strippers: Typically, two or three.
    - Feed stage: typically, 2-5 stages above the bottom stage.
    - Molar reflux ratio: typically, between 1 and 5.
    - Stripping steam to feed molar ratio for the main column: varies depending on type of crude and separation goals, usually between 10% and 50%.
    - Stripping steam to bottom product molar ratio for the side strippers: varies a lot depending on type of crude and separation goals, usually between 10% and 50% but can go below 10% or above 50%.
- Heat integration facilitates energy and cost savings that justify its implementation in most cases. However, the trade-off between the energy cost savings and the CAPEX increase needs to be considered on a case-by-case basis.
- The minimum temperature difference used in heat integration is between 10 and 15°C.

- Heat integration can be used for both a grassroots design and a retrofit design of a process.

4. Basis of Design

The Basis of Design (BoD) documented in this chapter contains the problem statement, battery limits, assumptions, specifications and restrictions of the problem.

4.1. Key word definitions

With respect to the scope of this project, the following words, as used in the subsequent chapters, are defined.

The atmospheric distillation unit (ADU) feed and products are:

- Naphtha is defined as the liquid distillate product from the ADU. The goal composition is hydrocarbons in the C_5-C_8 range.
- Kerosene is defined as the bottom product from the first stripper of the ADU. The goal composition is hydrocarbons in the C_9-C_{15} range.
- Gas oil is defined as the bottom product from the second stripper of the ADU. The goal composition is hydrocarbons in the C_{16}-C_{22} range.
- The bottom product from the ADU (hydrocarbons in the C_{23+} range) is defined as atmospheric residue (AR).
- The vapor distillate that contains C_4 and lighter hydrocarbons and other gases is defined as Light Ends.

The vacuum distillation unit (VDU) products are:

- HGO is defined as liquid distillate product from the VDU. The goal composition is hydrocarbons in the C_{23}-C_{27} range.
- LVGO is defined as the first (topmost) side product from the VDU. The goal composition is hydrocarbons in the C_{28}-C_{38} range.
- HVGO is defined as the second side product from the VDU. The goal composition is hydrocarbons in the C_{39}-C_{47} range.
- The bottom product of the VDU (hydrocarbons in the C_{48+} range) is defined as vacuum residue (VR).

The choice of carbon number range for the streams is derived from the boiling point ranges, as given in chapter 2.3, in combination with the boiling point data of linear alkanes and 1-alkenes obtained from Engineering Toolbox [36].

It must be noted at this point that the term HGO is used with respect to the name given to hydrocarbons of a specific boiling range (as explained in chapter 2.6) and not necessarily with respect to whether it is a product of the ADU or the VDU.

The purity and recovery of a stream are defined as:

- Purity is defined as the sum of the mass flows of all hydrocarbons in the desired range in the product stream over the total mass flow of the same stream.
- Recovery is defined as the sum of the mass flows of all hydrocarbons in the desired range in the product stream over the sum of the mass flows of all hydrocarbons in the desired range in the feed stream.

Stages are defined as theoretical equilibrium stages, and the convention followed in this project is that the top stage is stage 1.

4.2. Product specifications

The primary goal of the project is to model an atmospheric distillation column that separates the components of the feed into naphtha, kerosene and gas oil fractions. The goal is to achieve a minimum of 90% purity and 90% recovery for each fraction (naphtha, kerosene and gas oil). A vacuum distillation unit will be modelled as well in one of the cases, wherein the goal is to separate the atmospheric residue into heavy gas oil, light vacuum gas oil and heavy vacuum gas oil (HGO, LVGO and HVGO, respectively) with a minimum of 70% purity and 70% recovery. To meet those ends, the syncrude must be separated from the gases by flashing at a suitable temperature. To prevent losses, a minimum of 99.5% of the total syncrude mass in the raw feed must be recovered in the feed for the ADU. To ensure a stable ADU operation, syncrude purity must be at a minimum of 90% when entering the column. The purity specification is not as strict as the recovery specification, since the impurities can be separated from the syncrude products by the ADU itself.

4.3. Battery limits

The battery limits of this project include the distillation and its peripheral processes, such as separation of the syncrude from the gases and water, heat integration or vacuum distillation. Figure 3.2 illustrates the battery limits of the process. Syngas formation and cleaning, syncrude synthesis via the Fischer-Tropsch process, or refining of the fractions into useable final products are outside of the battery limits of this project.
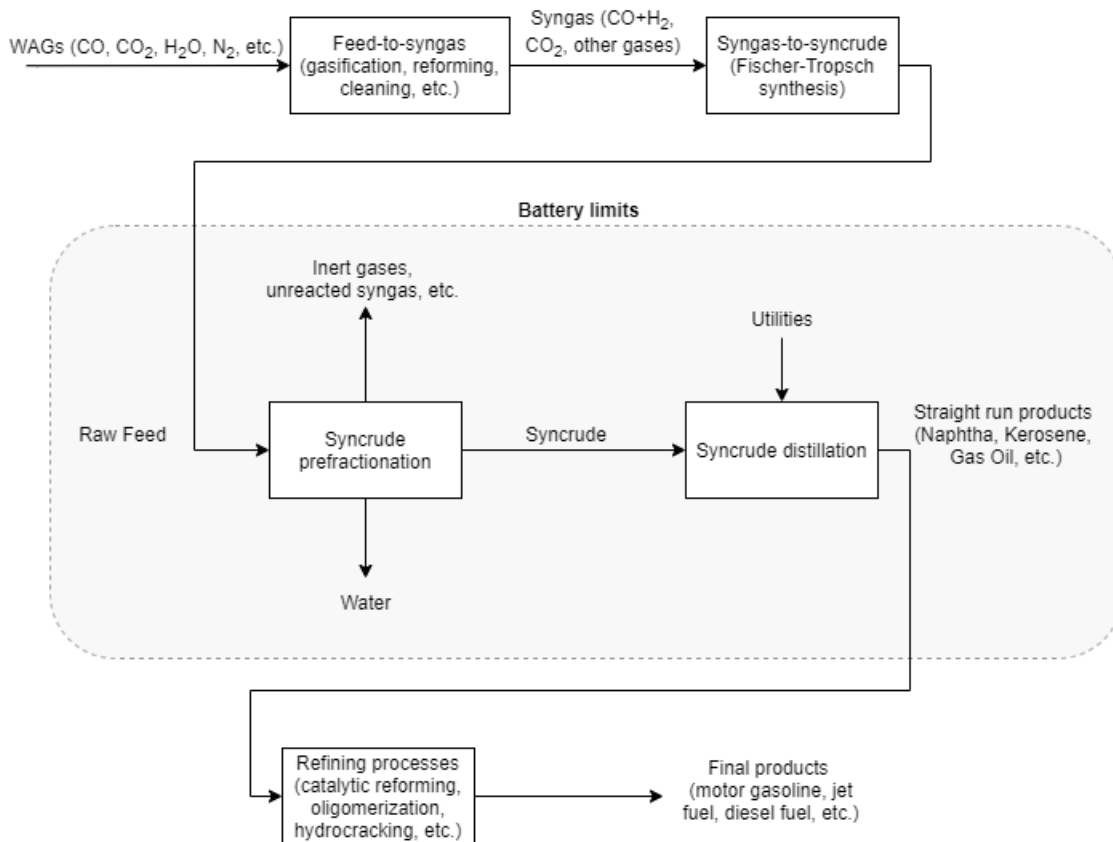
Figure 4.1: Battery limits block flow diagram

The raw feed is received at a rate of 130.7 kg/s, at a temperature of 204.2°C and a pressure of 23.6 bar. The majority of the raw feed is leftover compounds from the previous processes

that take place (syngas formation, FTS) such as H_2O, CO, N_2, CO_2. The actual flow rate of syncrude (hydrocarbons at the C_{5+} range) is 7.396 kg/s. For the scope of this project, syncrude is modelled as a mixture of light 1-alkenes and alkanes at the C_5-C_{50} range. According to the characteristics of Co-LTFT synthesis as described in chapter 2.2, this is an appropriate approximation. A detailed description of the composition and conditions of the raw feed is shown in Table A.1 in the Appendix. A short overview of the composition, on a mass basis, is shown in Figure 4.1 and Table 4.1.

Table 4.1: Raw feed composition

Component category	Mass flow [kg/s]	Mass fraction [-]
Inert gases (O_2, N_2, CO_2)	82.812	0.63
Water (H_2O)	11.362	0.09
Syngas ($CO+H_2$)	26.920	0.20
Light hydrocarbons (C_{1-4})	2.247	0.02
Syncrude	7.396	0.06
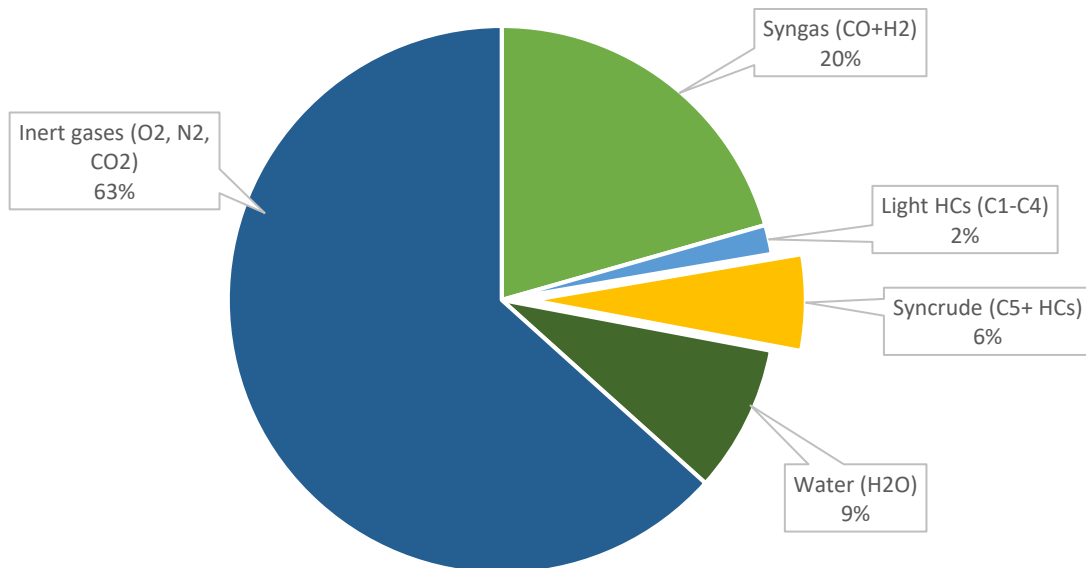
Figure 4.2: Raw feed composition

4.4. Utilities

The following utilities are used in the current project (design considerations in subchapter 4.5):

- The steam to the distillation units is superheated high pressure steam at 400°C and 20 bar.
- The steam to the side strippers is superheated low pressure steam at 175°C and 4 bar.
- Cooling water at 15°C is used for the first cooler of the raw feed, the condenser and pumparounds of all distillation units, and for the cooling of the product streams. The cooling water is used to cool down the product streams as low as 25°C.
- The term "subcooling duty" is used in this project to refer to cooling where the hot stream is at 25°C or lower and must be cooled down to 5°C or lower.

4.5. Cases

Modelling of the process will take place in ASPEN Plus. The components thermodynamic properties used, such as densities, specific heats, etc., will be those of the ASPEN Plus software. The equation of state used will be the Peng-Robinson EoS; an explanation is provided in section Thermodynamic property models of the Appendix.

Six different processes will be examined, one Base Case and five alternative processes of it. Subsection 4.5.1 contains the initial estimation for the initial estimates for the Base Case process. Subsection 4.5.2 of this chapter gives a detailed description of the Base Case process. Subsections 4.5.3 through 4.5.7 contain brief descriptions of the alternative processes that have been modelled. Since all the alternative cases have similar processes to the Base Case with one alteration in the input, only that alteration will be described.

Prior to the modelling, initial estimates for various parameters (such as number of ideal stages and feed stage) are taken using the Underwood method and the basic laws of thermodynamics. The latter part of the modelling includes heat integration and sensitivity analysis. Heat integration will be used to reduce the utility consumption. An approximation of the minimum energy approach will be used. Heat integration will not be used for steam production.

The Base Case includes the prefractionation train and atmospheric distillation unit (ADU). The condenser products are naphtha, light ends and condenser water. The bottom product is Atmospheric residue. The naphtha flow rate is fixed at 0.797 kg/s (explanation provided in section Product stream mass flow calculations of the Appendix), while the condenser duty is a dependent variable. In the alternative process cases, the condenser duty is fixed at the same value as the Base Case result, so that the results can be compared on the basis of similar ADUs.

The Base Case ADU has two side strippers, the bottom products of which are kerosene and gas oil. Both strippers utilize stripping steam. There is no heat integration taking place. The atmospheric residue is not further distilled in a vacuum unit. The utility consumption and separation quality are reported. Furthermore, for the Base Case, results of the syncrude prefractionation and a TBP curve for the cuts are reported. The TBP curves of the cuts are compared with findings from literature.

Case 2 is similar to the Base Case, but the kerosene side stripper of the ADU uses a reboiler instead of stripping steam to separate the light gases from the bottom product. The duty of the reboiler is the same as the duty necessary to heat up water from the temperature of the Base Case condenser stage to LPS temperature. Utility consumption and separation quality are compared to the Base Case.

Case 3 is similar to the Base Case, but there is an HGO product drawn off a third side stripper, which utilizes stripping steam, from the ADU. Utility consumption and separation quality are compared to the Base Case.

Case 4 is similar to the Base Case. In this case, what will be tested is the difference in separation quality if the collective duty of the pumparounds is added to the condenser duty. The goal is to illustrate the importance of distributing part of the cooling duty in the lower segments of the column. The total utility consumption will be of equal value, therefore only separation quality will be reported and compared to the Base Case.

Case 5 has the same exact ADU configuration as the Base Case, but there is a VDU as well. The AR stream is the feed to the VDU. It is used to produce HGO, LVGO and HVGO as distillates. The goal is to achieve a minimum of 70% purity and recovery (with respect to the AR feed) in all streams. The separation quality of the fractions produced is reported. Utility consumption is reported and compared to the Base Case.

Case 6 has the same exact ADU configuration as the Base Case. The difference with the Base Case is that this process makes use of heat integration in order to reduce utility consumption. The minimum temperature difference allowed in a heat exchanger is $\Delta T_{min}=10°C$. The heat exchanger network is explained in Chapter 4.5.7. The input parameters and internal configuration of the ADU are identical to the Base Case. Therefore, separation quality remains unaffected. Only utility consumption is reported. Two HENs will be designed, one that aims at decreasing total absolute duty (defined as the sum of the absolute values of heating and cooling duty) and one that aims at decreasing total subcooling duty.

4.5.1. Initial estimates

The first step is to decide on the feed temperature. The feed temperature is initially set at 370°C, after considering the literature review. The stripping steam temperature for the ADU is chosen to be 400°C so that it is always higher than the feed temperature, 370°C. The reason for that is that the stripping steam must always enter at a lower stage than the feed; stripping steam always enters the distillation unit at the bottom stage. Therefore, if the steam temperature were to be lower than the feed temperature, it would cause the stages below the feed stage to have a lower temperature than the feed stage, therefore the volatile components would not flow up with the vapor.

The next step is to decide on the light key and the heavy key. The Fenske method works for a simple distillation column with one feed, one distillate product and one bottom product. The light and heavy keys are chosen in a way that simulates the C_{23} and heavier components being the bottom product and the C_{22} and lighter components being the distillate, since that is the target composition for the naphtha, kerosene and gas oil streams collectively. Thus, the light and heavy keys are chosen to be $C_{22}H_{46}$ and $C_{23}H_{48}$ respectively.

The next step is to compute θ. This requires a calculation of some properties of the feed, namely volatilities (K-values), molar fractions (Z_f) and feed quality. First, the feed quality q must be calculated by using equation (2.7). This requires that an appropriate temperature for the feed be chosen. Initially, feed temperature was chosen to be 370°C, after considering the values from commercial experience. However, application of the method in ASPEN Plus resulted in failure of the process model calculations to converge, due to the column having a too high vapor content. Therefore, the process was repeated with a 20°C decrease in feed temperature in each iteration until convergence was achieved. The model converged after three iterations, with a feed temperature of 310°C. This chapter contains the application of the FUG method with this feed temperature. The feed is heated up to 310°C before entering the ADU. This results in a feed quality q:

$$q = \frac{H_G - H_F}{H_G - H_L} = \frac{-170124.3 - (-232135.4)}{-170124.3 - (-482602.9)} = 0.198 \Rightarrow 1 - q = 0.802$$

The K-values and the molar fractions of all the components in the feed can be found in the Appendix, subsection "K-values of syncrude components at 310°C". From the K-values, and with $C_{23}H_{48}$ having been decided as the heavy key, the relative volatility a_i of component i with respect to the heavy key can be computed. The value of θ can now be computed by using the goal seek method iteratively to solve equation (2.6):

$$\sum_{i=1}^{N_{comp}} \frac{a_i Z_{Fi}}{a_i - \theta} = 1 - q$$

In order to do that, the initial guess for θ is selected to be 1.01, to satisfy the condition $a_{LK} > \theta > a_{HK}$. The goal seek method converged at $\theta = 1.142$.

The next step is to calculate R_{min} by solving equation (2.5):

$$\sum_{i=1}^{N_{comp}} \frac{a_i x_{Di}}{a_i - \theta} = R_{min} + 1$$

where the target molar fractions x_{Di} of the components in the distillate are calculated by multiplying the molar flows of the components in the feed that are the light key or more volatile by 0.9 (given the target recovery of 90%), multiplying the less volatile ones by 0.1, and dividing by the target molar flow rate of the distillate.

This results in a minimum reflux ratio value $R_{min} = 1.47$, and by using equation (2.9), we get:

$$R = 1.2 * R_{min} = 1.77$$

Next, the Fenske equation (2.4) is used to calculate the minimum number of stages at total reflux:

$$N_{min} = \frac{\log\left(\left(\frac{x_{LK}}{x_{HK}}\right)_D \left(\frac{x_{HK}}{x_{LK}}\right)_B\right)}{\log(a_{LK})} = 16$$

After having used the Fenske and Underwood equations, the Gilliland correlation is used to calculate the necessary number of stages at reflux ratio $R = 1.77$. The Molokanov equation (2.8)(2.10) is used:

$$y = 1 - \exp\left(\left(\frac{1 - 54.4x}{11 + 117.2x}\right)\left(\frac{x - 1}{\sqrt{x}}\right)\right)$$

where

$$x = \frac{R - R_{min}}{R + 1}, \qquad y = \frac{N - N_{min}}{N + 1}$$

resulting in a total stage number of $N = 37$.

Finally, the Kirkbride equation is used to find an estimate for the feed stage.

$$\frac{m}{p} = \left(\left(\frac{B}{D}\right)\left(\frac{z_{HK}}{z_{LK}}\right)_F \left(\frac{x_{LK,B}}{x_{HK,D}}\right)^2\right)^{0.206}$$

$$m + p = N$$

resulting in the feed stage $m = 11$.

In the initial stages of modelling, the values for m, N and R were given as inputs. However, the results obtained by using the values $m = 11$, $N = 37$ and $R = 1.77$ do not meet the BoD targets; meaning that the purity and recovery of all products was below 90%. The final values used in subsections 4.5.2 and on were reached after running the process model through a

sensitivity analysis and applying the trial and error method as described in Figure 4.3. Confidential commercial experience data were used to assist with this step. The methodology by which the final values for the number of stages and reflux ratio are found is shown in the block flow diagram of Figure 4.3.
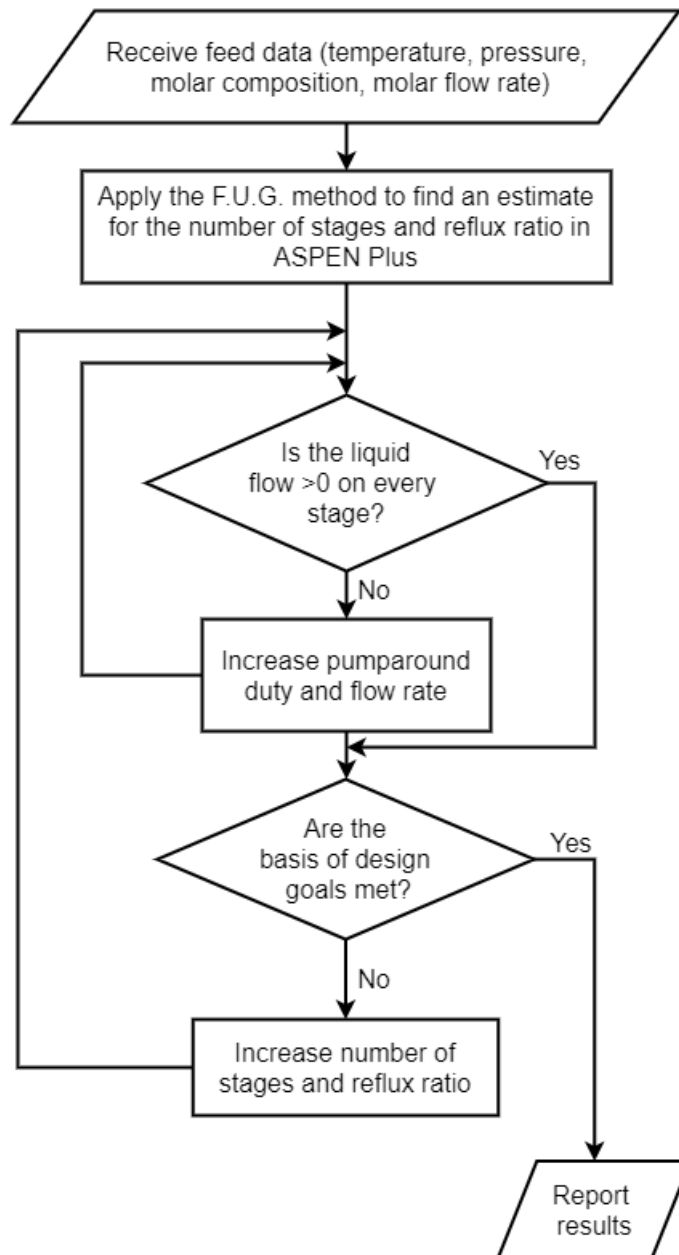

Figure 4.3: Block flow diagram for finding the final values for the number of stages and reflux ratio.

4.5.2. Base Case

The entire distillation process is shown in the process flow diagram (PFD) in Figure 4.4.

4. Basis of Design
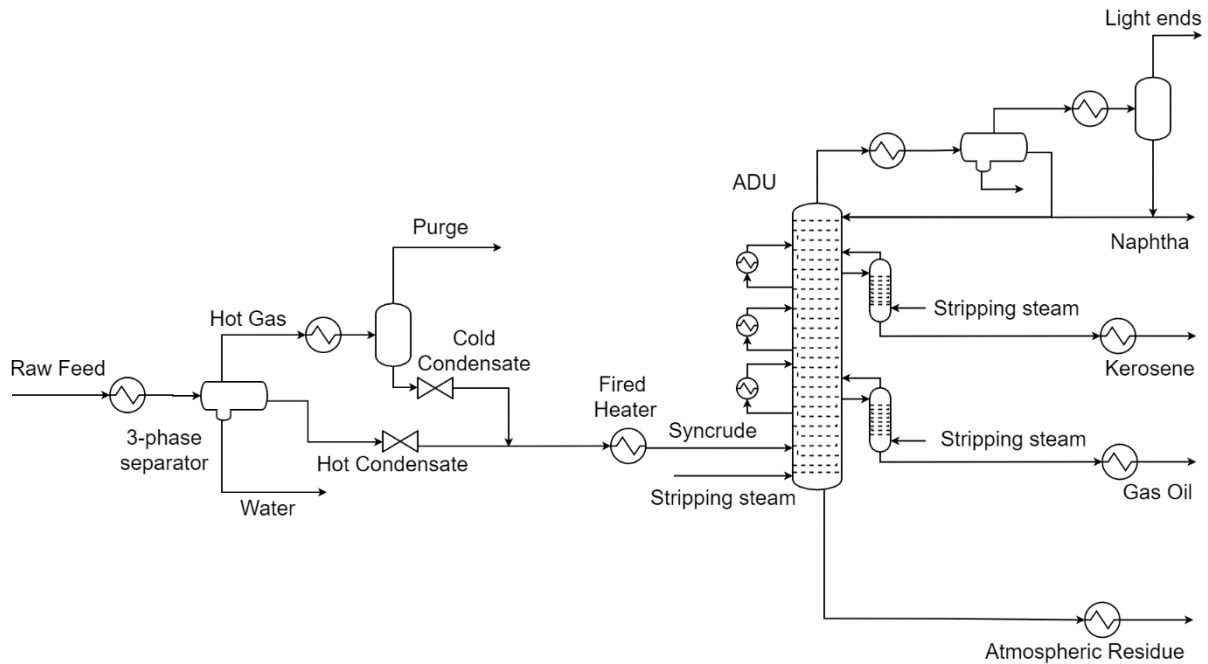
Figure 4.4: Base case PFD

The thermodynamic property model chosen for the calculation of thermodynamic properties in the Base Case process, as well as for the alternative processes (cases), is Peng-Robinson. The choice is justified in the Appendix, in sub-section Thermodynamic property models.

Regarding the processes upstream of the battery limits and the composition of the input (raw feed) stream: Blast furnace gases are captured from the blast furnace tower. These are also called works arising gases (WAGs). The WAGs are rich in N_2, CO and CO_2. The WAGs are first cleaned and then in Fischer-Tropsch synthesis (FTS) through the Fischer-Tropsch reactor (FTR). The FTR converts CO and H_2 to large hydrocarbon molecules, primarily alkanes, but also some alkenes at the lower carbon chain length (approximately C_{10} and lighter). The main product of the FTS is called syncrude. However, the FTS product contains a lot of unreacted syngas, inert gases, unwanted light hydrocarbons and water as well. Since it is not pure syncrude, it is termed raw feed for the purpose of this project.

The raw feed contains mostly gases and water, as described in chapter 3.1. Due to the high temperature of the raw feed (204°C), some of the syncrude is in the gas phase as well. The atmospheric column can only operate properly if it receives syncrude as its feed with little to no impurities. Therefore, the first step in the process is to recover the syncrude from the raw feed. Separation occurs by condensing the syncrude while keeping the unwanted components at the gas phase. For that purpose, raw feed is cooled down to separate the hydrocarbons from the water and the other gases twice.

Before the first separator, a heat exchanger using cooling water is used, bringing the temperature of the raw feed down to 20°C. The temperature is chosen to be 20°C because it is achievable with cooling water and also causes the syncrude stream to contain almost no impurities. The first separator is a 3-phase flash drum. It separates the raw feed into three streams: The gas product of the 3-phase separator (hot gas), which contains most of the unwanted gases and some light components of the syncrude, an organic liquid product which contains most of the syncrude (Hot Condensate), and an aqueous phase product (Water). The Hot Condensate contains most of the syncrude, and almost no impurities.

The aqueous product is discarded and sent outside the battery limits to a waste water treatment unit. Normally, the aqueous phase may contain 1-2% (mass basis) polar organic compounds, such as alcohols and carboxylic acids (see subchapter 2.2.2). However, since the raw feed to the process model only contains apolar hydrocarbons, carbon oxides, and inorganic elements and compounds, the aqueous phase will only contain H_2O.

In order to retrieve the light hydrocarbons contained in the hot gas stream, the second flash drum is at a much lower temperature. To that end, the hot gas is subcooled down to -70°C before entering the second separator The temperature of the hot gas before the flash drum is chosen to be -70°C because it results in >99.5% of recovery of the C_{5+} components from the raw feed and >90% purity of the C_{5+} components in the syncrude stream. Proof of that can be found in the sensitivity analysis (see chapter 6.1). The liquid product of the flash drum (Cold Condensate) contains most of the leftover C_{5+} hydrocarbons, with very few impurities. The gaseous product (Purge) is purged, as it contains almost no C_{5+} hydrocarbons and almost all of the components that are more volatile than C_5 hydrocarbons.

The Cold Condensate and Hot Condensate streams are mixed to form the syncrude stream. The syncrude stream is heated in a fired heater up to 310°C and enters the ADU.

The Petrofrac distillation model was used in ASPEN plus to model the ADU. The distillation unit has 40 stages. The syncrude enters above stage 37. Stripping steam enters the column below stage 40. The steam mass flow rate was initially chosen to be 1.9 kg/sec, or 25% of the feed (syncrude) mass flow rate, according to considerations of the literature. However, it was adjusted according to the results of the sensitivity analysis to be 1.3 kg/sec. At the top stage, there is a partial condenser with a duty of -5.65 MW. Heat is provided in the column by the feed preheating furnace and the stripping steam. The column does not have a reboiler.

At the top of the column there is a condenser with a 3-phase flash drum. The condenser produces a distillate product in vapor phase, a distillate product in liquid phase, and a water product. The vapor distillate contains some unwanted gases in addition to the naphtha range hydrocarbons, mostly lighter hydrocarbons (C_4 and more volatile), and other gases such as CO_2 that could not be purged at the flash drum at -70°C.

A heat exchanger with an outlet temperature of -20°C is used to condense the hydrocarbons in the vapor distillate. The cooled stream enters the second flash drum. The second flash drum produces a vapor product (Light Ends) which is purged, and a liquid product. The liquid product of the flash drum is mixed with the liquid distillate product of the condenser. The mixed liquid distillate stream is the naphtha stream. The mass flow rate for the naphtha stream is set at 0.797 kg/s. It is noted at this point that the calculation of the mass flow rate for all products in all cases is described in the Appendix, in subsection Product stream mass flow calculations.

There are two steam strippers in the Base Case ADU. The stripper products are kerosene and gas oil. The mass flow rates of the kerosene and gas oil streams are 1.27 and 1.25 kg/s, respectively. The first stripper draws liquid from stage 11 and returns vapor to stage 10 of the main column. The stripper has 10 stages, and low-pressure steam is injected at the bottom at 175°C, 4 bar and a flow rate of 0.025 kg/s. The stripping steam mass flow rate was chosen to be 2% of the bottom product flow rate, while steam conditions were chosen according to data from the literature. The second stripper draws liquid from stage 33 and returns vapor to stage 32 of the main column. The second stripper has 10 stages as well, and low-pressure steam is injected at the bottom at 175°C, 4 bar and a flow rate of 0.025 kg/s, maintaining the same LPS/bottom product mass ratio.

The column also has three pumparounds (named as pumparounds 1, 2 and 3 from top to bottom). Pumparound 1 draws liquid from stage 9 at a flow rate of 2.25 kg/s, cools it down to

50°C, and returns it to stage 6. Pumparound 2 draws liquid from stage 20 at a flow rate of 2.5 kg/s, cools it down to 150°C, and returns it to stage 17. Pumparound 3 draws liquid from stage 28 at a flow rate of 2 kg/s, cools it down to 80°C, and returns it to stage 25. The pumparounds ensure good separation between the kerosene and gas oil fractions with a utility consumption of -0.283, -0.382 and -0.757 MW from top to bottom. The choice of pumparound number and stage placement is based on ensuring liquid flow >0 in all stages; the duty and flow rate is based on the values documented in the literature review as well.

4.5.3. Case 2

The PFD of the case 2 process is shown in Figure 4.5.
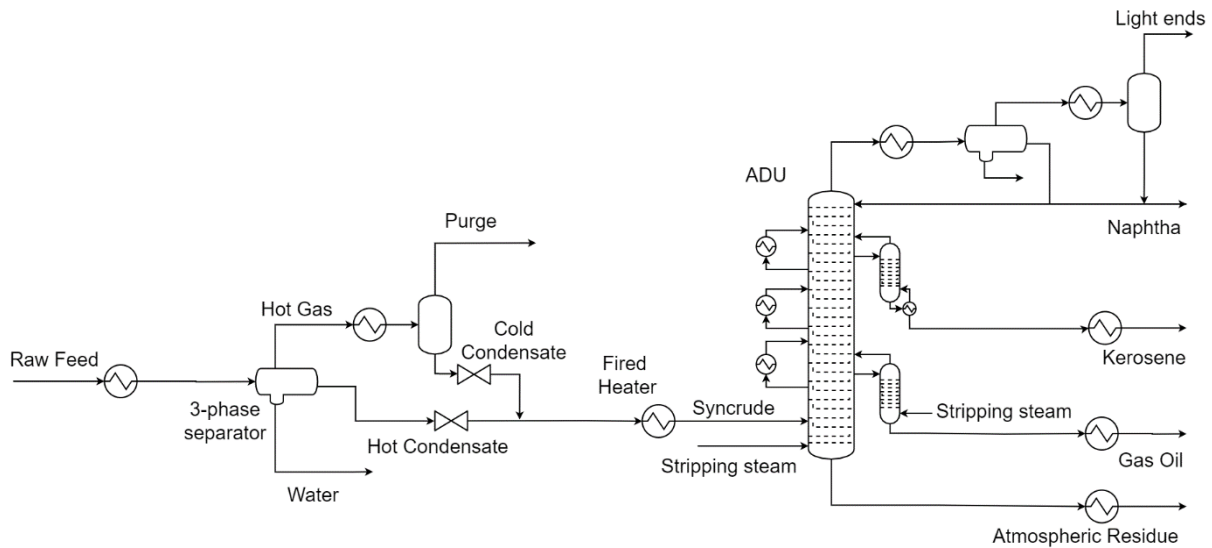
Figure 4.5: Case 2 PFD

The process of Case 2 is similar to that of the Base Case. The only difference is that the first stripper, where the bottom product is kerosene, is making use of a reboiler, instead of stripping steam. The duty of the reboiler is 63 kW, which is equal to the duty of the stripping steam boiler for the same stripper of the Base Case. Utilities aside from cooling water are equal by design between the Base Case and case 2. The separation quality of the product streams will be reported and compared to the Base Case.

4.5.4. Case 3

The PFD of the case 3 process is shown in Figure 4.6.
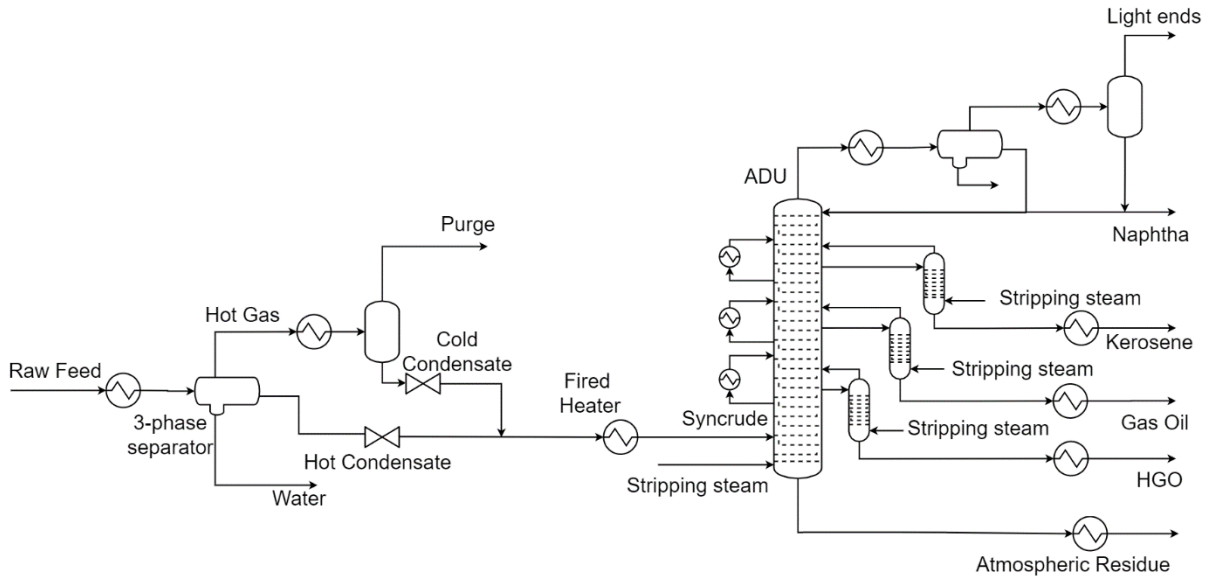
Figure 4.6: Case 3 PFD

The process of case 3 is similar to that of the Base Case. The only difference is that a third steam stripper is added. It has 10 stages and draws liquid from stage 38 and returns the stripped vapor to stage 37. The bottom product is HGO, at a rate of 0.92 kg/s. The mass flow of LPS in the stripper is 0.018 kg/s, in order to maintain the same 2% LPS/bottom product ratio used in the kerosene and gas oil strippers of the Base Case. Utilities and the separation quality of the product streams will be reported and compared to the Base Case.

4.5.5. Case 4

The PFD of the case 4 process is shown in Figure 4.7.
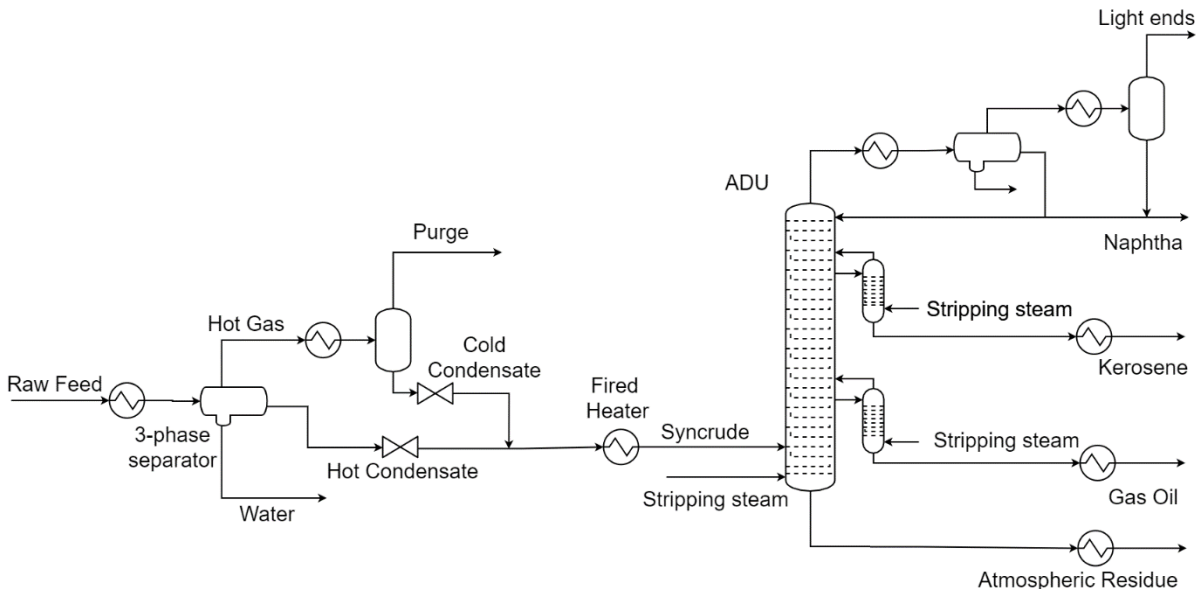
Figure 4.7: Case 4 PFD

The process of case 4 is similar to that of the Base Case. The only difference is that there are no pumparounds and their collective duty from the base case, a total of -1.42 MW, is added to the -5.65 MW of the condenser, resulting in a total cooling duty of -7.07 MW. Utilities do not need to be reported since the utility consumption is by design equal between the Base Case

and case 4. The separation quality of the product streams will be reported and compared to the Base Case.

4.5.6. Case 5

The PFD of the case 5 process is shown in Figure 4.8.
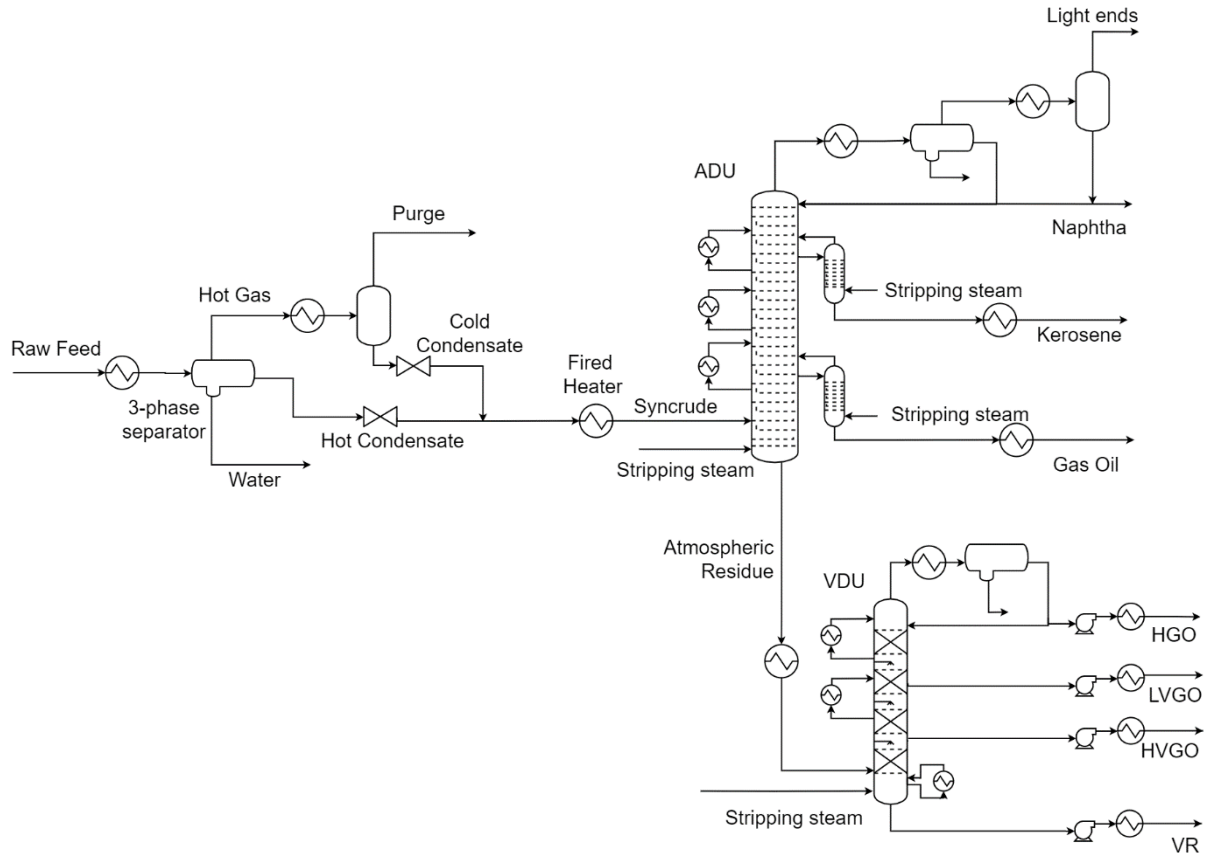
Figure 4.8: Case 5 PFD

The process of case 5 is similar to that of the Base Case. The only difference is that a VDU is added for the fractionation of the AR stream. The VDU is also modelled with the Petrofrac operation unit and has 12 stages. There is a feed preheating furnace that heats the AR stream up to 380°C. The feed enters the column at stage 11. More heat is provided to the column by an HPS stream that is fed at the bottom of the column. The stripping steam mass flow rate to the VDU is 1.25 kg/s. The flow rates of the HGO, LVGO and HVGO streams are 0.92, 1.95 and 0.95 kg/s respectively. The draw-off stages are stage 1, 4 and 8 respectively. All the streams are drawn off as side products.

The VDU has two pumparounds:

- Pumparound 1 draws liquid from stage 4 and returns it to stage 2. The flow rate is 0.5 kg/s, and the heat duty is -0.75 MW.
- Pumparound 2 draws liquid from stage 11 and returns it to stage 7. The flow rate is 1.5 kg/s, and the heat duty is -1 MW.

There is also an overflash stream with a mass flow of 0.5 kg/s which takes liquid from stage 12, passes through the fired heater, and returns to stage 12. The fired heater provides 0.5 MW to the overflash stream. The purpose of the overflash stream is to ensure adequate liquid flow at the bottom stage.

The utility consumption and separation quality of the product streams will be reported. Only the utilities will be compared to the Base Case, since the main product streams are identical.

4.5.7. Cases 6.1 and 6.2

Two heat integration networks are modelled for cases 6.1 and 6.2, one that aims at decreasing total absolute utility consumption and one that aims at decreasing total subcooling duty. All the temperatures, mass flows and stream compositions "seen" by the flash drums, pumps and the ADU are identical to those of the Base Case. Therefore, only utility consumption is reported.

The PFD of the case 6.1 process is shown in Figure 4.9.
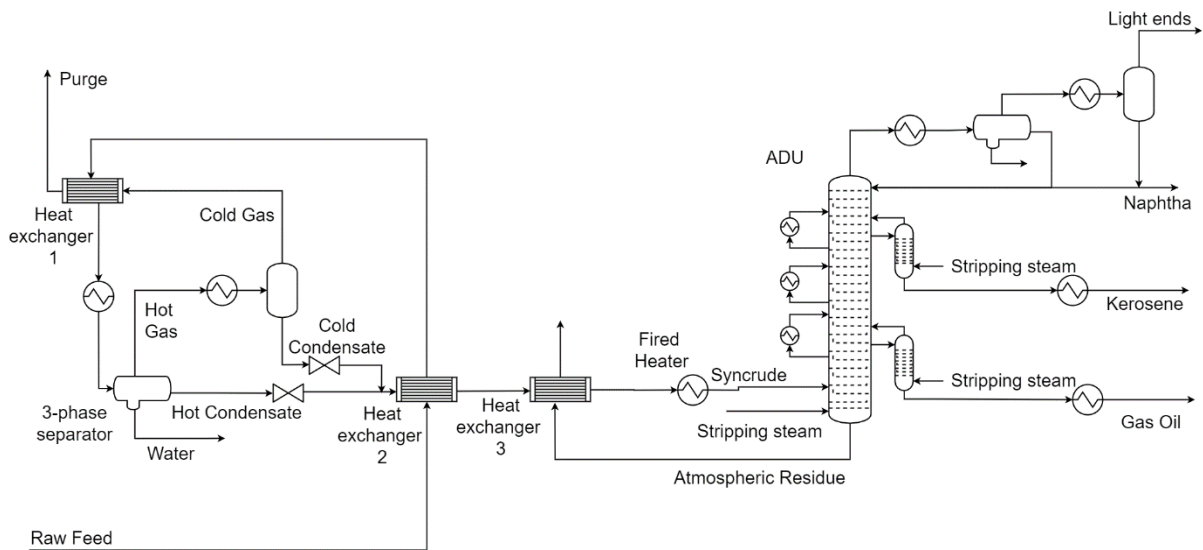
Figure 4.9: Case 6.1 PFD

The process of case 6.1 is similar to that of the Base Case. The only difference is that a heat exchanger network is employed to reduce total absolute duty. The raw feed and the AR are considered hot streams, since their temperature must decrease before the next unit process. The syncrude and the cold gas are considered cold streams, because the former has a temperature below ambient, so it can be used to cool down a hot stream, and the latter needs to increase in temperature before entering the ADU. Therefore, three countercurrent shell and tube heat exchangers are used.

- Heat exchanger 1: The hot stream is the raw feed and the cold stream is the purge stream. The minimum temperature difference is 10°C, which is given between the cold stream outlet and the hot stream inlet.
- Heat exchanger 2: The hot stream is the raw feed and the cold stream is syncrude. The minimum temperature difference is 10°C, which is given between the cold stream outlet and the hot stream inlet.
- Heat exchanger 3: The hot stream is the AR and the cold stream is syncrude. The minimum temperature difference is 10°C, which is given between the hot stream outlet and the cold stream inlet.

The PFD of the case 6.2 process is shown in Figure 4.10.
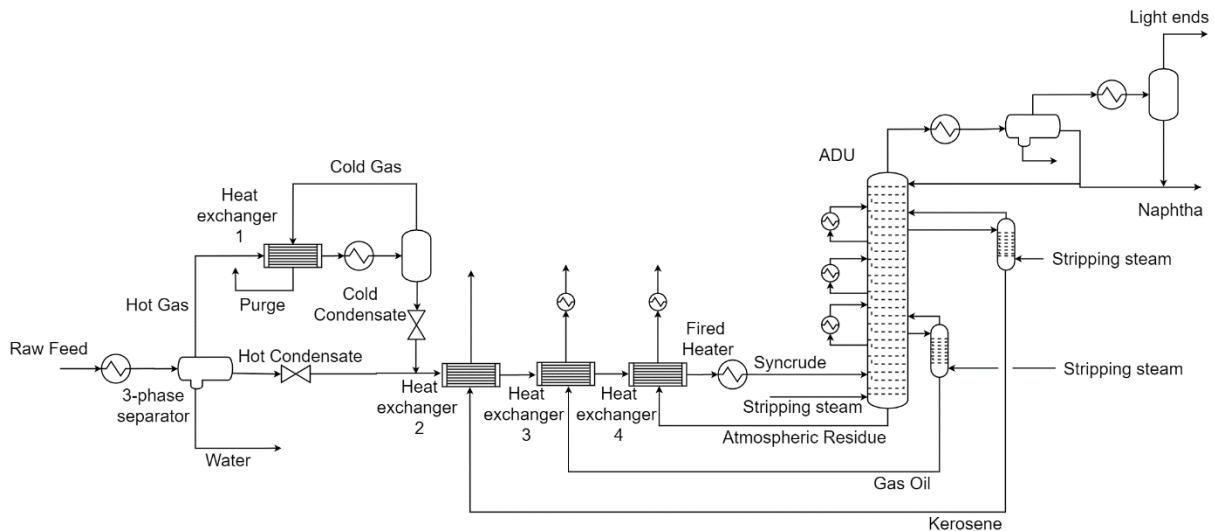
Figure 4.10: Case 6.2 PFD

The process of case 6.2 is similar to that of the Base Case. The only difference is that a heat exchanger network is employed to reduce total subcooling duty. Stream "hot gas" is considered a hot stream, since its temperature must decrease before the next unit process. This is the main difference between the HENs of case 6.1 and case 6.2. In case 6.1, the cold gas at -70°C is used to cool the raw feed down to 20°C, something which can be achieved with cooling water. In case 6.2, cooling water is used to cool down the raw feed instead, and the cold gas is used to cool down the Hot gas instead. Also, streams "kerosene", "gas oil" and "AR" are considered hot streams, since their temperature is above 15°C when exiting the column. Streams "Cold gas" and "syncrude" are considered cold streams, because the former has a temperature below ambient, so it can be used to cool down a hot stream, and the latter needs to increase in temperature before entering the ADU. Therefore, four countercurrent shell and tube heat exchangers are used.

- Heat exchanger 1: The hot stream is the gas from the Hot Condensate 3-phase separator and the cold stream is the Purge stream. The minimum temperature difference is 10°C, which is given between the cold stream outlet and the hot stream inlet.
- Heat exchangers 2-4: The streams kerosene, gas oil and AR are the hot streams of 3 heat exchangers in series and the cold stream is syncrude in all cases. The minimum temperature difference is 10°C, which is given between the cold stream outlet and the hot stream inlet.

4.6. Sensitivity analysis

A sensitivity analysis will be carried out in the Base Case. Five input parameters will be varied, one at a time, to ascertain their effect on the utility consumption and separation quality. The input parameters that will be varied are:

- Feed preheating furnace outlet temperature.
- Condenser duty.
- ADU stripping steam mass flow rate.
- Feed stage location.
- Cold condensate temperature.

The goal is to evaluate the effect varying these parameters has on the following dependent variables:

- Naphtha, kerosene and gas oil purity.
- Naphtha, kerosene and gas oil recovery.
- Utility consumption.

4. Basis of Design

5. Results and discussion

Subsection 5.1 contains the results of syncrude prefractionation, separation quality (purity and recovery) of the main product streams (naphtha, kerosene and gas oil for the Base case, Case 2 and Case 4; naphtha, kerosene, gas oil and HGO for case 3; naphtha, kerosene, gas oil, HGO, LVGO and HVGO for case 5), and utility consumption. Subsections 5.2 to 5.6 report the results of the separation quality of the main product streams of the ADU for each case. Graphs depicting the mass flow of each component group of the ADU feed and the product streams are given as well.

In the context of this chapter, component group is defined as hydrocarbons with the same carbon number.

Detailed tables of the individual stream physical properties and composition can be found in the Appendix.

5.1. Base case

The results of the syncrude prefractionation is shown in Figure 5.1. Recovery of the C_{5+} hydrocarbons in the syncrude (from the raw feed) is 99.66%, while purity of the C_{5+} components in the syncrude stream is 93.60%, which both meet the goals set in the BoD.
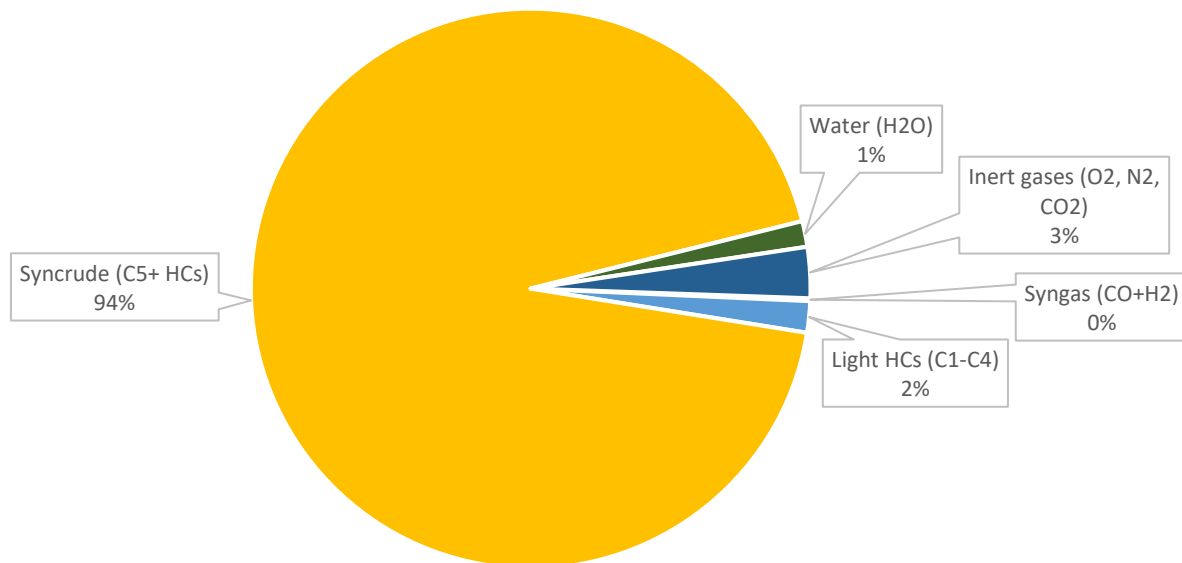
Figure 5.1: ADU feed stream composition

Table 5.1 shows the purity and recovery results of the naphtha, kerosene and gas oil streams for the Base Case process. Details of the stream composition and conditions for the syncrude prefractionation part of the process are shown in Table A.1. Details of the stream composition and conditions for the distillation unit of the Base Case process are shown in Table A.2.

5. Results and discussion

Table 5.1: Base case product stream results

Stream	Mass flow [kg/s]	Product purity (%)	Product recovery (%)
Naphtha	0.797	91.15%	93.42%
Kerosene	1.270	94.99%	97.39%
Gas Oil	1.250	92.40%	91.47%

Figure 5.2 shows the mass flow of each component group in the main feed and product streams. The mass flow of each product in Table 5.2 is equal to the area under the respective curve of Figure 5.2. Mass flow, recovery and purity of the atmospheric residue not reported because atmospheric residue is not a defined product, but a by-product.
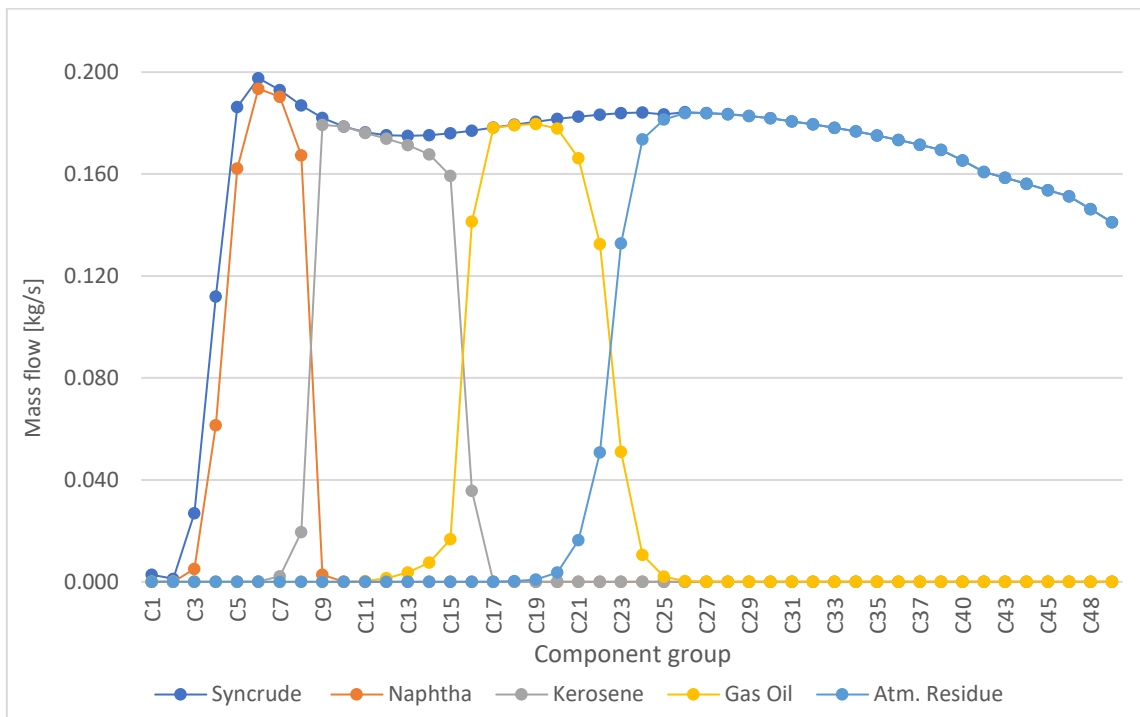
Figure 5.2: Component group mass flow in each stream (Base case)

The purity and recovery of the main products (naphtha, kerosene, gas oil) meet the >90% goals set in the basis of design. The separation quality of the kerosene fraction is especially high, with 97.39% of the components recovered and a stream purity of almost 95%. This indicates that the utility consumption can be reduced, or the column configuration can be altered, in order to have the kerosene purity and recovery closer to the 90% number. Attempts to meet that end however were unsuccessful, since any change in utility consumption or column configuration that successfully decreased kerosene purity and recovery, had an even stronger effect on either the naphtha or gas oil separation quality, bringing the purity and recovery numbers below 90%.

The utility consumption of the process is shown in Table 5.2. The largest duty, in absolute terms, is cooling duty (approximately -73 MW), due to the large mass flow of unwanted gases that are purged (110.619 kg/s). Electrical power consumption is negligible in comparison to the heating and cooling duties. The only cause of electrical power consumption is the pumps that pump the straight run products of the ADU up to atmospheric pressure and have not been depicted in the PFDs.

5. Results and discussion

Table 5.2: Base case utility consumption

Utilities	Utility consumption (MW)
Total heating duty	11.081
Total cooling duty (to ambient)	-72.918
Total cooling duty (below ambient)	-15.105
Total electrical power	0.00844

The total heat per mass of syncrude is:

$$\frac{\dot{Q}_{heating}}{\dot{m}_{syncrude}} = 1.407 \ \frac{MJ}{kg}$$

This value is about 3% of the LHV of liquid hydrocarbons (approximately 45 MJ/kg, [37]). This value will be used for comparison and discussion with cases 3, 5 and 6. In cases 2 and 4 no comparison is made because the heating duty is identical.

The TBP curves of the products are provided in Figure 5.3.
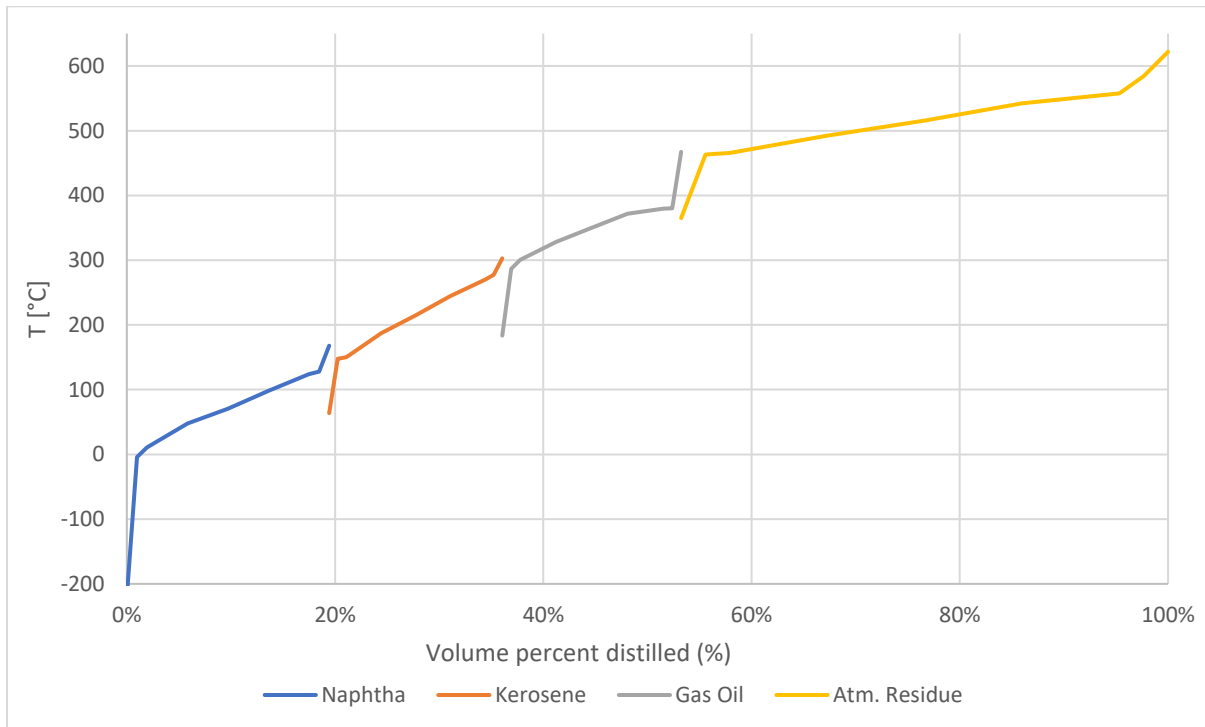
Figure 5.3: TBP curves of the cuts for the Base Case.

The cut point temperatures and volume percentages for each product are similar between the Base Case process and the cut points from literature. The differences can be attributed to a different crude (feed) composition, and different product specifications. For instance, one of the goals of this project was maximizing kerosene yield. To that end, the ADU is configured in a way such that C_{9-10} hydrocarbons, which are usually part of the heavy naphtha cut, are in this case part of the kerosene cut. The kerosene yield is about 15% of the total product volume in the Base Case. The 5% and 95% distilled product points are 148°C and 277°C, which are nearly identical to the same cut points in the Bintulu plant (see Figure 2.9). On the contrary, the yield of kerosene from the Middle Eastern crude is only about 10.5%, and the 5% cut point is around 210°C.

The TBP curve of the residue fraction of the Base Case resembles closely the one of the Middle Eastern crude (see Figure 2.10), with it taking up 45% of the total product volume, and having a final boiling point in the order of 600°C. The corresponding cut from the Bintulu plant (see Figure 2.9) is much smaller in volume and has a steeper TBP curve, reaching up to a final boiling point of about 900°C. This means that the hydrocarbons in the C_{23+} range make up much less of the total crude feed volume, and the composition is shifted more towards components heavier than C_{50+}.

5.2. Case 2

The duty required to heat up water, with a mass flow of 0.025 kg/sec, from 15°C to 175°C at 4 bar of pressure is 62 kW. Thus, a reboiler with a duty of 62 kW is added to the first side stripper of the ADU, replacing the stripping steam. Table 5.3 shows the purity and recovery of the naphtha, kerosene and gas oil streams for the case 2 process and the comparison to the Base Case. Details of the stream composition and conditions for the distillation unit of the Case 2 process are shown in Table A.3.

Table 5.3: Case 2 product stream results

Stream	Mass flow [kg/s]	Product purity (%)	Purity difference from Base Case (%)	Product recovery (%)	Recovery difference from Base Case (%)
Naphtha	0.717	89.50%	-1.65%	84.06%	-9.37%
Kerosene	1.270	92.52%	-2.47%	94.86%	-2.53%
Gas Oil	1.250	92.14%	-0.26%	91.21%	-0.26%

Figure 5.4 shows the mass flow of each component group in the main feed and product streams.
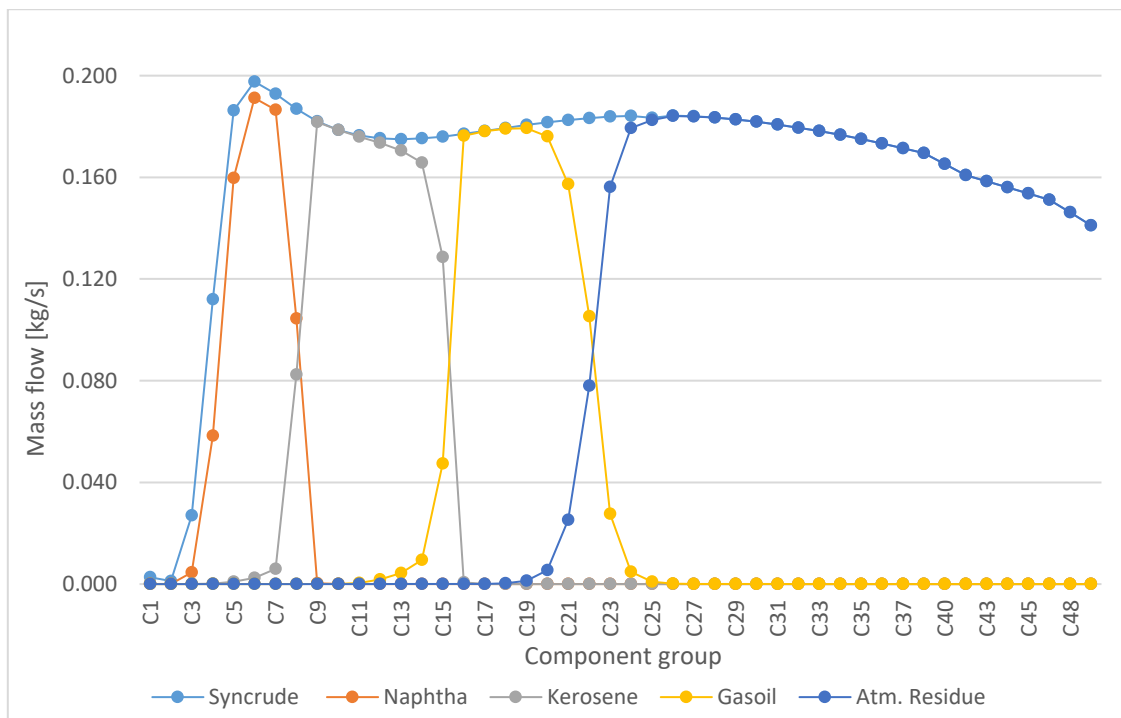
Figure 5.4: Component group mass flow in each stream (Case 2)

A steep decrease of 0.062 kg/s is observed for the C_8 components in the naphtha stream, causing recovery to decrease by -9.37% compared to the Base Case. Naphtha purity also decreases by -1.65% compared to the Base Case.

The C_{8+} components not drawn off in the naphtha stream end up in the kerosene stream. In order to maintain the mass balance, a small amount of C_{15} components is lost. This causes purity and recovery to both decrease by approximately -2.5% with respect to the Base Case.

Gas oil purity and recovery are mostly unaffected, with a decrease of -0.26% each compared to the Base Case.

Table 5.4 shows the utility consumption for Case 2, while comparing it to the Base Case. The formula used in the calculation of the difference between the current case and the Base Case is:

$$D_i = \frac{A_i - B}{B}$$

where D is the difference in consumption of Case i

A is the utility consumption of Case i

B is the utility consumption of the Base Case

Table 5.4: Case 2 utility consumption

Utilities	Utility consumption of Case 2 (MW)	Utility consumption of the Base Case (MW)	Difference of Case 2 from the Base Case (%)
Total heating duty	11.081	11.081	0.00%
Total cooling duty (to ambient)	-72.986	-72.918	0.09%
Total cooling duty (below ambient)	-15.105	-15.105	0.00%
Total electrical power	0.00844	0.00844	0.00%

Cooling duty is slightly higher (0.09% increase compared to the Base Case), due to small differences in product stream mass flow rate and composition. Heating utility consumption is the same as the Base Case.

5.3. Case 3

A third steam stripper is added to the Base Case ADU, in order to draw HGO as the bottom product. Table 5.5 shows the purity and recovery of the naphtha, kerosene and gas oil streams for the case 3 process. Details of the stream composition and conditions for the distillation unit of the Case 3 process are shown in Table A.4.

Table 5.5: Case 3 product stream results

Stream	Mass flow [kg/s]	Product purity (%)	Purity difference from Base Case (%)	Product recovery (%)	Recovery difference from Base Case (%)
Naphtha	0.773	89.57%	-1.57%	90.66%	-2.77%
Kerosene	1.270	94.78%	-0.21%	97.17%	-0.22%
Gas Oil	1.250	90.18%	-2.23%	89.26%	-2.21%

5. Results and discussion

Figure 5.5 shows the mass flow of each component group in the main feed and product streams, so that the separation quality can be visualised.
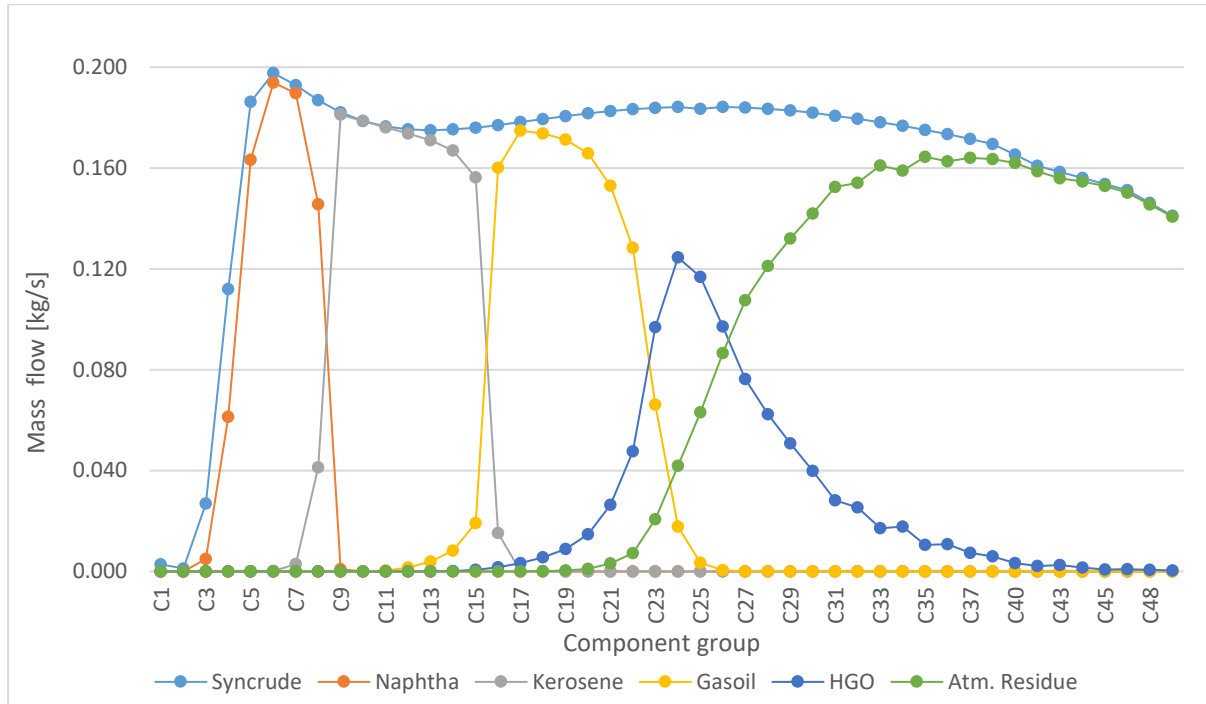
Figure 5.5: Component group mass flow in each stream (case 3)

The decrease in naphtha recovery is -2.77% compared to the Base Case. This can be mostly attributed in the loss of some C_8 components in the kerosene stream. Naphtha purity decreases by -1.57% compared to the Base Case, due to the higher draw-off of C_4 components.

Kerosene purity and recovery are not affected, with an absolute difference of -0.21% and -0.22% compared to the Base Case.

The purity and recovery decrease are most apparent in the case of the gas oil stream, where there is a -2.23% and -2.21% decrease, respectively. The HGO product contains about 0.61 kg/s of gas oil range components, causing the gas oil recovery to decrease. Purity also decreases, since an equal amount of C_{23+} components are now part of the gas oil stream.

Table 5.6 shows the utility consumption for case 3as compared to the Base Case.

Table 5.6: Case 3 utility consumption

Utilities	Utility consumption of Case 3 (MW)	Utility consumption of the Base Case (MW)	Difference of Case 3 from the Base Case (%)
Total heating duty	11.131	11.081	0.45%
Total cooling duty (to ambient)	-73.011	-72.918	0.13%
Total cooling duty (below ambient)	-15.105	-15.105	0.00%
Total electrical power	0.008	0.00844	0.00%

Despite the higher utility consumption, separation quality for the main streams has deteriorated. This is consistent with literature, where it is stated that increasing the number of

draw-off streams from any given ADU decreases separation quality (see section 2.3). Heating duty is increased by 0.45% due to the extra steam necessary for the third stripper.

The total heat per mass of syncrude is:

$$\frac{\dot{Q}_{heating}}{\dot{m}_{syncrude}} = 1.413 \frac{MJ}{kg}$$

which is a 0.45% increase with respect to the Base Case. Since the heating duty per unit mass of syncrude increases, while the purity and recovery of the main products decrease, this is not an appropriate addition to the column if the goal is recovering naphtha, kerosene and gas oil only. However, if HGO is a desirable product, it can be obtained with the addition of a small side column. In this last case, the increase in heating duty is minimal, and the decrease in purity and recovery of the main streams is small.

5.4. Case 4

The heat duties of pumparounds 1, 2 and 3 are -0.28, -0.38 and -0.76 MW respectively, summing up to a total of -1.42 MW. This value, added to the -5.65 MW of the condenser heat duty, gives us the new value of -7.07 MW for the cooling duty of the condenser.

Table 5.7 shows the purity and recovery of the naphtha, kerosene and gas oil streams for the case 4 process. Details of the stream composition and conditions for the distillation unit of the Case 4 process are shown in Table A.5.

Table 5.7: Case 4 product stream results

Stream	Mass flow [kg/s]	Product purity (%)	Product recovery (%)	Purity difference from Base Case (%)	Recovery difference from Base Case (%)
Naphtha	0.808	87.42%	92.51%	-3.73%	-0.91%
Kerosene	1.270	92.64%	94.99%	-2.35%	-2.40%
Gas Oil	1.250	90.18%	89.26%	-2.23%	-2.21%

Figure 5.6 shows the mass flow of each component group in the main feed and product streams, so that the separation quality can be visualised.
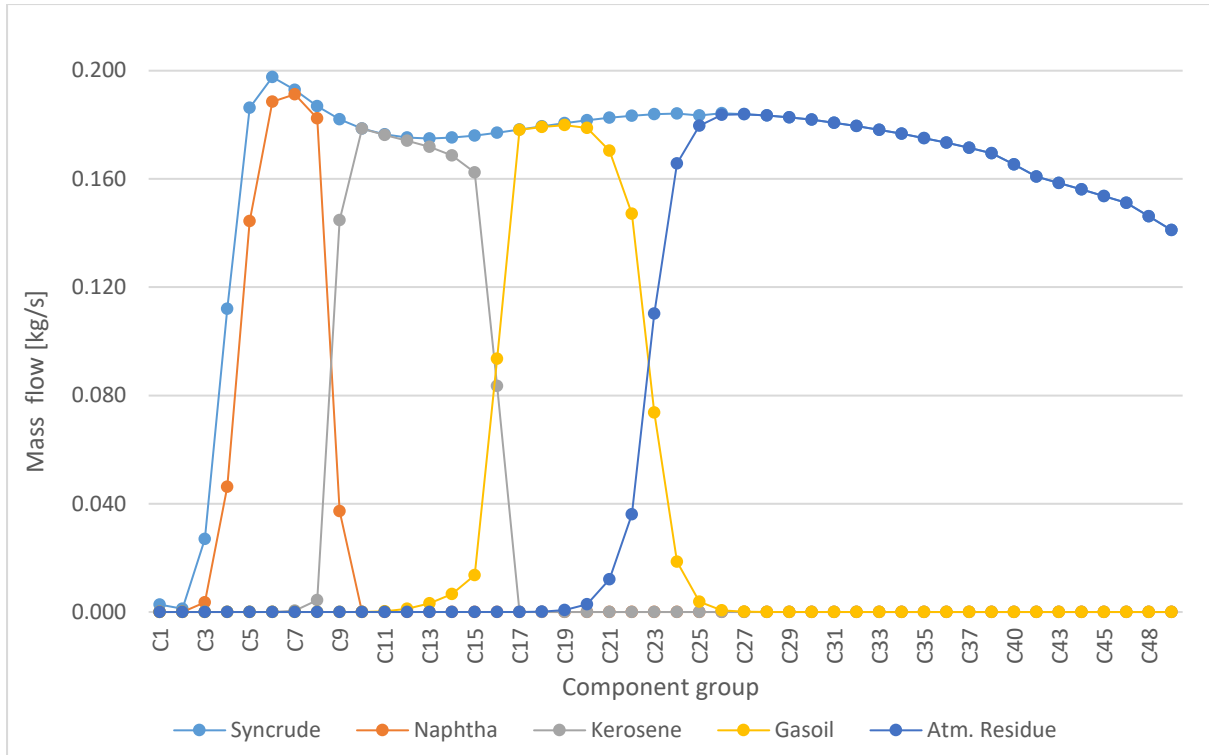
Figure 5.6: Component group mass flow in each stream (case 4)

Due to the concentration of the cooling duty in the condenser stage, purity and recovery for all product streams is decreasing. The small increase in cooling duty is due to the differences in product stream temperature and composition.

Naphtha yield is slightly higher compared to the Base Case, mostly due to the increase in C_9 component uptake. This causes a -3.73% decrease in purity. The recovery of all the components in the C_{5-8} range is slightly decreased, causing naphtha recovery to decrease by -0.91%.

Kerosene recovery and purity also decrease by -2.40% and -2.35% respectively, compared to the Base Case. The recovery decrease is attributed to the rather steep decrease in C_9 component uptake, as well as a decrease in the C_{10-15} uptake. An additional mass flow of 0.78 kg/s of C_{16} components are recovered in the kerosene stream to maintain mass balance, causing the decrease in purity.

In a similar vein, gas oil recovery and purity decrease by -2.21% and -2.23% respectively, due to the lower recovery of C_{16-22} components and the higher recovery of C_{23+} components.

5.5. Case 5

The atmospheric residue can be further fractionated into HGO, LVGO and HVGO with the use of a vacuum distillation unit. The results of this fractionation is shown in Table 5.8. Details of the stream composition and conditions for the vacuum distillation unit of the Case 5 process are shown in Table A.6.

5. Results and discussion

Table 5.8: Case 5 product stream results

Stream	Mass flow [kg/s]	Component purity (%)	Component recovery (%)
Naphtha	0.797	91.15%	93.42%
Kerosene	1.270	94.99%	97.39%
Gas Oil	1.250	92.40%	91.47%
HGO	0.920	74.59%	74.56%
LVGO	1.953	85.13%	85.08%
HVGO	0.946	75.29%	71.91%

Figure 5.7 shows the mass flow of every component group in each stream.
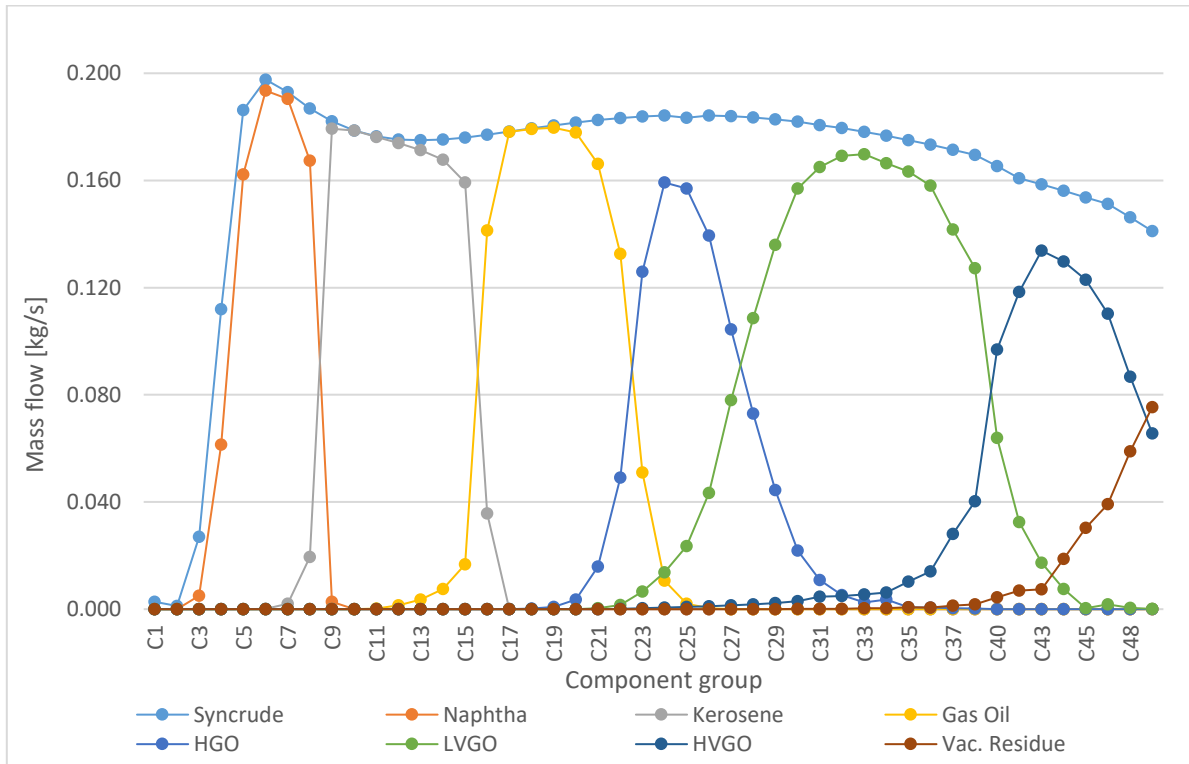
Figure 5.7: Component group mass flow in each stream (case 5)

Table 5.9 shows the utility consumption for case 5, while comparing it to the Base Case.

Table 5.9: Case 5 utility consumption

Utilities	Utility consumption of Case 5 (MW)	Utility consumption of the Base Case (MW)	Difference of Case 5 from the Base Case (%)
Total heating duty	16.869	11.081	52.23%
Total cooling duty (to ambient)	-81.421	-72.918	11.66%
Total cooling duty (below ambient)	-15.105	-15.105	0.00%
Total electrical power	0.018	0.00844	110.61%

5. Results and discussion

Utility consumption increases across the board, especially in heating duty. The heat to syncrude mass ratio is:

$$\frac{\dot{Q}_{heating}}{\dot{m}_{syncrude}} = 2.142 \ \frac{MJ}{kg}$$

Which is a 52.23% increase with respect to the Base Case.

The VDU meets the 70% goal for purity and recovery of HGO, LVGO and HVGO streams. Its implementation is desirable when HGO, LVGO and HVGO separation is desirable for fuel, lubricant and hydrocracker feedstock preparation.

The TBP curves of the cuts from Case 5 are shown in Figure 5.8.
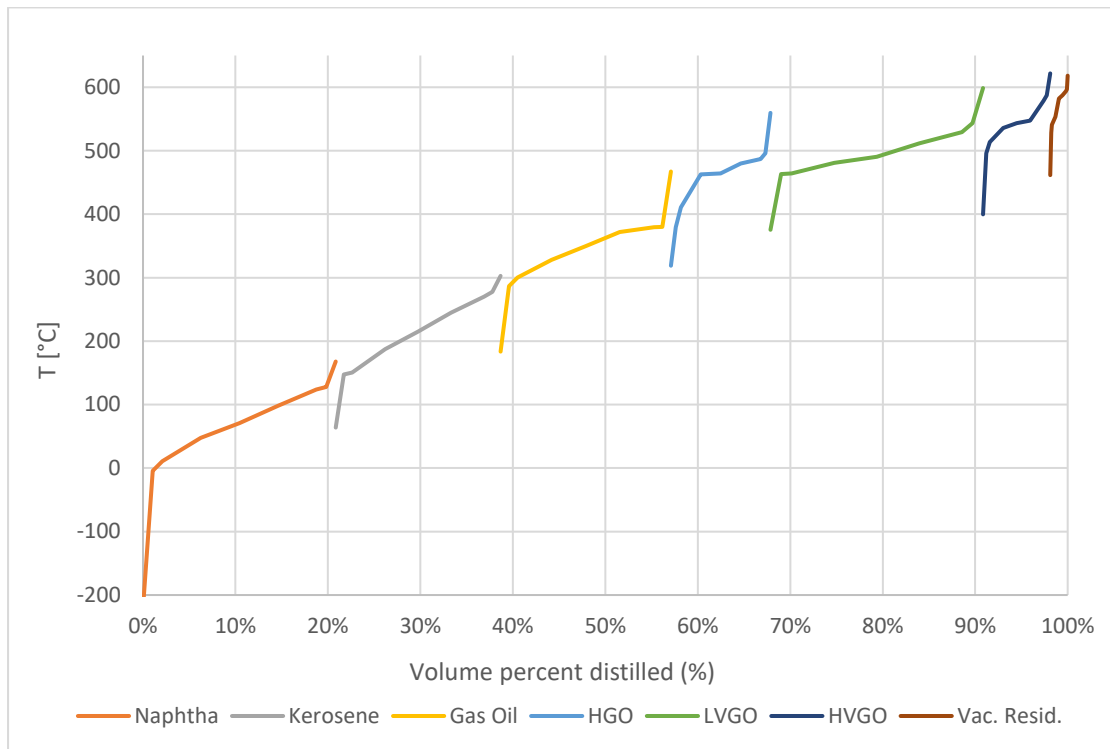
Figure 5.8: TBP curves of the cuts for Case 5.

There is significant boiling point overlap in the VDU products compared to the ADU products, especially between HVGO and VR.

With respect to the VDU alone, the heat to syncrude ratio is:

$$\frac{U_{heating}}{\dot{m}_{syncrude}} = 1.406 \ \frac{MJ}{kg}$$

which is the same as the heating utility to feed ratio for the Base Case. However, the purity and recovery of the VDU product streams is much lower than that of the ADU. This is attributed to the closer boiling points of the components in the C_{23+} range, as well as the smaller number of equilibrium stages. It is worth mentioning, however, that the separation quality of both the ADU products and the HGO stream is higher in case 5 compared to case 3.

5.6. Cases 6.1 and 6.2

The HENs of cases 6.1 and 6.2 are shown in Figure 5.9.
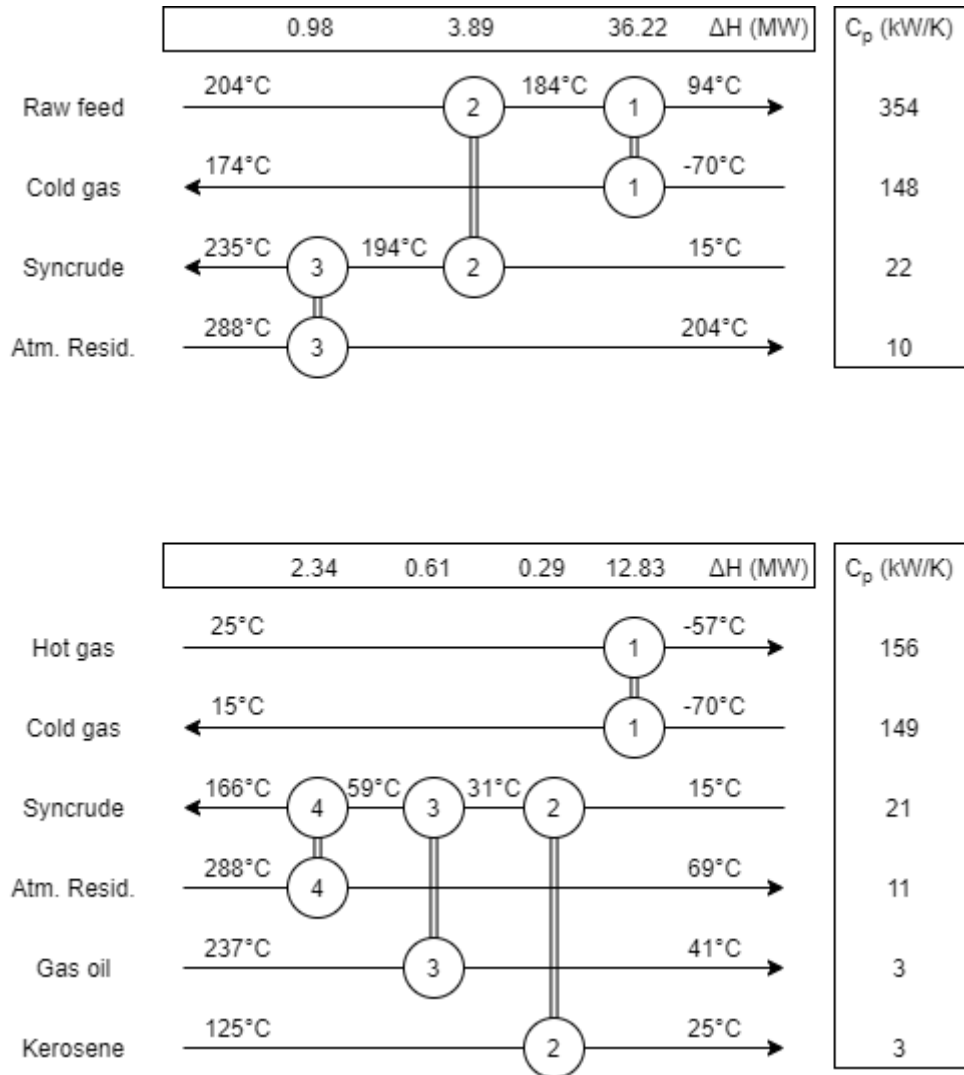
Figure 5.9: HEN schematics for cases 6.1 and 6.2. Right facing arrows indicate a hot stream, left facing arrows indicate a cold stream. Heat exchanger duties shown above the schematics, stream names shown at the left, heat exchanger number on the heat exchanger symbol, heat capacity flows shown at the right. Only heat exchangers between streams are shown, heat sources and sinks are not.

The separation quality in the heat integration cases is identical to the Base Case, so separation quality and stream composition results are not reported. The utility consumption for cases 6.1 and 6.2 is shown in Table 5.10 and Table 5.11 respectively.

5. Results and discussion

Table 5.10: Case 6.1 utility consumption

Utilities	Utility consumption of Case 6.1 (MW)	Utility consumption of the Base Case (MW)	Difference of Case 6.1 from Base Case (%)
Total heating duty	6.136	11.081	-44.62%
Total cooling duty (to ambient)	-27.551	-72.918	-62.22%
Total cooling duty (below ambient)	-15.105	-15.105	0.00%
Total electrical power	0.008	0.008	0.00%
Total absolute consumption	48.801	99.112	-50.76%

Table 5.11: Case 6.2 utility consumption

Utilities	Utility consumption of Case 6.2 (MW)	Utility consumption of the Base Case (MW)	Difference of Case 6.2 from Base Case (%)
Total heating duty	7.770	11.081	-29.88%
Total cooling duty (to ambient)	-62.602	-72.918	-14.15%
Total cooling duty (below ambient)	-2.255	-15.105	-85.07%
Total electrical power	0.008	0.008	0.00%
Total absolute consumption	72.635	99.112	-26.71%

In case 6.1, heating duty, cooling duty and total absolute duty see a decrease of about half compared to the Base Case. Meanwhile, the heating duty, cooling duty and total absolute duty have a smaller decrease compared to the Base Case in case 6.2, but subcooling duty decreases by almost an order of magnitude.

Utility consumption decreases in both case 6.1 and case 6.2. The heat to syncrude ratio for case 6.1 is:

$$\frac{\dot{Q}_{heating}}{\dot{m}_{syncrude}} = 0.779 \frac{MJ}{kg}$$

which is a -44.62% decrease compared to the Base Case. The heat to syncrude ratio for case 6.2 is:

$$\frac{\dot{Q}_{heating}}{\dot{m}_{syncrude}} = 0.987 \frac{MJ}{kg}$$

which is a -29.88% decrease compared to the Base Case.

6. Sensitivity analysis

In the present chapter, the results of the sensitivity analysis for the Base Case are reported. Five different parameters are varied: Cold condensate temperature, feed stage, condenser duty, stripping steam mass flow and feed preheating temperature.

6.1. Cold condensate temperature

As mentioned in the basis of design, a sensitivity analysis is carried out in order to evaluate whether -70°C is an appropriate temperature for the subcooling of the hot condensate gas when the goal is to have >90% purity of the C_{5+} hydrocarbons in the syncrude and >99.5% recovery of the C_{5+} hydrocarbons from the Raw feed.

The controlled variable is the output temperature of the cooler before the cold condensate flash drum, and the dependent variables are syncrude recovery (the ratio of the total mass flow of C_{5+} components in the ADU feed over the same components in the raw feed) and syncrude purity (the mass fraction sum of C_{5+} components in the syncrude).

The results of the sensitivity analysis of syncrude purity and recovery as functions of the Cold Condensate cooling temperature is shown in Figure 6.1.
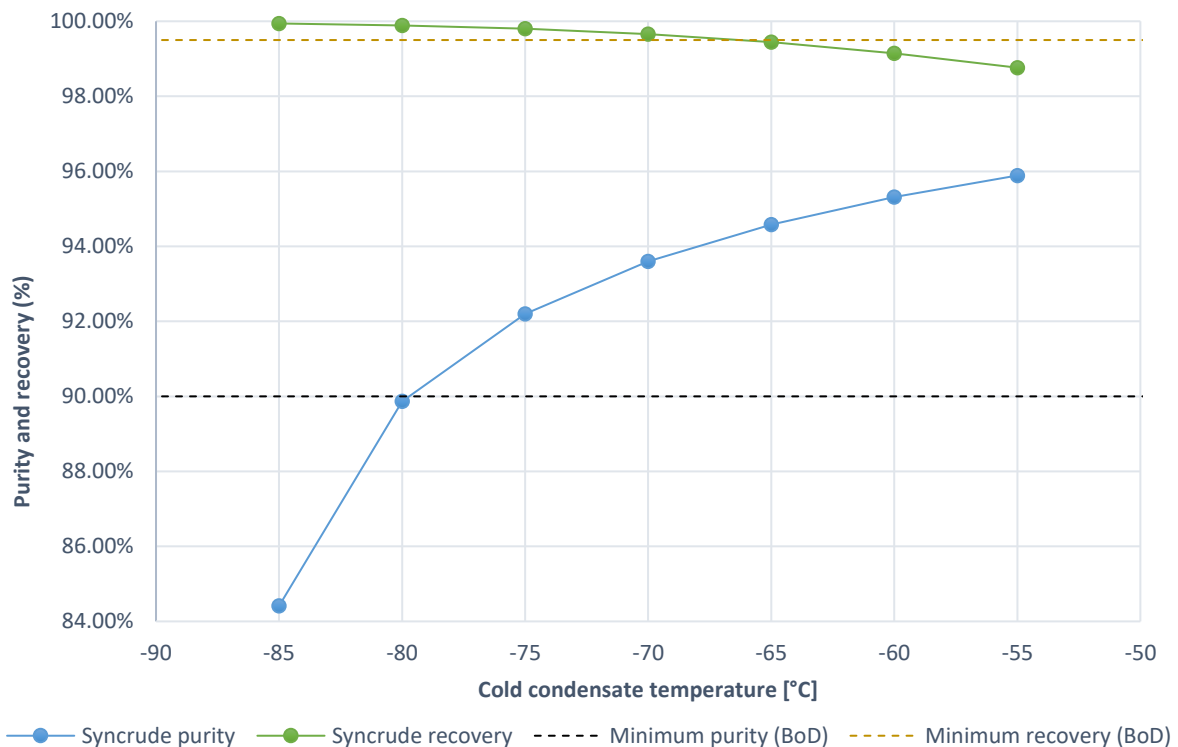
Figure 6.1: Syncrude purity and recovery as a function of the Cold Condensate cooling temperature

It is shown, from the intersections of the dotted lines for the required purity and recovery according to the basis of design with their respective curves for the purity and recovery of syncrude, that Cold condensate cooling temperatures between -67°C and -79°C are acceptable. Therefore, the BoD value of -70°C is acceptable.

6.2. Feed stage

The results of the sensitivity analysis of the purity and recovery of the naphtha, kerosene and gas oil streams as functions of the feed stage location is shown in Figure 6.2 and Figure 6.3.
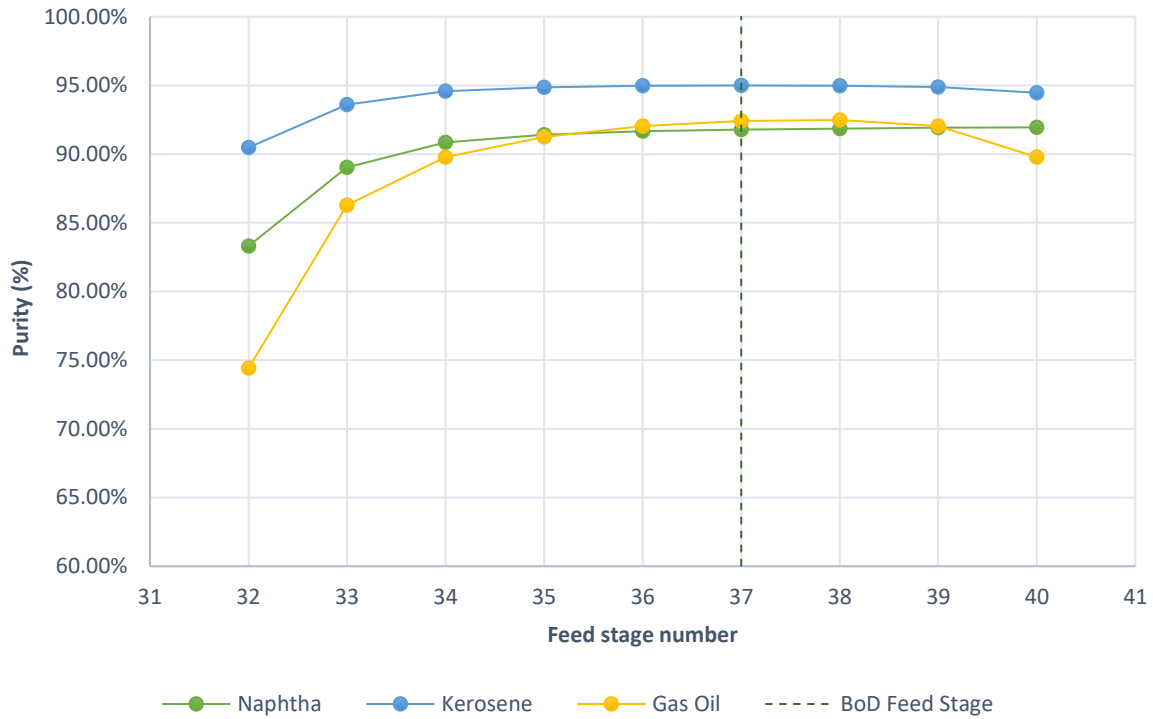
Figure 6.2: Product Purity as a function of Feed Stage
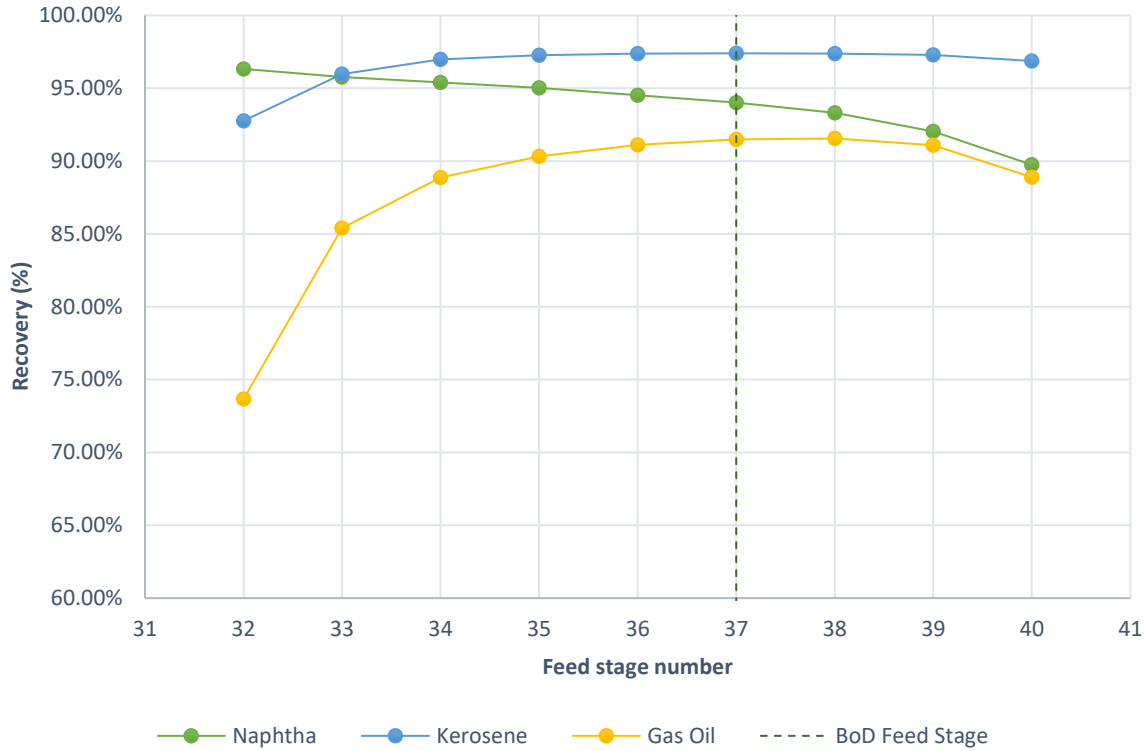
Figure 6.3: Product Recovery as a function of Feed Stage

Gas oil exhibits maximum purity and recovery when the feed enters the column at the 37th stage. Both purity and recovery display a steep drop when the feed enters at stage 32, which in part is attributed to the feed stage being above stage 33, where the liquid draw-off for the gas oil stripper occurs. This means that the gas oil stripper draw-off, so the composition of the gas oil stream is much closer to the syncrude composition. Kerosene recovery and purity are not affected at all between stages 35 and 39 and decrease slightly when the feed stage is above or below that.

Naphtha recovery decreases when the feed stage is below the 37th. This is in part because the feed comes in contact with the less volatile components of the lower stages and does not increase the temperature of the lighter, naphtha-range hydrocarbons enough. Therefore, some of the C_{5-8} components condense at a stage below 1, and naphtha recovery decreases. In order to retain the energy balance, the AR stream is at a higher temperature. Conversely, when the feed stage is higher than 37, naphtha purity decreases. This is attributed to more kerosene range hydrocarbons being vaporized from the higher equilibrium stages, condensing at the top stage.

6.3. Condenser duty

The results of the sensitivity analysis of the purity and recovery of the naphtha, kerosene and gas oil streams as functions of the condenser duty is shown in Figure 6.4 and Figure 6.5.

6. Sensitivity analysis
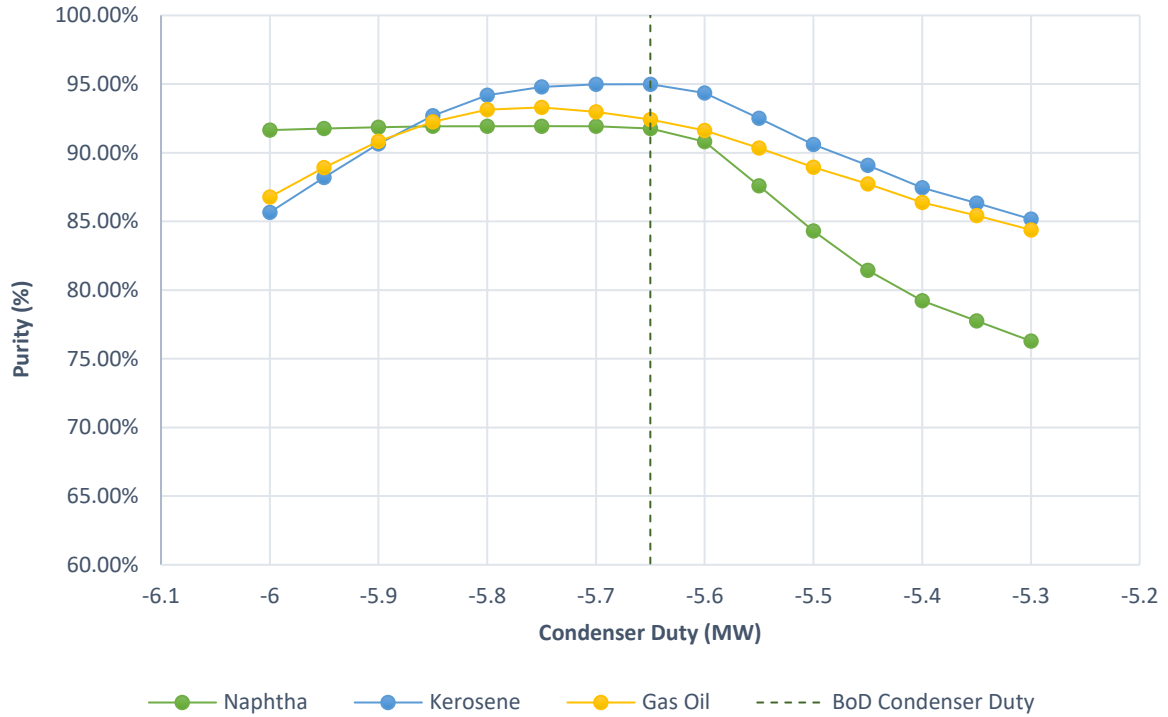
Figure 6.4: Product Purity as a function of Condenser Duty
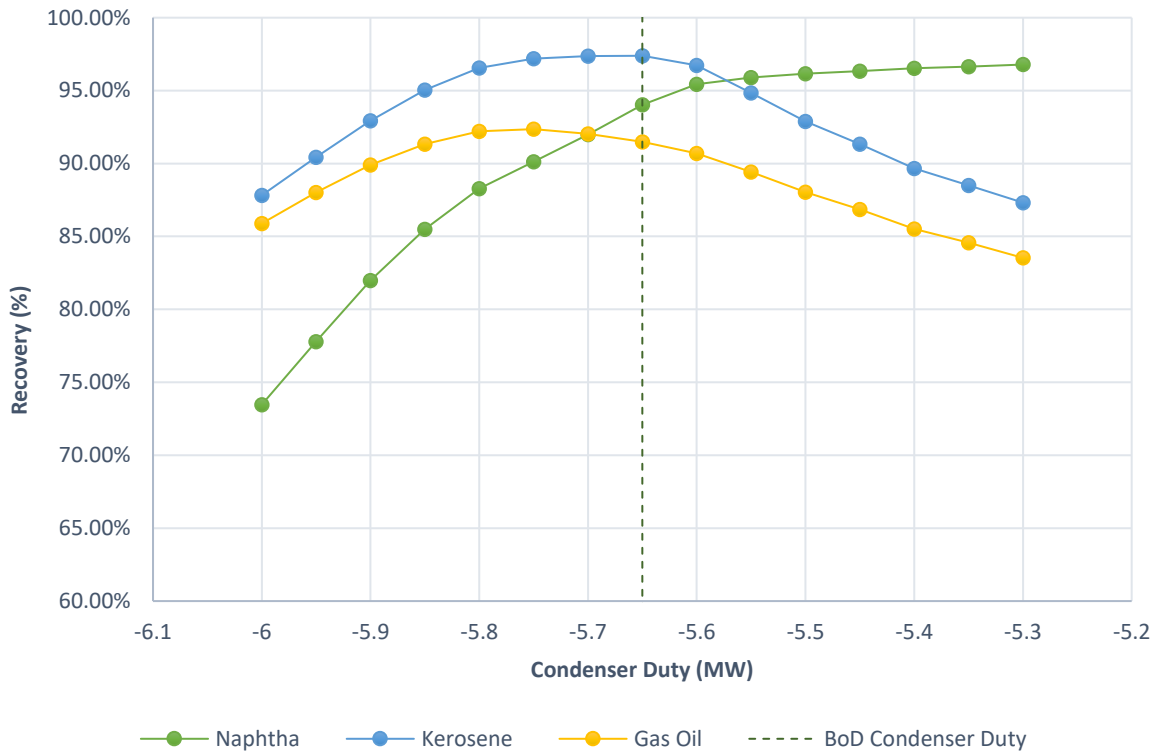
Figure 6.5: Product Recovery as a function of Condenser Duty

It can be observed that purity and recovery for the kerosene stream reach their maximum values at and around the BoD condenser duty set point, i.e., -5.65 MW. Gas oil purity and recovery reach a maximum value at a slightly higher condenser duty: -5.8 MW. Naphtha purity decreases sharply at -5.6 MW of condenser duty or less, while naphtha recovery sharply

decreases at -5.75 MW of condenser duty or higher. Naphtha purity and recovery between those values is >90%.

A higher condenser duty means that the temperature at the top stages decreases more, causing hydrocarbons in the naphtha range (e.g., C_8 hydrocarbons), to condense at lower stages. Therefore, naphtha recovery decreases with increasing condenser duty. Purity is increased, since only the most volatile components condense at the top stage to be drawn off as distillate while almost all the C_{9+} components condense at stages below the first and are not drawn off in the naphtha stream. The purity of the kerosene and gas oil products both decreases with a higher condenser duty, because both products contain more light components outside the desired components range. Similarly, the recovery of both products decreases because they contain less components from the heavy part of their desired component range.

Conversely, a lower condenser duty means that the top stages are at a higher temperature. This causes naphtha recovery to increase since more C_{5-8} components are vaporized, move higher in the column and condense at the top stage. Due to the higher temperature at the top stages, some of the light kerosene range components condense at the top stage, which decreases naphtha purity. As in the case of higher condenser duty, the purity and recovery of the kerosene and gas oil products decreases. However, the explanation in the case of lower condenser is different. With a lower condenser duty, both products contain more heavy components outside the desired components range, thus decreasing purity. Additionally, the recovery of both products decreases because they contain less components from the light part of their desired component range.

6.4. ADU Stripping steam

The results of the sensitivity analysis of the purity and recovery of the naphtha, kerosene and gas oil streams as functions of the high pressure stripping steam mass flow rate in the ADU is shown in Figure 6.6 and Figure 6.7.
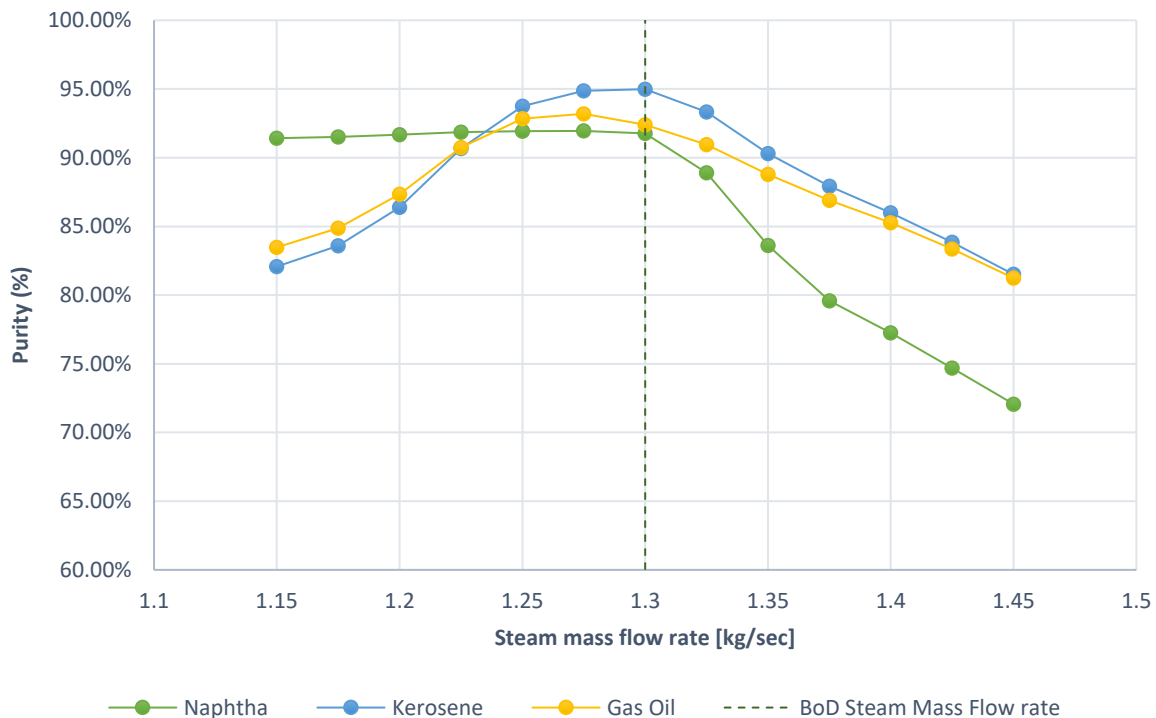
Figure 6.6: Product Purity as a function of Steam Mass Flow
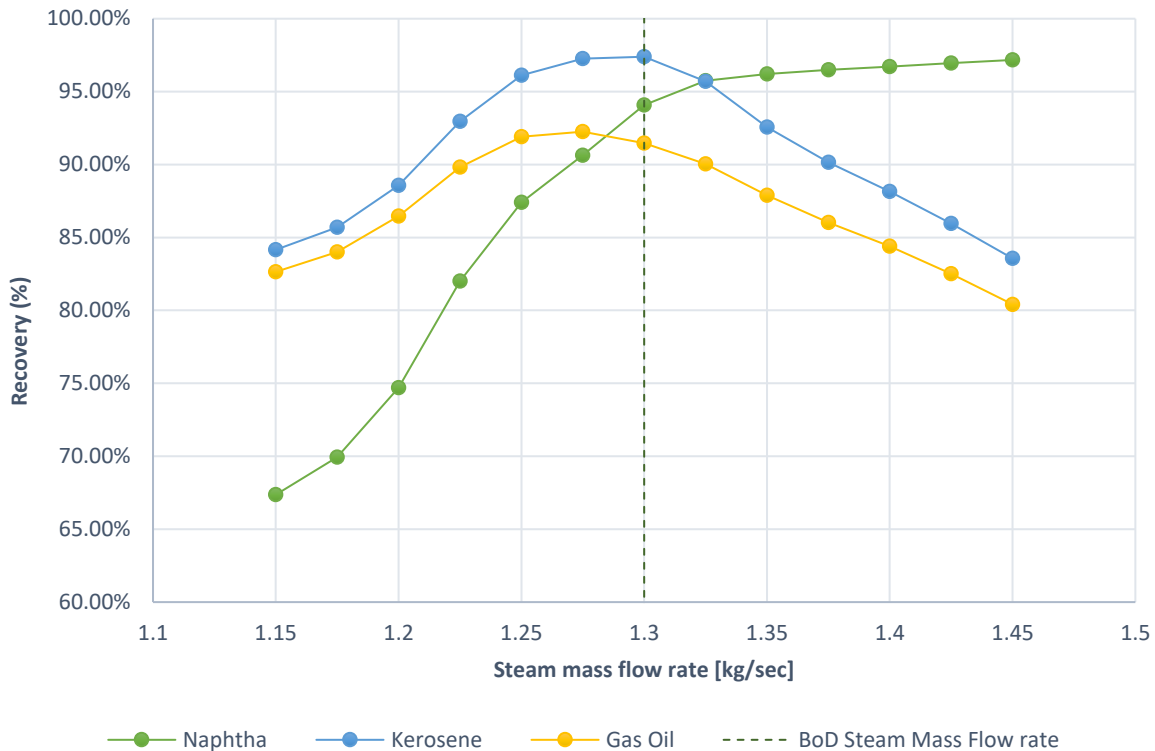
Figure 6.7: Product Recovery as a function of Steam Mass Flow

Varying the stripping steam mass flow to the ADU shows that the maximum for the purity and recovery of the kerosene stream is at the BoD set point, 1.3 kg/s. Gas oil purity and recovery has a maximum at a slightly smaller flow, 1.275 kg/s.

Naphtha recovery decreases especially steeply with steam flow rates below 1.275 kg/s, while purity decreases with increasing steam flow, especially above 1.3 kg/s. The former is explained by some heavier components from the naphtha range condensing at a stage lower than the first, decreasing recovery. C_{9+} impurities that are present in the naphtha stream in the BoD steam flow case also condense at lower stages when steam flow decreases, thus increasing purity. In the case of higher steam flow, the opposite result takes place. The increased steam flow in the ADU causes more components both from the heavy end of the naphtha range and from the light end of the kerosene range to be drawn off as distillate. Therefore, there are more naphtha range hydrocarbons in the naphtha stream, increasing recovery. However, there are more non-naphtha range hydrocarbons in the naphtha stream as well, reducing purity.

In the case of lower steam flow, kerosene and gas oil purity and recovery both decrease because both products contain more light hydrocarbons outside their range and less heavy hydrocarbons from inside their range. In contrast, when steam flow is higher, kerosene and gas oil purity both decrease because the products contain less light hydrocarbons from inside their range and more heavy hydrocarbons from outside their range.

6.5. Preheating furnace outlet temperature

The results of the sensitivity analysis of the purity and recovery of the naphtha, kerosene and gas oil streams as functions of the feed preheating furnace outlet temperature is shown in Figure 6.8 and Figure 6.9.
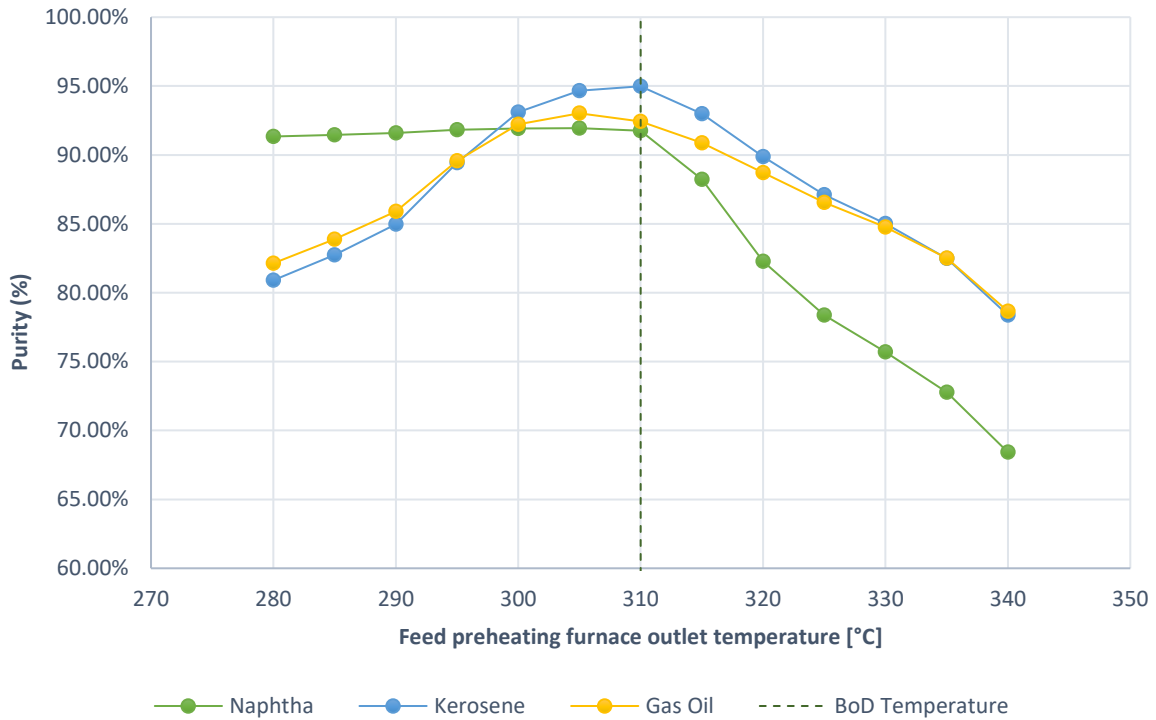
Figure 6.8: Product Purity as a function of the ADU Feed Temperature
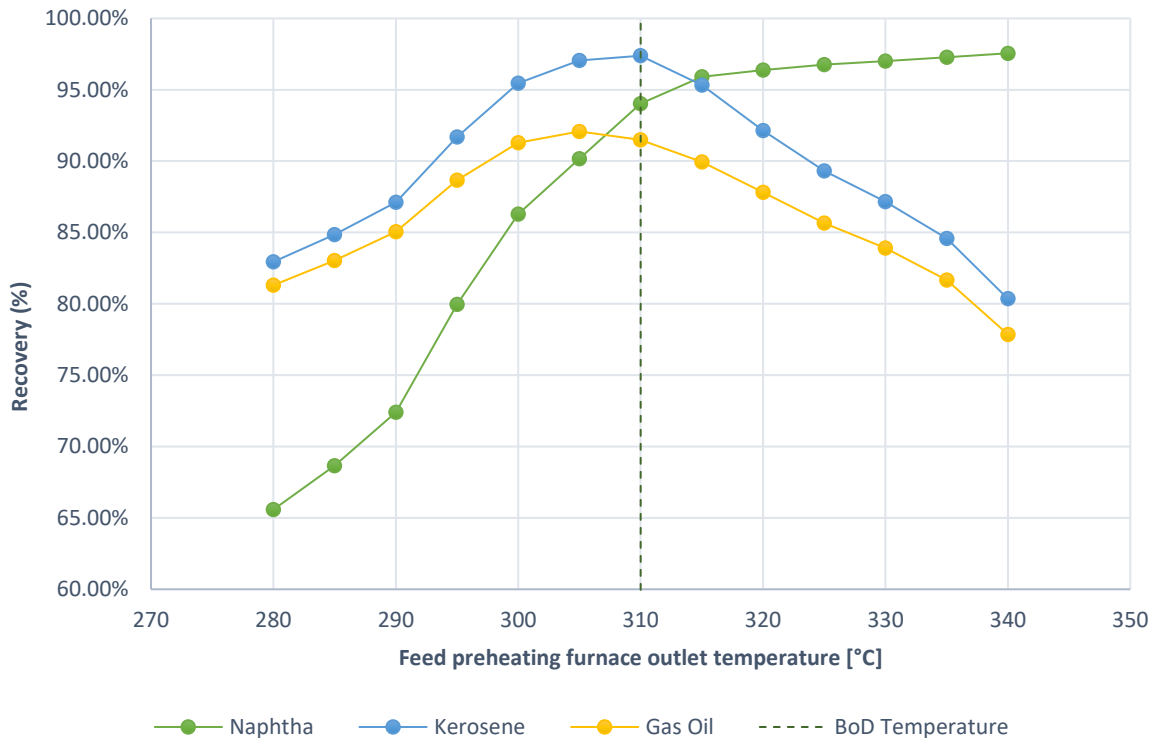
Figure 6.9: Product Recovery as a function of the ADU Feed Temperature

By varying the ADU feed temperature it is seen that kerosene purity and recovery, are at their maximum value at the BoD temperature set point value, i.e., 310°C. Gas oil purity and recovery reach a maximum value at a slightly colder temperature, 305°C.

Similarly to the previous point, naphtha is displaying a decrease in purity below the 90% mark if the ADU feed is heated to 305°C or lower, while purity decreases below 90% if the ADU feed is heated to 312°C or higher. This is attributed to higher temperatures causing more components in the heavy naphtha and light kerosene range to be drawn off in the naphtha stream, which means more naphtha range material is in the naphtha stream (increasing recovery), but more non-naphtha range material is in the naphtha stream as well (decreasing purity). In contrast, a lower feed temperature causes less heavy naphtha components and less light kerosene components to condense at the top stage, thus decreasing recovery and increasing purity of the naphtha stream.

Kerosene and gas oil purity decrease with lower temperature as well as with high temperature. In the former case, it is attributed to the presence of more light components outside the product range, while in the latter case it is attributed to the presence of more heavy components outside the product range. Recovery of these products also decreases with an increase or decrease in feed temperature. In the former case, recovery decreases due to a lower presence of light components from the product range, while in the latter case the missing components are from the heavy end of the product range.

7. Conclusions

The goal of this project was to create a computer simulation model of a syncrude distillation process in ASPEN Plus for the distillation of 235 kton/year of Co-LTFT derived syncrude to naphtha, kerosene and gas oil with at least 90% purity and recovery of the target components. The input stream to the process was a syncrude product containing non-hydrocarbon impurities. A Base Case process and five alternative processes were simulated.

- In the Base Case process, the water, the unreacted syngas and the syncrude were separated into different streams. The syncrude stream was used as feed to an ADU with two steam strippers, producing one distillate product (naphtha) and two stripper side products (kerosene and gas oil).
- In the Case 2 process, the kerosene stripper of the ADU used a reboiler instead of stripping steam.
- In the Case 3 process, there is a third steam stripper that produces heavy gas oil.
- In the Case 4 process, the duty of the pumparounds is added to the condenser.
- In the Case 5 process, there is a VDU separating the atmospheric residue into heavy gas oil, light and heavy vacuum gas oil.
- In the Case 6.1 and 6.2 processes, a heat exchanger network is used to decrease utility consumption.

The simulation of the processes was successfully implemented, and results of the design and process parameters and utility consumption were obtained. A sensitivity analysis was carried out for certain parameters of the Base Case process to assess the optimal operating point. The Base Case was compared in utility consumption and separation quality with the five alternative processes.

The results of the process model show that most of the cooling duty is used to separate the syncrude from inert gases (mostly N_2), unreacted syngas and water. It is concluded that if the FT reactor has a higher recycle to increase CO utilisation, thus decreasing the molar and mass fraction of non-hydrocarbons in the output stream, then the consumption of cooling water used to remove the gases from the syncrude would be decreased. The same holds true for reducing the amount of inert gases in the FT reactor input.

According to the results for Case 2, replacing the stripping steam of the kerosene stripper with a reboiler that has the same duty as the heater for the LPS leads to a minor decrease in purity and recovery of the kerosene fraction. At atmospheric pressure conditions, the temperature necessary at the bottom stage of the gas oil stripper or the main column if stripping steam is replaced by a reboiler of equal duty to the heater used in creating the steam is prohibitively high, since it would lead to thermal cracking and coking. Therefore, it is concluded that for the given feed composition, steam strippers are more suitable than reboiler strippers.

According to the results for Case 3, adding another stripper with the goal of producing an extra product, decreases the quality of fractionation. This happens even if the heaviest hydrocarbon component of the stripper product drawn off from a higher stage of the ADU has a lower boiling point than the lightest hydrocarbon component of the stripper product drawn off from a lower stage in the ADU. In other words, drawing off an extra product decreases purity and recovery of all the other products, given the same BoD specifications (duties, internal configuration, etc). This is shown in Case 3 where drawing HGO from the main column by adding a stripper lowers the purity and recovery of naphtha, kerosene and gas oil. This is consistent with literature. However, the increase in heating utility is very small, and the decrease in separation

quality of the main products is not prohibitively high. Thus, it is concluded that only the necessary cuts should be drawn off in order to have good purity and recovery with minimum utility use.

Next, according to the results for Case 4, concentrating the duty of the pumparounds in the condenser decreases separation quality for all fractions. This is consistent with literature and commercial experience. It is concluded that pumparounds are necessary not only to ensure adequate liquid flow and prevent dumping, but also to increase separation quality with no increase in utilities consumption.

According to the Case 5 results, separation quality between products is lower in the case of a VDU compared to an ADU. This happens despite having equal heating utility consumption per unit mass of feed and an equal number of products in the ADU and VDU. This is caused by the lower relative volatilities of the components in the atmospheric residue (VDU feed) compared to the syncrude (ADU feed). Furthermore, installation, operation and maintenance of a VDU increase the capital, operation and maintenance costs of the refinery as a whole. Therefore, it is concluded that the implementation of a VDU in the refinery should only be carried out if there is either a market for VGOs, or if there are downstream refinery units that require different cuts of the AR as feedstock.

Finally, according to the Case 6 results, heat integration can decrease the total utility consumption by almost half while providing identical separation quality to the Base Case (without heat integration). It can also decrease the subcooling duty by a factor of 6 while also reducing heating duty by 25% and providing identical separation quality to the Base Case (without heat integration). This is possible due to the low temperature (-70°C) and large content of the purge stream from the prefractionation step, and the high temperature of the product streams, which are above ambient temperature upon exiting the column. It is thus concluded that heat integration is highly recommendable from an energy efficiency point of view when designing the distillation section of a refinery.

In the sensitivity analysis chapter, the cold condensate temperature was varied to assess changes in syncrude purity and recovery from the FTR output stream. Additionally, the ADU feed stage, ADU feed temperature, ADU condenser duty, and ADU stripping steam flow rate were varied to assess changes in product purity and recovery. The sensitivity analysis was used to find the optimal operating point for the Base Case process column to meet the BoD goals. Variations in the feed stage, feed temperature and condenser duty are permissible while still meeting the BoD goals. It can be concluded from the results obtained from the Base Case process model sensitivity analysis that the prefractionation design parameters and the column configuration are optimal.

The ADU feed temperature may be decreased, or condenser duty may be slightly increased, in order to maximize gas oil purity and recovery. It is concluded that, given an existing ADU, and given the same feed, operating parameters such as condenser duty, feed temperature and can be optimized differently in order to maximize the purity and recovery of different products.

8. Recommendations

The implementation of a process model for the prefractionation and distillation of Co-LTFT derived syncrude in ASPEN Plus has been documented in this report.

The process model developed in this project can be tested in future research projects for different types of crude feed, such as crude oil or Fe-HTFT derived syncrude.

Vacuum distillation is an energy intensive process that produces relatively low-value products compared to the products of the ADU. Therefore, it is recommended that hydrocracking of the atmospheric residue is modelled as an alternative to vacuum distillation, which increases the yield of the naphtha, kerosene and gas oil products.

A refinery model can also be part of a research project. The products of this project are all "straight-run" products, not final products. Catalytic reformers, oligomerisation units and other refining units can be modelled with the goal of producing on-specification final products. Units that recover propane and butane from the Light Ends stream can be modelled.

A cost estimation of the process model can be conducted, in order to compare the capital cost, operating and maintenance cost that the different cases have. A cost-benefit analysis can be conducted to estimate if it is beneficial to refine naphtha to motor gasoline, kerosene to jet fuel, or gas oil to diesel fuel. A comparison can be made between a hydrocracking reactor and a VDU for the atmospheric residue.

Crude oil has different compositions depending on origin. Some crude compositions may be more suitable for chemical, instead of fuel, production. Studies can be conducted regarding the suitability of each type of crude for fuel or chemical production, and the distillation and refining of suitable crude types for petrochemicals. Integrated fuel and chemical refinery systems are also interesting and deep as a topic to explore.

A market study is also recommended in order to assess the potential sales benefit of each product and consider the consequences of Tata Steel's entry in the fuel or chemical market.

8. Recommendations

Bibliography

[1]   Reaching zero carbon emissions from steel, Energy Transitions Comm. (2018). http://www.energy-transitions.org/mission-possible.

[2]   J.A. Ricketts, HOW A BLAST FURNACE WORKS, Am. Iron Steel Inst. (2011). https://web.archive.org/web/20110223081722/http://www.steel.org:80/AM/Template.cfm?Section=Home&template=/CM/HTMLDisplay.cfm&ContentID=5433 (accessed May 7, 2020).

[3]   G. Parker, Encyclopedia of materials: science and technology, (2001).

[4]   W.T. Lankford, The making, shaping, and treating of steel, Association of Iron & Steel Engineers, 1985.

[5]   C.G. Davis, J.F. McFarlin, H.R. Pratt, Direct-reduction technology and economics, Ironmak. Steelmak. 9 (1982) 93–129.

[6]   W.S. Association, World Direct Reduction Statistics [EB/OL. f2014—06—03]. http, I. Midrex. Co. (2013).

[7]   R.J. Fruehan, O. Fortini, H.W. Paxton, R. Brindle, Theoretical minimum energies to produce steel for selected conditions, Carnegie Mellon University, Pittsburgh, PA (US); Energetics, Inc., Columbia …, 2000.

[8]   R. Béchara, H. Hamadeh, O. Mirgaux, F. Patisson, Carbon Impact Mitigation of the Iron Ore Direct Reduction Process through Computer-Aided Optimization and Design Changes, Metals (Basel). 10 (2020) 367.

[9]   I.I. and S.I.C. on Technology, The Electric Arc Furnace, 1990, International Iron and Steel Institute, 1990. https://books.google.nl/books?id=9QQJAQAAMAAJ.

[10] Fleur Templeton, "Iron and steel - Attempts to extract iron", Te Ara - the Encyclopedia of New Zealand, http://www.TeAra.govt.nz/en/diagram/5885/electric-arc-furnace (accessed 8 May 2020), (n.d.).

[11] WorldSteel, Fact Sheet: Climate change mitigation., Worldsteel Assoc. (2019). https://doi.org/10.4018/978-1-5225-0803-8.ch003.

[12] ENVIRONMENT AND CLIMATE CHANGE, World Steel Assoc. (2019).

[13] STEEL'S CONTRIBUTION TO A LOW CARBON FUTURE, World Steel Assoc. (2020).

[14] M. Pooler, Cleaning up steel is key to tackling climate change, Financ. Times. (2019).

[15] D. Semih Eser, Petroleum Processing - Distillation terminology: Cut Points, PennState Coll. Earth Miner. Sci. (2018).

[16] A. De Klerk, Fischer-tropsch refining, John Wiley & Sons, 2012.

[17] A. Sajeev Kumar, Modelling of Multi-Tubular Fixed-Bed Reactor for Fischer-Tropsch Synthesis to Produce Synthetic Crude Using Syngas Obtained from the Work's Arising Gases of an Integrated Steel Mill, (2019).

[18] R. Socolow, M. Desmond, R. Aines, J. Blackstock, O. Bolland, T. Kaarsberg, N. Lewis, M. Mazzotti, A. Pfeffer, K. Sawyer, Direct air capture of CO2 with chemicals: a technology assessment for the APS Panel on Public Affairs, American Physical Society, 2011.

[19] C. Graves, S.D. Ebbesen, M. Mogensen, K.S. Lackner, Sustainable hydrocarbon fuels

by recycling CO2 and H2O with renewable or nuclear energy, Renew. Sustain. Energy Rev. 15 (2011) 1–23.

[20]   A. de Klerk, Refining Fischer-Tropsch Syncrude: Perspectives on Lessons from the Past, in: Adv. Fischer-Tropsch Synth. Catal. Catal., CRC Press, 2009: pp. 343–376.

[21]   A. de Klerk, Fischer–Tropsch fuels refinery design, Energy Environ. Sci. 4 (2011) 1177–1205. https://doi.org/10.1039/C0EE00692K.

[22]   Annual Energy Outlook 2019 with projections to 2050, U.S. Energy Inf. Adm. (2019). https://www.eia.gov/outlooks/aeo/pdf/aeo2019.pdf.

[23]   B. Todic, W. Ma, G. Jacobs, B.H. Davis, D.B. Bukur, CO-insertion mechanism based kinetic model of the Fischer–Tropsch synthesis reaction over Re-promoted Co catalyst, Catal. Today. 228 (2014) 32–39.

[24]   R.A. Meyers, R.A. Meyers, Handbook of petroleum refining processes, McGraw-Hill New York, 2004.

[25]   D.S.J. Jones, P.R. Pujadó, Handbook of petroleum processing. 2006, (n.d.).

[26]   L.P. Dancuart, R. de Haan, A. de Klerk, Chapter 6 - Processing of Primary Fischer-Tropsch Products, in: A. Steynberg, M.B.T.-S. in S.S. and C. Dry (Eds.), Fischer-Tropsch Technol., Elsevier, 2004: pp. 482–532. https://doi.org/https://doi.org/10.1016/S0167-2991(04)80463-4.

[27]   J. Liu, Predicting the products of crude oil distillation columns, (2012).

[28]   J.P. Wauquier, Petroleum Refining, Vol. 2, Separation Processes; Editions Technip: Paris, 1995, There Is No Corresp. Rec. This Ref. Sch. (n.d.).

[29]   A. Gorak, H. Schoenmakers, Distillation: Operation and applications, Academic Press, 2014.

[30]   R. Ravi, A rigorous analysis of McCabe-Thiele assumptions and their consequences: critical role of parallel enthalpy lines, Chem. Eng. Commun. 193 (2006) 55–68.

[31]   L. Chen, M. Jobson, R. Smith, Heat-integrated crude oil distillation system design, University of Manchester UK, 2008.

[32]   L.M. Ochoa-Estopier, M. Jobson, R. Smith, The use of reduced models for design and optimisation of heat-integrated crude oil distillation systems, Energy. 75 (2014) 5–13.

[33]   Y. Luo, L. Wang, H. Wang, X. Yuan, Simultaneous optimization of heat-integrated crude oil distillation systems, Chinese J. Chem. Eng. 23 (2015) 1518–1522.

[34]   A.N. Khalaf, Steady State Simulation of Basrah Crude Oil Refinery Distillation Unit using ASPEN HYSYS, Univ. Thi-Qar J. Eng. Sci. 9 (2018) 29–39.

[35]   A.K. Coker, Ludwig's applied process design for chemical and petrochemical plants, gulf professional publishing, 2014.

[36]   Engineering ToolBox, (2017). Hydrocarbons - physical data. [online] Available at: https://www.engineeringtoolbox.com/hydrocarbon-boiling-melting-flash-autoignition-point-density-gravity-molweight-d_1966.html [Accessed 20 Jan 2020], (n.d.).

[37]   Engineering ToolBox, (2003). Fuels - Higher and Lower Calorific Values. [online] Available at: https://www.engineeringtoolbox.com/fuels-higher-calorific-values-d_169.html [Accessed 20 January 2020], (n.d.).

[38]   S. Ramdharee, E. Muzenda, M. Belaid, A review of the equations of state and their applicability in phase equilibrium modeling, in: Int. Conf. Chem. Environ. Eng.

Bibliography

Johannesbg., 2013.

Appendix

Stream composition and conditions

Table A.1: Syncrude prefractionation stream composition and conditions

		Raw feed	Hot condensate	Cold condensate	Water	Purge	Syncrude	HPS	LPS
Temperature	°C	204.2	-70.5	-19.5	25.5	-70.5	310.0	400.0	175.0
Pressure	bar	23.6	23.0	23.0	23.6	23.6	1.0	20.0	4.0
Molar Vapor Fraction	-	1.0	0.0	0.0	0.0	1.0	0.8	1.0	1.0
Mole Flows	kmol/s	5.428	0.027	0.019	0.624	4.759	0.045	0.072	0.001
Molar fractions of components and component groups	CO	0.164	0.012	0.006	0.000	0.187	0.010	0.000	0.000
	H2	0.179	0.005	0.001	0.000	0.204	0.003	0.000	0.000
	H2O	0.116	0.009	0.337	1.000	0.000	0.144	1.000	1.000
	N2	0.451	0.034	0.013	0.000	0.514	0.025	0.000	0.000
	CO2	0.054	0.030	0.200	0.000	0.060	0.100	0.000	0.000
	O2	0.008	0.001	0.001	0.000	0.009	0.001	0.000	0.000
	C1-C4	0.022	0.011	0.136	0.000	0.025	0.062	0.000	0.000
	C5-C8	0.002	0.115	0.295	0.000	0.000	0.189	0.000	0.000
	C9-C15	0.001	0.273	0.012	0.000	0.000	0.166	0.000	0.000
	C16-C22	0.001	0.178	0.000	0.000	0.000	0.105	0.000	0.000
	C23-C27	0.000	0.098	0.000	0.000	0.000	0.058	0.000	0.000
	C28-C38	0.001	0.159	0.000	0.000	0.000	0.094	0.000	0.000
	C39-C47	0.000	0.058	0.000	0.000	0.000	0.034	0.000	0.000
	C48+	0.000	0.016	0.000	0.000	0.000	0.009	0.000	0.000
Mass flow	kg/s	130.736	6.968	0.907	11.242	111.619	7.875	1.300	0.025

Table A.2: Base case ADU products composition and conditions

		Light Ends	Naphtha	Kerosene	Gas Oil	Atm. Residue
Temperature	°C	-20.0	10.3	124.8	237.3	287.7
Pressure	bar	0.9	1.0	1.0	1.0	1.0
Molar Vapor Fraction	-	1.0	0.0	0.0	0.0	0.0
Mole Flows	kmol/s	0.008	0.010	0.008	0.005	0.009
Molar fractions of components and component groups	CO	0.052	0.000	0.000	0.000	0.000
	H2	0.018	0.000	0.000	0.000	0.000
	H2O	0.002	0.050	0.043	0.016	0.015
	N2	0.136	0.000	0.000	0.000	0.000
	CO2	0.525	0.011	0.000	0.000	0.000
	O2	0.005	0.000	0.000	0.000	0.000
	C1-C4	0.207	0.112	0.000	0.000	0.000
	C5-C8	0.057	0.823	0.024	0.000	0.000
	C9-C15	0.000	0.002	0.914	0.031	0.000
	C16-C22	0.000	0.000	0.020	0.913	0.026
	C23-C27	0.000	0.000	0.000	0.041	0.269
	C28-C38	0.000	0.000	0.000	0.000	0.471
	C39-C47	0.000	0.000	0.000	0.000	0.173
	C48+	0.000	0.000	0.000	0.000	0.046
Mass flow	kg/s	0.358	0.784	1.270	1.250	4.115

<

Table A.3: Case 2 ADU products composition and conditions

		Light Ends	Naphtha	Kerosene	Gas Oil	Atm. Residue
Temperature	°C	-33.1	0.9	144.6	233.3	285.7
Pressure	bar	0.9	1.0	0.9	1.0	1.0
Molar Vapor Fraction	-	1.0	0.0	0.0	0.0	0.0
Mole Flows	kmol/s	0.008	0.010	0.008	0.005	0.009
Molar fractions of components and component groups	CO	0.056	0.000	0.000	0.000	0.000
	H2	0.019	0.000	0.000	0.000	0.000
	H2O	0.001	0.040	0.017	0.016	0.015
	N2	0.148	0.000	0.000	0.000	0.000
	CO2	0.568	0.016	0.000	0.000	0.000
	O2	0.005	0.000	0.000	0.000	0.000
	C1-C4	0.175	0.154	0.000	0.000	0.000
	C5-C8	0.027	0.789	0.101	0.000	0.000
	C9-C15	0.000	0.000	0.881	0.063	0.000
	C16-C22	0.000	0.000	0.000	0.900	0.039
	C23-C27	0.000	0.000	0.000	0.021	0.272
	C28-C38	0.000	0.000	0.000	0.000	0.460
	C39-C47	0.000	0.000	0.000	0.000	0.168
	C48+	0.000	0.000	0.000	0.000	0.045
Mass flow	kg/s	0.315	0.752	1.270	1.250	4.185

≤.

Table A.4: Case 3 ADU products composition and conditions

		Light Ends	Naphtha	Kerosene	Gas Oil	Heavy Gas Oil	Atm. Residue
Temperature	°C	-24.1	7.0	120.5	235.0	280.6	299.5
Pressure	bar	0.9	0.9	0.9	1.0	1.0	1.0
Molar Vapor Fraction	-	1.0	0.0	0.0	0.0	0.0	0.0
Mole Flows	kmol/s	0.008	0.010	0.008	0.005	0.003	0.007
Molar fractions of components and component groups	CO	0.053	0.000	0.000	0.000	0.000	0.000
	H2	0.018	0.000	0.000	0.000	0.000	0.000
	H2O	0.001	0.047	0.046	0.016	0.014	0.015
	N2	0.140	0.000	0.000	0.000	0.000	0.000
	CO2	0.539	0.012	0.000	0.000	0.000	0.000
	O2	0.005	0.000	0.000	0.000	0.000	0.000
	C1-C4	0.198	0.125	0.000	0.000	0.000	0.000
	C5-C8	0.046	0.814	0.048	0.000	0.000	0.000
	C9-C15	0.000	0.001	0.898	0.035	0.001	0.000
	C16-C22	0.000	0.000	0.008	0.893	0.146	0.006
	C23-C27	0.000	0.000	0.000	0.056	0.578	0.134
	C28-C38	0.000	0.000	0.000	0.000	0.253	0.548
	C39-C47	0.000	0.000	0.000	0.000	0.007	0.233
	C48+	0.000	0.000	0.000	0.000	0.001	0.063
Mass flow	kg/s	0.343	0.773	1.270	1.250	0.910	3.231

viii

Table A.5: Case 4 ADU products composition and conditions

		Light Ends	Naphtha	Kerosene	Gas Oil	Atm. Residue
Temperature	°C	-9.5	17.8	135.6	239.8	289.1
Pressure	bar	1.0	1.0	0.9	1.0	1.0
Molar Vapor Fraction	-	1.0	0.0	0.0	0.0	0.0
Mole Flows	kmol/s	0.009	0.010	0.008	0.005	0.009
Molar fractions of components and component groups	CO	0.049	0.000	0.000	0.000	0.000
	H2	0.017	0.000	0.000	0.000	0.000
	H2O	0.003	0.059	0.035	0.015	0.015
	N2	0.129	0.000	0.000	0.000	0.000
	CO2	0.500	0.010	0.000	0.000	0.000
	O2	0.004	0.000	0.000	0.000	0.000
	C1-C4	0.217	0.093	0.000	0.000	0.000
	C5-C8	0.080	0.807	0.006	0.000	0.000
	C9-C15	0.000	0.030	0.912	0.026	0.000
	C16-C22	0.000	0.000	0.047	0.896	0.019
	C23-C27	0.000	0.000	0.000	0.063	0.262
	C28-C38	0.000	0.000	0.000	0.000	0.480
	C39-C47	0.000	0.000	0.000	0.000	0.176
	C48+	0.000	0.000	0.000	0.000	0.047
Mass flow	kg/s	0.386	0.808	1.270	1.250	4.063

Table A.6: Case 5 VDU products composition and conditions

		Heavy Gas Oil	LVGO	HVGO	Vac. Residue
Temperature	°C	24.1	255.1	314.1	336.1
Pressure	bar	0.0	0.0	0.0	0.0
Molar Vapor Fraction	-	0.0	0.0	0.0	0.0
Mole Flows	kmol/s	0.003	0.004	0.002	0.000
Molar fractions of components and component groups	CO	0.000	0.000	0.000	0.000
	H2	0.000	0.000	0.000	0.000
	H2O	0.013	0.001	0.000	0.001
	N2	0.000	0.000	0.000	0.000
	CO2	0.000	0.000	0.000	0.000
	O2	0.000	0.000	0.000	0.000
	C1-C4	0.000	0.000	0.000	0.000
	C5-C8	0.000	0.000	0.000	0.000
	C9-C15	0.000	0.000	0.000	0.000
	C16-C22	0.087	0.002	0.000	0.000
	C23-C27	0.748	0.105	0.008	0.000
	C28-C38	0.152	0.838	0.167	0.024
	C39-C47	0.000	0.054	0.684	0.545
	C48+	0.000	0.000	0.141	0.430
Mass flow	kg/s	0.920	1.953	0.946	0.294

xi

K-values of syncrude components at 310°C

Table A.7: K-values of syncrude components at 310°C

Component	K-value	Component	K-value
CO	275.0287262	C36H74	0.013547868
H2	360.5059706	C37H76	0.009431429
H2O	68.37393806	C38H78	0.00767827
N2	265.4248165	C40H82	0.004403542
CO2	154.3215277	C42H86	0.002986679
O2	229.4279632	C43H88	0.003612202
CH4	191.9501612	C44H90	0.002144573
C2H6	122.9469241	C45H92	0.001146031
C3H8	86.68225987	C46H94	0.001448342
C4H10	61.22427125	C48H98	0.001027292
C5H12	44.02614393	C50H102	0.000736465
C6H14	31.88175526	C2H4	137.6300404
C7H16	23.39552777	C3H6	91.03514008
C8H18	17.1772146	C4H8	64.84081827
C9H20	12.68694677	C5H10	46.64356261
C10H22	9.344016632	C6H12	33.92229865
C11H24	6.969220691	C7H14	25.03224413
C12H26	5.159612788	C8H16	18.42444626
C13H28	3.846716683	C9H18	13.53948966
C14H30	2.8375569	C10H20	9.971391413
C15H32	2.134884373	C11H22	7.366572521
C16H34	1.604628251	C12H24	5.463473436
C17H36	1.216910059	C13H26	4.046036692
C18H38	0.935570554	C14H28	3.010503406
C19H40	0.716897296	C15H30	2.293347727
C20H42	0.54780692	C16H32	1.727050855
C21H44	0.422959192	C17H34	1.318917242
C22H46	0.33050806	C18H36	1.003515269
C23H48	0.25094665	C19H38	0.764106439
C24H50	0.194240642	C20H40	0.576002281
C25H52	0.153395211	C21H42	0.2459539
C26H54	0.118110543	C22H44	0.340773264
C27H56	0.09065086	C23H46	0.208316279
C28H58	0.073588485	C24H48	0.203371487
C29H60	0.059973361	C26H52	0.123616648
C30H62	0.047413853	C27H54	0.069288865
C31H64	0.03357261	C28H56	0.077018979
C32H66	0.030616313	C29H58	0.050905226
C33H68	0.02082728	C30H60	0.048587472
C34H70	0.021511645	C36H72	0.012784092
C35H72	0.013147508	C40H80	0.005506893

Thermodynamic property models

The purpose of this chapter is to explain the process by which the Peng-Robinson thermodynamic property model was selected among the other options in ASPEN Plus for the modelling of the process.

All chemical processes, distillation included, are governed by the laws of thermodynamics. The first law describes the conservation of energy, while the second law states that in a closed system, entropy always increases. The entropy S of a system is a function of pressure and temperature, and it is path independent. Rewriting and combining the first and second laws of thermodynamics gives us:

$$dU = TdS - pdV$$

which means that the internal energy function U is also path independent, thus making equations of state necessary and sufficient for its calculation. In order to calculate pressure, volatility and internal energy, as functions of temperature and molar density, equations of state are required. The ideal-gas equation of state,

$$p = \frac{nRT}{V}$$

is inaccurate for non-ideal gases. For non-ideal gases, a large number of state equations are offered in literature that more accurately predict thermodynamic properties. For example, there is the van der Waals equation of state, expressed as:

$$p = \frac{RT}{V_m - b} - \frac{a}{V_m^2}$$

where

V_m is the molar volume,

$a = 3p_C V_{mC}^2 = \frac{27R^2 T_C^2}{64 p_C}$, and

$b = V_C/3 = RT_C/(8p_C)$.

In distillation, the most commonly used equations of state are the Redlich-Kwong (RK), Soave-Redlich-Kwong (SRK), Benedict-Webb-Rubin (BWR) and Peng-Robinson (PR).

The Benedict-Webb-Rubin EoS is not described in this chapter. Despite it being regarded as an accurate predictor of liquid and vapor properties of mixtures, it is not included among the options provided by the ASPEN Plus software.

The Redlich-Kwong state equation, proposed in 1949 by Otto Redlich and Joseph Neng Shun Kwong, is an empirical equation that better predicts pressure compared to the van der Waals equation that preceded it. It is given by:

$$p = \frac{RT}{V_m - b} - \frac{a}{\sqrt{T} V_m (V_m + b)}$$

where a is a constant that corrects for the attractive forces between molecules and b is a constant that corrects for volume, both functions of critical temperature T_C and critical pressure P_C as follows:

$$a = \frac{1}{9(\sqrt[3]{2} - 1)} \frac{R^2 T_c^{2.5}}{P_c} = 0.42748 \frac{R^2 T_c^{2.5}}{P_c},$$

$$b = \frac{\sqrt[3]{2} - 1}{3} \frac{R T_c}{P_c} = 0.08664 \frac{R T_c}{P_c},$$

The Redlich-Kwong equation was modified in 1972 by Soave, forming the SRK EoS. The reason was that the RK fails to accurately predict vapor-liquid equilibria, so Soave updated the original equation to include the (then) recently discovered accentric factor. The SRK is given by:

$$P = \frac{RT}{V_m - b} - \frac{a\alpha}{V_m(V_m + b)}$$

The SRK still inadequately predicted liquid densities, especially liquid densities of non-polar materials or liquid densities close to the critical point. Thus, the accentric term was updated by Ding-Yu Peng and Donald Robinson in 1976, forming the Peng-Robinson equation of state. The PR EoS is given by:

$$p = \frac{RT}{V_m - b} - \frac{a\alpha}{V_m^2 + 2bV_m - b^2}$$

The literature suggests that the most suitable equations of state for multicomponent distillation applications are the SRK and the PR EoS. Of those two, the SRK EoS is better at predicting properties of polar mixtures, while the PR EoS is better at predicting liquid densities and volatilities of hydrocarbons [38]. The feed to the ADU contained mostly non-polar hydrocarbons, therefore the PR EoS was used.

Product stream mass flow calculations

According to Wauquier [28], calculation of the concentration of each individual component on each stage necessitates:

- material balance (mass or mole basis),
- enthalpy balance and
- equilibrium equations

as inputs. The purpose of this subchapter is to illustrate the method by which the mass flow rate of each product in each case was calculated and set as a fixed input parameter in the ASPEN Plus model of the process.

The mass flow rates of each required product stream are the same in all cases (as long as the cases in question have the same product streams). The only exception is the AR stream. However, the flow rate of this stream is a dependent variable and is thus not necessary to calculate.

Case 5 is the case where all the possible products need to be defined, so this calculation will be performed with respect to Case 5. In most cases (with the exception of Case 5), only some of the streams need to have their mass flow rate defined. In those cases, there is simply no input parameter for the other streams.

The independent variables that require a fixed value for the successful convergence of the process are:

- Naphtha
- Kerosene
- Gas Oil
- HGO
- LVGO
- HVGO

Ideally, the composition of any distillation stream would be 100% of the goal components that exist in the feed to the same distillation unit, and 0% of any other component. Therefore, the mass flow of each product is set at the sum of the mass flows of all the components in the target range. All the mass flows of values needed for the calculation are in the Appendix, in Stream composition and conditions. The resultant mass flows are:

Table A.8: Product mass flow specifications

	Mass flow [kg/s]
Naphtha	0.80
Kerosene	1.27
Gas Oil	1.25
HGO	0.92
LVGO	1.95
HVGO	0.95